FACULTY OF BIOSCIENCE ENGINEERING

EXPLORING THE SMALL INTESTINAL MICROBIOTA: OPTIMIZATION AND VALIDATION OF A PERSONALIZED SMALL INTESTINAL MODEL

Margot Smet

Student number: 01907067

Promotor(s): Prof. dr. ir. Tom Van de Wiele and dr. Ludovica Marinelli

Tutor: Ir. Karen Delbaere and dr. ir. Kim De Paepe

Master's Dissertation submitted to Ghent University in partial fulfillment of the requirements for the degree of Master of Science in Bioscience Engineering: Cell and Gene Biotechnology

Academic year: 2023-2024

UNIVERSITEIT GENT

COPYRIGHT

Ghent, 7th of Juin 2024

The promoter(s),

Prof. dr. ir. Tom Van de Wiele

Dr. Ludovica Marinelli

The tutor(s),

Ir. Karen Delbaere

Dr. ir. Kim De Paepe

The author,

Margot Smet

ACKNOWLEDGMENTS

Reflecting on my thesis year, I am grateful for the valuable lessons I've learned. I believe I have grown throughout this journey, especially in my scientific writing and communication. None of this would have been possible without the guidance and support of several people, whom I would like to acknowledge.

First of all, I would like to express my gratitude to my promotors prof. dr. ir. Tom Van de Wiele, dr. ir. Kim de Paepe, and dr. Ludovica Marinelli. Your insights into the microbial community and your constructive feedback have enriched my understanding and scientific competences. I am also grateful for my tutor, Karen. Your support and willingness to answer all my questions were truly valuable throughout this trajectory. Your enthusiasm motivated me and made it very enjoyable to work with you.

Next, I would like to thank members of CMET, especially the HAM cluster, who created a positive environment where one feels motivated to come in and be supported. Furthermore, I would like to thank the ATP team. Your commitment to laboratory safety, your expertise, and your readiness to answer any question really facilitated lab work.

Finally, I want to thank my friends and family, especially Merel, Rita, mom, dad, Emma, Michiel, and Thomas who were always ready to hear my stories about the lab, read through my thesis, and served as my audience for my presentations. Your support was truly invaluable.

SUMMARY

Several diseases such as small intestinal bacterial overgrowth and inflammatory bowel disease are associated with shifts in the small intestinal microbiota. However, diagnosing and treating these diseases is challenging due to the limited knowledge about these bacteria, primarily because *in vivo* sampling is invasive, time-consuming, and prone to contamination. To address this, an *in vitro* model was developed and validated to study the small intestinal bacteria, bypassing the need for invasive sampling and allowing for a mechanistic understanding of the dynamics and composition of these bacteria. The *in vitro* model, based on the well-studied M-SHIME, includes six compartments: the mouth, stomach, proximal small intestine (duodenum and jejunum), ileum, proximal colon and distal colon. A dialysis membrane between the proximal small intestine and ileum simulates nutrient absorption. The system was inoculated with both salivary and fecal microbiota from healthy human donors, allowed the colonization by both saliva (e.g. *Streptococcus* and *Veillonella*) and fecal microbial genera (e.g. *Bacteroides* and *Enterococcus*) in the small intestine, similar to the *in vivo* situation. Validation of the system against *in vivo* data demonstrated that the microbial genera in the compartments were representative, maintaining individual signatures. The functionality and bacterial abundances of the compartments were consistent with *in vivo* conditions, except for the proximal small intestinal cell counts, which were higher *in vitro*. Based on these findings, we concluded that the developed small intestinal M-SHIME can effectively recapitulate the *in vivo* situation.

SAMENVATTING

Verschillende ziekten, zoals bacteriële overgroei in de dunne darm en inflammatoire darmziekte, worden geassocieerd met verschuivingen in de dunne darm microbiota. Het diagnosticeren en behandelen van deze ziekten is echter uitdagend door de beperkte kennis over deze bacteriën, voornamelijk omdat *in vivo* bemonstering invasief tijdrovend, en vatbaar voor contaminatie is. Daarom werd een *in vitro* model ontwikkeld en gevalideerd om de dunne darm bacteriën te bestuderen, waardoor invasieve bemonstering niet nodig is en er een mechanistisch begrip van de dynamiek en samenstelling van deze bacteriën kan worden verkregen. Het *in vitro* model, gebaseerd op de M-SHIME, omvat zes compartimenten: de mond, maag, proximale dunne darm (duodenum en jejunum), ileum, proximale colon en distale colon. Een dialysemembraan tussen de proximale dunne darm en het ileum simuleert nutriënt absorptie. Het systeem word geïnoculeerd met speeksel en fecale microbiota van gezonde, menselijke donoren zodat zowel speeksel microbiële genera (bijv. *Streptococcus* en *Veillonella*) als fecale genera (bijv. *Bacteroides* en *Enterococcus*) aanwezig zijn in de dunne darmcompartimenten, vergelijkbaar met de *in vivo* situatie. Validatie van het systeem met *in vivo* data toonde aan dat de microbiële genera in de compartimenten representatief waren, met behoud van typerende genera. De functionaliteit en bacteriële abundantie van de compartimenten waren consistent met *in vivo* omstandigheden, behalve voor de bacteriële cel concentraties in de proximale dunne darm, die hoger waren *in vitro*. Op basis van deze bevindingen concludeerden we dat het ontwikkelde M-SHIME-model voor de dunne darm de *in vivo* situatie effectief kan nabootsen.

TABLE OF CONTENTS

Summary 4

Abbreviations 7

List of tables 8

List of figures 9

1 Introduction 11

2 Literature 12

2.1 The gastrointestinal tract *12*
2.1.1 Structure 12
2.1.2 Function 13
2.1.3 Physicochemical environment 15
2.1.4 Colonization of the gastrointestinal tract by micro-organisms 16
2.1.5 Microbial metabolism 21

2.2 Modeling the small intestinal microbiota in vitro *24*
2.2.1 Batch fermentation models 25
2.2.2 Continuous and semi-continuous models 25
2.2.3 Model overview 28

3 Objectives 30

4 Material and methods 31

4.1 Dialysis absorption efficiency *31*
4.1.1 Dialysis membrane operation 32
4.1.2 Carbohydrate analysis 32

4.2 SI M-SHIME validation experiment *33*
4.2.1 Experimental set-up 33
4.2.2 Inoculation and SI M-SHIME operation 35

4.3 Chemical and microbial analysis *36*
4.3.1 Bacterial cell counts 36
4.3.2 Short-chain fatty acid, organic acid, and ammonium composition 37
4.3.3 cDNA extraction and 16S rRNA gene amplicon sequencing 37
4.3.4 Gas composition 38
4.3.5 Bioinformatics and statistics 38

5 Results 40

5.1 Carbohydrate absorption dialysis membrane *40*

5.2 SI M-SHIME results *42*
5.2.1 Bacterial cell counts 42
5.2.2 Organic acid profiles 45
5.2.3 Ammonium concentration 49
5.2.4 Gas composition 49
5.2.5 The bacterial composition of the first donor is more diverse compared to the second donor. 52
5.2.6 Phenotypic diversity 60

6 Discussion 62

6.1 The Small Intestinal M-SHIME can recapitulate genera found in vivo 62

6.1.1 Validation of the system by comparison to literature data 62

6.1.2 Validation based on donor *in vivo* data 65

6.1.3 Origin of the bacteria present in the SHIME 66

6.2 The dialysis membrane filters fibers next to the sugars. 67

6.3 The bacterial load in the proximal small intestinal compartment was higher than in vivo reported values, while the bacterial load of the other compartments was within expected values. 67

6.4 The organic acid profiles of the first and third donors were representative of the in vivo environment 69

6.4.1 The metabolite composition of the mouth compartment contained lower levels of lactate and formate compared to *in vivo*, along with higher levels of butyrate. 69

6.4.2 The small intestinal compartments were characterized by rapid carbohydrate fermentation. 69

6.4.3 The proximal colon was characterized by saccharolytic fermentation, while the distal colon by proteolytic fermentation. 70

7 Conclusion 72

8 Future perspectives 73

9 Sustainability paragraph 74

10 Appendix 75

10.1 Material and methods 75

10.2 Results 79

11 References 85

ABBREVIATIONS

SIBO	Small Intestinal Bacterial Overgrowth
IBD	Inflammatory Bowel Disease
GIT	Gastrointestinal tract
IgA	Immunoglobulin A
Ccf	Commensal Colonization Factor
CFU	Colony Forming Units
CAZymes	Carbohydrate Active Enzymes
SCFA	Short Chain Fatty Acids
FXR	Farnesoid-X-Receptor
TIM-1	TNO gastric and small intestinal model 1
TSI	The Smallest *in vitro* model
(SI M-)SHIME	(Small Intestinal Mucosal) Simulator of the Human Intestinal Microbial Ecosystem
PVC	PolyVinyl Chloride
HA	Hydroxy Apatite
SGPI	SYBR Green Propidium Iodide
SG	SYBR Green
GC	Gas Chromatography
IC	Ion Chromatography
ASV	Amplicon Sequencing Variant
QMP	Quantitative Microbial Profile
PCoA	Principal Coordinate Analysis
BCFA	Branched Short Chain Fatty Acid

LIST OF TABLES

Table 1: Genera found in the mucus and lumen of the duodenum, jejunum, and ileum. 1: (Li et al., 2015) 2: (Nagasue et al., 2022), 3: (Vasapolli et al., 2019), 4: (Seekatz et al., 2019), 5: (Dlugosz et al., 2015), 6:(Wang et al., 2005), 7: (Sundin et al., 2017), 8: (Villmones et al., 2018), 9: (Villmones et al., 2021), 10: (Hayashi et al., 2005), 11: (Booijink et al., 2010), 12 : (Van den Bogert et al., 2013) 19
Table 2: Organic acid composition detected in sudden death victims (mmol/kg) or ileostomy (mM) effluent in the different compartments of the small intestine (Cummings et al., 1987; Zoetendal et al., 2012). N.d. = no data 23
Table 3: The inoculation strategy, simulated gut compartments, transit time, and pH of each small intestinal bacterial in vitro model with TIM-1 = TNO GastroIntestinal Model, TSI = The Smallest intestinal model, M-SHIME = Mucosal Simulator of the Human Intestinal Microbial Ecosystem 28
Table 4: Advantages and disadvantages of the discussed small intestinal bacterial in vitro models with TIM-1 = TNO Gastrointestinal Model, TSI = The Smallest intestinal model, M-SHIME = Mucosal Simulator of the Human Intestinal Microbial Ecosystem 29
Table 5: SI-SHIME medium of the first donor used in dialysis absorption efficiency experiment. 31
Table 6: Concentration (g L^{-1}) of twelve compounds dialyzed in the dialysis absorption efficiency experiment. Concentrations are based on the concentration of each compound normally present in the proximal small intestine of the SI-SHIME 31
Table 7: Composition of buffer solution used in the dialysis absorption efficiency experiment 32
Table 8: Flowrate (mL/min) between the mucin Schott bottles and its respective biofilm compartment. 33
Table 9: Set-up parameters of the SI-M-SHIME 34
Table 10: SI M-SHIME medium composition of the first donor. 35
Table 11: Different buffer solutions added during the DNA extraction and their effect. 38
Table 12: Mucosal (cells/g) and luminal (cells/mL) counts in the proximal small intestine and the ileum of the second and third donors. The mean and standard deviation was calculated on day 16, with two replicates (n = 2) for the second donor, while over day 18 and 20, with each time two replicates (n = 4) for the third donor. 43
Table 13: Intact luminal flow cytometry and plating counts in the proximal small intestine and the ileum of the third donor. The mean and standard deviation were calculated over days 18 and 21, with each time 2 replicates (n = 4). 43

LIST OF FIGURES

Figure 1: Diagram of the gastrointestinal tract (made with BioRender.com) (Treuting et al., 2018a, 2018b).....12
Figure 2: Schematic overview of the small intestinal wall (Rumsey, 2005).....13
Figure 3: Overview of the different functions and environmental factors (pH, transit time, and secretions or enzymes) of the mouth, stomach, small intestine, and colon (made with BioRender.com) (Aburub et al., 2018; Ali & Tanwir, 2012; Cummings & Macfarlane, 1992; Davidson et al., 1998; Guerra et al., 2012; He et al., 1999; Korpela, 2018; Machen & Paradiso, 1987; Maurer & Krevsky, 1995; Singhal & Shah, 2020; Wilson, 2004).....16
Figure 4: The adapted TIM-1 model (a) with medium in a cooling chamber (b) (7 °C), a pH meter (c) and pH-dependent NaOH dosage (d), a hollow fiber membrane (e) and nitrogen supply (h) can be sampled through sampling port (i), Efflux is collected in a bottle (j). Dialysis fluid (f) and a flask for metabolites and digestion products (g) are placed in a cooling chamber (7°C) on a weighing scale (Stolaki et al., 2019).....26
Figure 5: Schematic overview of the Smallest Intestine in vitro model (Cieplak et al., 2018).....27
Figure 6: Schematic overview of the SHIME model (Van de Wiele et al., 2015).....27
Figure 7: Schematic overview of the dialysis absorption efficiency experiment. At the serosal side, the buffer goes into the dialysis unit and out of the system.....32
Figure 8: Schematic overview of SI-M-SHIME validation experiment with NS: nutritional saliva, BA/PJ : bile acids and pancreatic juice, PSI: proximal small intestine, PC: proximal colon, distal colon: distal colon. The orange arrows indicate the outflow of the compartments, the blue arrows show the different input flows, and the gray arrows reveal the serosal fluid flow. At the start of the experiment, saliva was used to inoculate the mouth, whereas the fecal slurry inoculated the colon compartments. Each compartment is connected to a base and acid compartment (not shown on figure).....34
Figure 9: Timeline of the stable days of the different sampling points for different chemical analysis for the different donors. Donor 2 is not included in the plot, since it never reached stability.....36
Figure 10: The carbohydrate concentration (g glucose eq. /L) of the SI M-SHIME medium before dialysis, determined in three different ways. (i) "Combined experimental" is experimentally determined by separately analyzing each medium component and adding the determined values together (1.05 g L^{-1} pectin, 0.11 g L^{-1} xylan, 0.31 g L^{-1} mucin type II, 0.80 g L^{-1} glucose, 0.60 g L^{-1} fructose, 0.27 g L^{-1} galactose, 0.26 g L^{-1} mannose, 0.37 g L^{-1} maltose, 0.32 g L^{-1} sucrose, 0.48 g L^{-1} lactose), (ii) "Complete" indicates the experimental determination of the complete SI M-SHIME medium, and (iii) "Theoretical" shows the carbohydrate content of SI M-SHIME medium based on its composition.....40
Figure 11: The carbohydrate concentration (mg glucose eq./L) before and after dialysis of the different compounds present in the SI M-SHIME medium ordered on ascending molecular weight. Before and after dialysis are plotted on the left axis, while the % removal is plotted on the right axis.....41
Figure 12: Dialysis efficiency evaluated by the carbohydrate concentration of the proximal small intestine and ileum over four cycles during the SHIME of the first donor (n = 2). The "Theoretical carbohydrate concentration" was calculated based on the SI M-SHIME medium in the proximal small intestine. The "Difference" was determined by subtracting the ileal carbohydrate concentration from the proximal small intestinal concentration.....41
Figure 13: Mean bacterial intact cell counts (cells/mL) of **A** the first donor, **B** the second donor, and **C** the third donor, separated by compartment, determined by flow cytometry and SGPI staining. Means and standard deviations are calculated based on two technical replicates (n = 2). PSI stands for proximal small intestine. Stable days are indicated by a dashed line, the non-stable phase is indicated by a full line.....44
Figure 14: Organic acids concentration (mM) during the SHIME run of **A** the first donor, **B** the second donor, and **C** the third donor, per compartment and day. Prox. SI indicates the proximal small intestine and Prox. colon the proximal colon.....47
Figure 15: Daily net organic acid production in the proximal colon and distal colon during the stable days of **A** day 16, 18, 19, and 21 for the first donor (n = 4), **B** day 9, 12, and 13 for the second donor (n = 3), **C** day 18, 19, and 21 for the third donor (n = 3).....48
Figure 16: Ammonium concentration of **A** the first donor and **B** the third donor in the proximal colon and distal colon of the SHIME run of the second donor.....49

Figure 17: **A** O_2 ,**B** CO_2,and **C** H_2 composition in the different SI-M-SHIME compartments during the SHIME of the first donor. 50
Figure 18: **A** O_2 ,**B** CO_2,and **C** H_2 composition in the different SI-M-SHIME compartments during the SHIME of the second donor. 51
Figure 19: **A** O2 ,**B** CO2,and **C** H2 composition in the different SI-M-SHIME compartments during the SHIME of the second donor. 52
Figure 20: Principle coordinate analysis of the bacterial composition of the different compartments of the first donor and second donor. Prox. SI stands for proximal small intestine and Prox. colon for proximal colon 54
Figure 21: Proportional bacterial composition based on 16S rRNA gene amplicon sequencing in the different SHIME compartments of the first donor. On the x-axis the days were displayed, and the M represents the mucosal sample of the day, Prox. SI stands for proximal small intestine and Prox. colon for proximal colon. The ASV of Muribaculaceae could not be classified on genus level, therefore f_Muribaculaceae stands for the family of Muribaculaceae 55
Figure 22: Proportional bacterial composition of the aspirates and biopsies from the first donor. Prox. colon stands for proximal colon 55
Figure 23: **A** Blanks added during extraction and PCR of the SHIME of the first donor and **B** extracted inputs of the SHIME with BA/PJ = Bile acids and pancreatic juice, SI M-SHIME Feed, Concentrated SI SHIME Fiber medium, mucus extracted from the small intestinal beads, and NS = Nutritional saliva. The ASV of Caulobacteraceae could not be classified on genus level, therefore f_Caulobacteraceae stands for the family of Caulobacteraceae. 57
Figure 24: The different ASVs of **A** Streptococcus, **B** Enterococcus, **C** Escherichia-Shigella, and **D** Bacteroides in the lumen of the compartments during day 21 (PSI = proximal small intestine, PC = proximal colon, DC = distal colon), saliva, feces, feed, nutritional saliva (NS), mucus of the small intestine (mucus), Bile acids and pancreatic juice (BA/PJ), and fiber solution (Fiber) added to the SHIME of the first donor. Each ASV within a genus is indicated with another color. 58
Figure 25: Proportional bacterial composition based on 16S rRNA gene amplicon sequencing in the different SHIME compartments on day 12 of the second donor. Prox. SI stands for proximal small intestine and Prox. colon for proximal colon. 59
Figure 26: Principle coordinate analysis of the bacterial composition of the different compartments of the second donor. Prox. SI stands for proximal small intestine and Prox. colon for proximal colon. 60
Figure 27: Phenotypic diversity of the three donors for the different compartments. Day 21 is considered for the first and third donors, while day 12 for the second donor, with two technical replicates. 60
Figure 28: Community beta diversity of the three donors for the different compartments 61

1 INTRODUCTION

Our body is the habitat of approximately 10^{13} bacterial cells (Sender et al., 2016). Interactions among these bacteria, involving an exchange of metabolites, enzymes, and genetic material, typically maintain a healthy balance known as eubiosis, which confers various benefits to the host, including protection against pathogen colonization. However, disruption to this bacterial community can lead to dysbiosis, with associated effects on host health (Kern et al., 2021).

The importance of gut bacteria is increasingly recognized. While most research focuses on the bacterial community of the large intestine, alterations in the small intestinal bacteria have also been linked to conditions such as small intestinal bacterial overgrowth (SIBO) and inflammatory bowel disease (IBD). In particular, IBD includes conditions such as Crohn's disease and ulcerative colitis. It is a prevalent chronic illness, affecting the quality of life of 2.5-3.0 million individuals in Europe, with a direct cost related to healthcare of €4.5-5.6 billion annually (Burisch et al., 2013). Conversely, SIBO is characterized by symptoms ranging from bloating to nutrient deficiencies. An estimation of the prevalence of SIBO is more difficult due to the lack of clear definitions of a "healthy" small intestinal microbiome and the one associated with SIBO (Bushyhead & Quigley, 2022).

Unlike the large intestine, which is commonly studied using fecal samples, the small intestine is more difficult to access and sample, resulting in limited information on the composition and dynamics of its bacteria. Current sampling methods such as endoscopy, enteroscopy, or surgery, are invasive, time-consuming, and susceptible to contamination. These challenges can be circumvented by *in vitro* models, enabling the exploration of the dynamics and composition of the small intestinal bacteria, as well as the produced metabolites. Furthermore, they can provide mechanistic insights into various diseases, facilitating a deeper understanding and potentially aiding in the identification of diagnostic markers.

Currently, there are few existing *in vitro* models designed to replicate the microbiota of the ileum. These models are typically inoculated with either a synthetic community, fecal sample, or ileostomy effluent, each with its advantages. However, the use of a synthetic community fails to account for inter-individual variability, whereas fecal matter does allow for such variability but fails to reproduce some key small intestinal taxa. As well, using ileostomy effluent as inoculum can induce bias due to the altered composition (Deyaert et al., 2023), compared to the normal *in vivo* condition. Moreover, to date, no models represent the duodenum and jejunum, which are also important parts of the small intestine.

To address these limitations, this thesis proposes the development of an *in vitro* model inoculated with both feces and saliva to mimic the small intestinal microbiota. Furthermore, parameters such as bacterial composition, metabolite composition, and cell counts will be measured and compared to *in vivo* samples, to validate the efficacy of the system.

2 LITERATURE

The gastrointestinal tract is a crucial part of the body, responsible for food digestion, nutrient absorption, immune and enteroendocrine function as well as interactions with the microbiome. Despite the recognized importance of the gastrointestinal microbiota, the small intestine environment and its interaction with the resident microbiota remains an understudied topic in the broad domain of gut microbiology, gastroenterology, and dietetics. This literature study will therefore address the structure, functionality, environmental parameters, microorganisms, and metabolism within the small intestine as well as existing *in vitro* models to mimic the small intestinal processes.

2.1 The gastrointestinal tract

2.1.1 Structure

The gastrointestinal tract (GIT) can be divided into two parts. Firstly, the upper gastrointestinal tract comprises the oral cavity, esophagus, stomach, and small intestine. The small intestine is the longest organ of the gastrointestinal tract measuring 6 to 7m, starting from the pylorus and ending at the ileocecal valve. It can be divided into three sections: duodenum, jejunum, and ileum (Campbell et al., 2019). The duodenum consists of four parts: the bulb, ascending, transverse, and descending parts. The bile duct and pancreas ducts come together and empty into the ascending part. The distinction between the jejunum and ileum is based on anatomic differences. The jejunum has larger and closer (10-18 per cm) circular folds, a thicker wall with more blood vessels, less prominent lymphoid follicles, and a larger diameter compared to the ileum (Campbell et al., 2019; Federle et al., 2019). The ileum is separated from the colon by the ileocecal valve which regulates the outflow of the ileum and prevents backflow (Campbell et al., 2019).

Secondly, the lower gastrointestinal tract, also known as the colon or large intestine (Petras & Frankel, 2009) consists of the cecum with the appendix, the ascending colon, the transverse colon, the descending colon, the rectum, and lastly, the anal canal (Figure 1) (Treuting et al., 2018a).

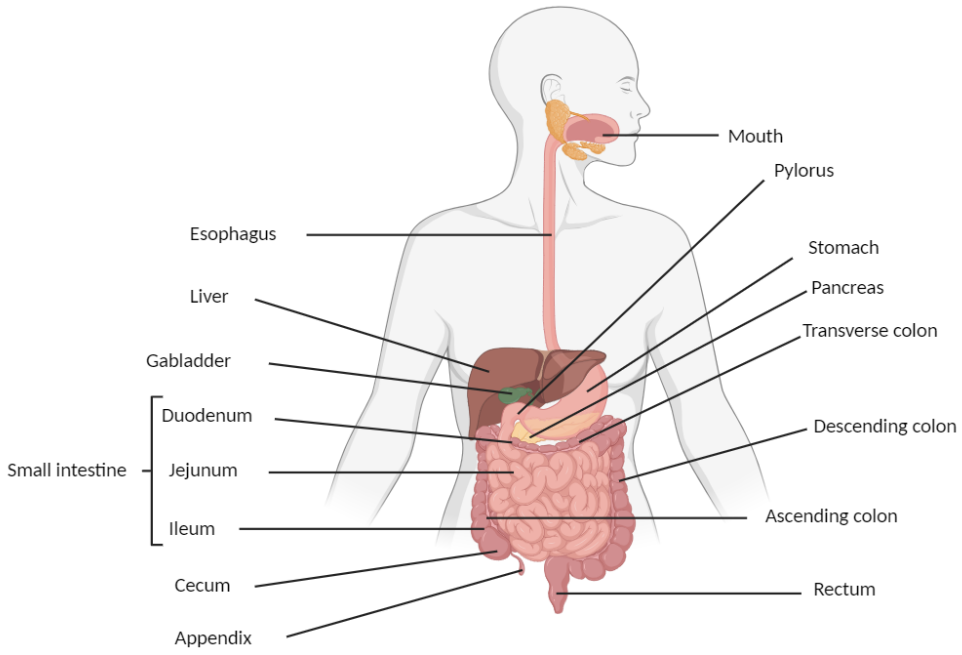

Figure 1: Diagram of the gastrointestinal tract (made with BioRender.com) (Treuting et al., 2018a, 2018b).

The intestinal wall is composed of five layers (Figure 2). The mucosa, closest to the lumen, consists of the epithelium, lamina propria (connective tissue), and a muscle layer. The underlying submucosa holds the blood ducts and nerves.

Subsequently, two muscle layers; an inner circular layer and an outer longitudinal layer, known as the muscularis layer. The outermost serosa varies along the gastrointestinal tract in function and thickness (Van de Graaff, 1986).

The mucosa has a surface area of 30 m^2 due to the presence of villi, microvilli, and plicae circulares of Kerckring, with the former two ensuring a 6.5-13-fold enlargement. The villi (0.5-1 mm long) arise as finger-like protrusions of the mucosa, whereas the microvilli appear on the epithelial cells of the villi, constituting the "brush border" (Figure 2) (Campbell, 2015; Helander & Fändriks, 2014; Höllwarth, 1999).

The mucosa is coated with mucus throughout the gastrointestinal tract (Allen et al., 1993). No studies exist yet concerning the thickness of the small intestinal mucus in humans. Nevertheless, in the rat the mucus layer of the small intestine is estimated to be 170 ± 38 µm in the duodenum, 123 ± 4 µm in the jejunum, and 480 ± 47 µm in the ileum. Interestingly, several tops of villi in the jejunum are free of mucus (Atuma et al., 2001). In rats, the mucosal thickness in the large intestine is approximately 830 ± 110 µm, compared to an estimated range of 107-155 µm in humans, indicating an interspecies difference (Atuma et al., 2001; Pullan et al., 1994).

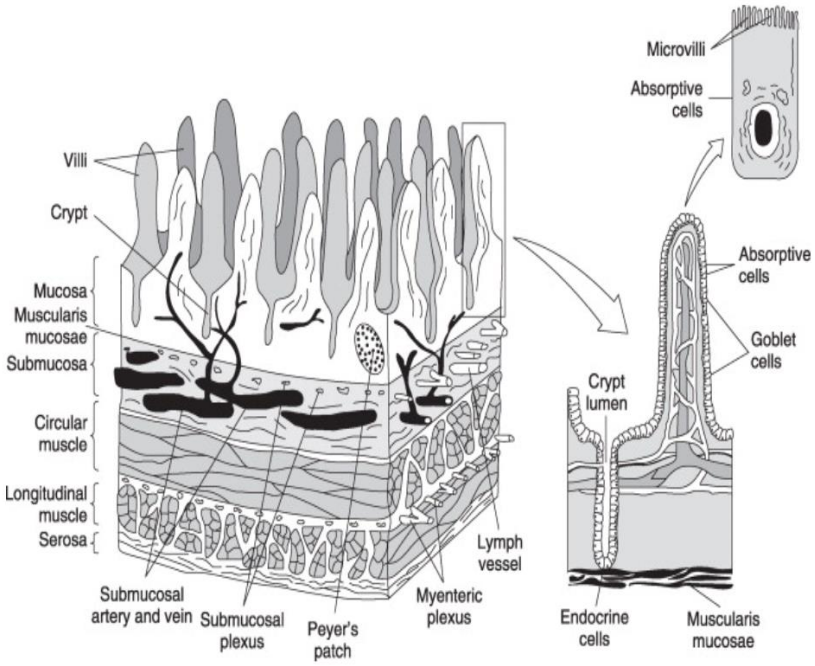

Figure 2: Schematic overview of the small intestinal wall (Rumsey, 2005).

2.1.2 Function

The overall function of the gastrointestinal tract is to digest food and absorb nutrients while maintaining immune homeostasis (Ahluwalia et al., 2017).

Food digestion starts in the mouth, where food is reduced in size by chewing, lubricated by salivary mucins and digested by salivary enzymes, such as amylase which breaks down starch. Lipases, aiding in lipid digestion have also been cited as an enzyme present in the saliva, although this is not unambiguous within literature (Barret et al., 2018; Neyraud et al., 2017; Pepino et al., 2012; Voigt et al., 2014). Besides being a digestive aid, saliva safeguards the mouth from bacterial overgrowth through the presence of immunoglobulin A and lysozymes (Barret et al., 2018). Furthermore, saliva is an alkaline and hypotonic solution attributed to the presence of K^+ and bicarbonate (HCO_3^-), which protects the esophagus from gastric acid in conditions of reflux. Peristaltic movements of the esophagus lead food to the stomach (Barret et al., 2018; Haschek et al., 2010).

In the stomach, food will be further macerated and digested. Serving as a reservoir, it retains food until signals such as the release of the hormone gastrin, gastric food volume, and feedback signals from the duodenum indicate optimal absorption and digestion rates (Day, 2019; Haschek et al., 2010; Soybel, 2005). The mucus layer acts in this part as a pH controller by secreting mucosal bicarbonate (Flemström & Kivilaakso, 1983). Protein breakdown is facilitated by the stomach acids and pepsin. Initially secreted as an inactive molecule, pepsinogen is activated by the low pH to prevent autodigestion (see 2.1.3) (Ramsay & Carr, 2011; Soybel, 2005).

The so-processed material, termed chyme, leaves the stomach and arrives in the small intestine. The most important function of the small intestine is the digestion and absorption of nutrients, including sugars, amino acids, and fatty acids from the lumen and the discharge of undigestible components such as fibers (see 2.1.1) (Day, 2019). In the small intestine, as well as the large intestine, the mucus protects the underlying epithelium from mechanical stress by lubricating the food to ensure smooth passage and forms the first barrier against microorganisms (Allen et al., 1993; Haschek et al., 2010).

The first part of the small intestine, the duodenum, receives the contents of the stomach, digestive juices of the pancreas, intestinal wall, and liver. Pancreatic juice consists of digestive enzymes such as amylases, proteases and lipases, water, and sodium bicarbonate ($NaHCO_3$) which neutralize the stomach contents. Furthermore, cells of the intestinal wall secrete digestive juice containing digestive enzymes, such as disaccharidases (e.g. maltase, isomaltase, sucrase), exopeptidases (aminopeptidase, dipeptidases), nucleosidases, and mucus (Fish & Burns, 2022; Guerra et al., 2012; Nightingale & Spiller, 2023; Richardson, 2006). Additionally, brush border enzymes (e.g. glycosidases, phosphatases, peptidases) at the surface of the microvilli further break down the components (Holmes & Lobley, 1989; Hooton et al., 2015). Bile acids, secreted by the liver, are released into the small intestine where it plays a crucial role in fat digestion and absorption (Barret et al., 2018; Fish & Burns, 2022; Richardson, 2006). In the duodenum, the presence of digestive enzymes ensures that the food is primarily chemically digested. Moreover, iron and some folate (vitamin B9) are also absorbed in this part of the small intestine (Fish & Burns, 2022; Richardson, 2006).

In contrast to the enzymatic digestion of the duodenum, the jejunum is mainly involved in mechanical digestion. Food turbulently moves back and forward, while being mixed with digestive juices (Fish & Burns, 2022). Furthermore, the jejunum absorbs folate (vitamin B9), sugars, amino acids, and fatty acids (Collins et al., 2017). The digestible carbohydrates are broken down into the monomers glucose, galactose, and fructose and are then actively absorbed in the case of glucose and galactose, while fructose is absorbed using facilitated diffusion (Wright et al., 2018). For example, starch is broken down into glucose and is absorbed in the small intestine for 80-98% of the intake (Stephen et al., 1983). In the ileum, vitamin B12, unabsorbed nutrients, and bile salts are absorbed, more specifically, 95% of the bile acids are actively absorbed in the small intestine (Collins et al., 2017; Di Ciaula et al., 2018; ZR, 1990).

The epithelium of the gastrointestinal tract is at the interphase between the host and the environment and needs to discriminate between beneficial and harmful environmental stimuli. This is accomplished by the gastrointestinal tract immune system, which is composed of a mucosal barrier and the gut-associated lymphoid tissue (GALT) consisting of scattered immune cells and organized lymphoid tissues (e.g., Peyer's patches in the small intestine) (Ahluwalia et al., 2017). The crypts of the small intestine also contain Paneth cells that release antimicrobial peptides and regulate the microbial composition by distinguishing between symbiotic microorganisms and pathogens (Collins et al., 2017; Garabedian et al., 1997). Finally, the immune system also has to differentiate between toxins and harmless food compounds (Profet, 1991).

Food components resistant to human enzymes such as fibers, some peptides, and resistant starch enter the large intestine *via* the ileocecal valve and will be fermented by the resident microbiota to extract additional energy (Grabitske & Slavin, 2008). Besides hosting bacteria, the large intestine is involved in the absorption and secretion of water, electrolytes, and digestive matter storage (Haschek et al., 2010). Alongside the food components in the lumen, the mucus layer in the colon is an important niche for mucus-degrading and attaching bacteria such as *Bacteroides thetaiotaomicron* and *Akkermansia muciniphila* (Lee et al., 2013).

2.1.3 Physicochemical environment

The physicochemical environment throughout the gastrointestinal tract varies to ensure optimal enzyme performance and digestion (Figure 3). The pH and oxygen levels and transit time are important physicochemical determinants (Guerra et al., 2012).

The mouth pH varies between 5 and 8 in fed and 6 and 7.4 in fasting conditions (Davidson et al., 1998; Guerra et al., 2012; Machen & Paradiso, 1987). The stomach has a pH ranging between 1 and 5 (Guerra et al., 2012). When food enters the stomach, the pH temporarily rises to approximately 5 before dropping to 1.5-2 due to the addition of hydrochloric acid (HCl) produced by the parietal cells (Barret et al., 2018; Malagelada et al., 1976). This drop in pH creates an optimal environment for the enzyme pepsin to digest proteins. The acidic contents of the food bolus are neutralized along the small intestine by intestinal juice, pancreatic juice, bile, and the secretion of bicarbonate by the mucosa. This results in a pH increase from pH 5.7 – 6.4 in the duodenum to pH 5.9 – 6.8 in the jejunum and pH 7.3-7.5 in the ileum (Aburub et al., 2018; Wilson, 2004). The colon maintains a pH between 5 and 7 (Guerra et al., 2012). The pH is influenced by the microbial fermentation (Topping & Clifton, 2001). For example, carbohydrate fermentation results in a pH decrease, which also explains the pH profile in the large intestine. As carbohydrates become depleted further along the colon, the pH increases, ranging from 5.4-5.9 in the ascending colon to about 6.2 in the transverse colon and 6.6-6.9 in the descending colon (Cummings & Macfarlane, 1992; Korpela, 2018).

Like the pH, oxygen concentrations also fluctuate throughout the gastrointestinal tract (Singhal & Shah, 2020). Freshly produced saliva has an oxygen pressure of 65 mmHg which is reduced to 35 mmHg after 30 to 60 seconds (Ali & Tanwir, 2012). The stomach has a partial oxygen pressure of 46.3 ± 15.44 mm Hg at the luminal surface of the mucosa. In the small intestine, the partial pressure is between 34 and 36 mm Hg (Wilson, 2004) and it decreases to 11 mmHg in the ascending and to 3 mmHg in the sigmoid colon in mice (He et al., 1999). Noteworthy, the oxygen concentration at the serosal side of the sigmoid colon in humans is 39 mmHg which is approximately ten times higher than the concentration found in the lumen in mice, indicating an oxygen gradient in the axial direction (He et al., 1999; Savage, 1978).

Another influential parameter differing between the segments of the gastrointestinal tract is the transit time. The upper gastrointestinal tract has a fast transit (mouth 10 seconds to 2 minutes, stomach 15 minutes to 3 hours, small intestine 2 to 5 hours), while the lower gastrointestinal tract has a slower transit (colon 12 up to 72 hours) facilitating more microbial growth (Guerra et al., 2012; Maurer & Krevsky, 1995).

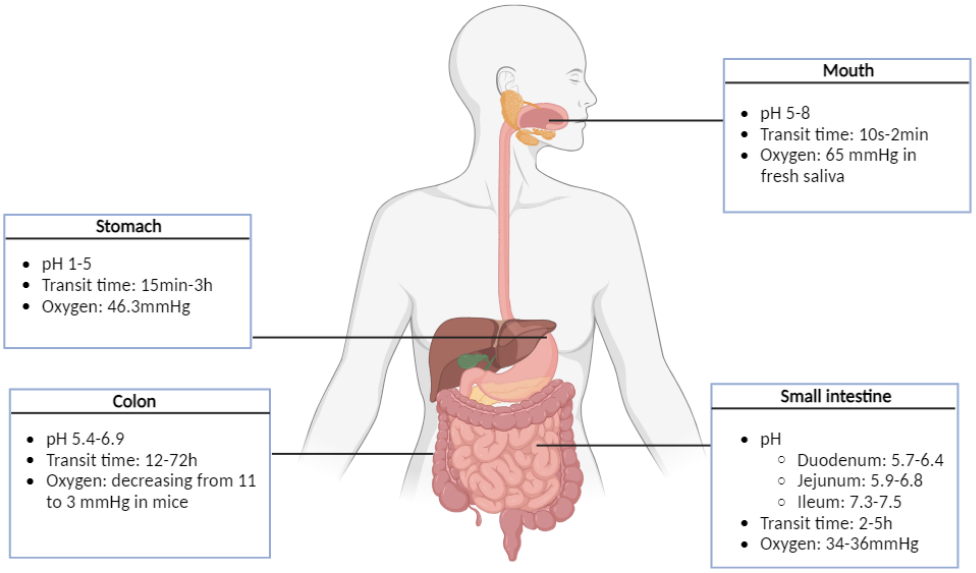

Figure 3: Overview of the different functions and environmental factors (pH, transit time, and secretions or enzymes) of the mouth, stomach, small intestine, and colon (made with BioRender.com) (Aburub et al., 2018; Ali & Tanwir, 2012; Cummings & Macfarlane, 1992; Davidson et al., 1998; Guerra et al., 2012; He et al., 1999; Korpela, 2018; Machen & Paradiso, 1987; Maurer & Krevsky, 1995; Singhal & Shah, 2020; Wilson, 2004).

The physicochemical environment along the gastrointestinal tract not only ensures optimal enzyme performance and digestion but also results in a stringent selection process for the microbes. Firstly, the small intestine is a highly dynamic region with a high risk for bacterial washout. Daily, nine liters of fluid passes through the small intestine, encompassing pancreatic juice (1.5L), saliva (1.5L), bile (0.5L), intestinal juices (1L), gastric juices (2.5L) and the daily liquid (2L) intake. Roughly 7.5L of this fluid is absorbed within the small intestine, with about 5.5L reabsorption in the jejunum and 2L in the ileum. Due to the short transit time in the small intestine, the bacteria have less time to double (Wilson, 2004). Additionally, the presence of proteolytic enzymes and the high concentration of bile salts further limit microbial proliferation (Barret et al., 2018; Wilson, 2004). As well, antimicrobial components such as secretory IgA and antimicrobial peptides from the aforementioned Paneth cells play a crucial role in maintaining a low microbial load (Pabst, 2012). The reduction of oxygen content and initiation of fermentative processes create reducing conditions in the ileum with a redox potential of around -150 mV: this also contributes to a stringent bacterial selection (see 2.1.3). At last, the low pH contributes to a selective environment (see 2.1.3) (Wilson, 2004). As a result, the specific small intestinal environment results in a controlled bacterial load. Yet, despite the harsh environment, the microbiota can grow on the multitude of nutrients, retrieved from the chyme, shed intestinal cells, mucins, and molecules made by other microbes (cross-feeding) (Wilson, 2004). Moreover, in the ileum, the abundance of microbiota increases due to slowed peristalsis, the neutral pH, and the decrease of bile acids due to absorption (Di Ciaula et al., 2018; Wilson, 2004).

2.1.4 Colonization of the gastrointestinal tract by micro-organisms

The gastrointestinal tract is characterized by the presence of a dense and diverse community of microorganisms, known as the microbiota. This community develops alongside the human immune system and plays a crucial role in human health and diseases such as irritable bowel syndrome and Crohn's disease (Chung et al., 2016; Hooper et al., 2012; Kaoutari et al., 2013; Martinez-Medina et al., 2006).

The bacterial phyla present throughout the gastrointestinal tract include Bacillota, Pseudomonata, Fusobacteria, Bacteroidota, and Actinomycetota. Additionally, Saccharibacteria are commonly found in the esophagus, duodenum, and ileum, while Spirochaetes are prevalent in the oral cavity (Ahn et al., 2011; Bik et al., 2006; Dlugosz et al., 2015; Leite et al., 2020; Pei et al., 2004; Verma et al., 2018; Villmones et al., 2018; Vuik et al., 2019).

The diversity on genera and species level is greater compared to phylum level. More inter-individual variability is observed on the genera/species level due to a higher diversity on these taxonomic levels. On this level, researchers try to determine a core microbiome, defined as the predominant species common within all individuals during health and at specific sites of the body. In contrast, the variable microbiome is unique for each individual and depends on the lifestyle, genotypic, and phenotypic determinants (Turnbaugh et al., 2007).

This inter-individual variation is caused by numerous factors, including host environment (e.g. genetic factors concerning immunity) (Benson et al., 2010) and initial colonization (Cavender-Bares et al., 2009). Despite this inter-individual variation, the functions and formed metabolites are highly conserved, which is the result of redundancy in the metabolome and genome of the gastrointestinal tract microbiota (Tap et al., 2009). Moreover, there is variation within an individual both in time and sampling location (intraindividual variation) (Delaroque et al., 2022). As mentioned in 2.1.3, various parameters like transit time, pH, and oxygen concentration vary longitudinally across the gastrointestinal tract, creating unique niches, with each a specific resident microbial community. This community is dynamic and is modulated by among others diet, age, and disease (Bresalier & Chapkin, 2020).

Conditions also vary in the axial direction, between the lumen and mucus (Sommer & Bäckhed, 2016). For example, due to diffusion of oxygen from the blood, the oxygen concentration is higher in the mucus than in the lumen. This is illustrated in the cecum where the underlying tissue contains 40 mmHg of oxygen, while the average oxygen concentration in the lumen is less than 1 mmHg (Albenberg et al., 2014). Moreover, mucus presents a nutrient source for bacteria such as *Bacteroides thetaiotaomicron* and *Akkermansia muciniphila* (Lee et al., 2013; Sheridan et al., 1990; Singhal & Shah, 2020). Mucus utilization is tightly linked with mucus attachment. *Bacteroides fragilis*, for instance, grows on mucus because it expresses commensal colonization factors (ccf). Deletion of the *ccf* gene leads to reduced mucosal association and interferes with colonization in the colonic crypts of mice (Lee et al., 2013). The conditions lead to a different community in the mucus and lumen, with the composition of luminal bacteria fluctuating throughout the day depending on the carbohydrate intake, while the mucosal microbiota are more stable (Johansson et al., 2011; Rogowski et al., 2015; Zoetendal et al., 2012).

2.1.4.1 *Mouth, esophagus, and stomach*

The mouth is colonized by a wide range of microbiota, with a bacterial load of 10^{8-9} bacterial cells/ml (Walter & Ley, 2011). The core microbiome constitutes of *Actinomyces, Atopobium, Corynebacterium, Rothia, Campylobacter, Cardiobacterium, Haemophilus, Neisseria, Granulicatella, Streptococcus, Veillonella, Bergeyella, Derxia, Leptotrichia, Capnocytophaga,* and *Prevotella.* Genera belonging to the variable microbiome include *Chryseobacterium, Filifactor, Anaeroglobus, Lactobacillus, Hohnsonella, Shuttleworthia, Brachymonas, Propiniovibrio, Olsenella, Scardovia, Cryptobacterium* (Bik et al., 2010; Chen & Jiang, 2014). The mouth accommodates several microbial niches such as the gingival sulcus, tongue, hard and soft palates, the cheek, the floor of the mouth, the throat, the teeth, and the saliva, each with its unique microbiome (Benn et al., 2018; Dewhirst et al., 2010). For instance, *Rothia* species are commonly found on the tongue or tooth surfaces, *Simonsiella* colonizes the hard palate, *Streptococcus salivarius* predominantly resides on the tongue, and *Treponemes* are generally restricted to the subgingival crevice (Aas et al., 2005; Kazor et al., 2003; Mager et al., 2003; Segata et al., 2012; Walter & Ley, 2011).

As food enters the body *via* the mouth, it is initially mixed with saliva and microorganisms. These microorganisms are transferred, after passage through the stomach, to the small intestine. Some strains such as *Streptococcus, Veillonella, Actinomyces, Haemophilus* are suggested to be regularly transmitted, while other species including *Prevotella* show indication of transmission on occasion or even no transmission at all. Moreover, profound inter-individual variability within the oral transmission was proposed (Dewhirst et al., 2010; Schmidt et al., 2019).

The community of the esophagus is similar to the community of the oral cavity. *Prevotella*, *Veillonella,* and *Streptococcus* are the most prevalent genera in the esophagus, with a dominance of *Streptococcus* (Pei et al., 2004).

The stomach is an extremely acidic environment with only 10^3 CFU/mL and is the least diverse of the gut segments (Berg, 1996; Stearns et al., 2011; Wilson, 2004). A commonly found species in the stomach is *Helicobacter pylori* (Tomb et al., 1997). In addition, genera such as *Streptococcus*, *Fusobacterium*, *Veillonella*, *Rothia*, *Neisseria*, *Haemophilus*, *Porphyromonas*, *Pasteurellaceae* and *Prevotella* have been detected in the stomach, with several of these genera also found in the oral cavity (Bik et al., 2006; Engstrand & Lindberg, 2013; Li et al., 2009).

2.1.4.2 Small intestine

The community of the small intestine is not yet fully unraveled due to the inaccessibility of this site. While samples can be obtained during gastroduodenoscopy and colonoscopy, these procedures present several challenges and limitations. Intraluminal naso-ileal catheters can aid in sample collection, yet this approach also presents some limitations. Patients typically need to fast before undergoing these procedures or require flushing before sampling. Furthermore, due to the invasiveness of the procedure, sampling of healthy individuals is unsuitable, and repeated sampling is hindered, complicating the study of dynamics (El Aidy et al., 2015; Kastl Jr et al., 2020; Rehan et al., 2024; Villmones, 2022).

Efforts to overcome these limitations have led to the development of swallowable capsules for small intestinal sampling, although further optimization is still needed. Besides the sampling of healthy participants, stoma bags of ileostomy subjects or colectomy patients can be sampled, allowing repeated sampling. Nevertheless, during the process of sampling, there is a risk of contamination of the skin, mouth, or colon (El Aidy et al., 2015; Kastl Jr et al., 2020; Rehan et al., 2024; Villmones, 2022).

Some sampling methods are more prone to contamination than others. For example, surgery and autopsy sampling can be executed in a more sterile manner, while endoscopy, enteroscopy, and biopsies require passage through other parts of the gastrointestinal tract, resulting in more contamination (Villmones, 2022). While surgery offers a more sterile approach, it is only feasible when necessary.

Besides the sampling method, variations in population and sample size also influence the obtained microbial composition. For example, several studies involve elderly (patients older than 65 years of age), for which it is already known that the colonic gut microbiome undergoes a shift (O'Toole & Jeffery, 2018), while studies on a small intestinal shift are still lacking. Therefore, extrapolating elderly data to healthy adults could introduce different genera. Furthermore, small-scale studies make it difficult to research inter-individual variability. To conclude, comparing the results of the different studies is difficult due to differences in study design.

Despite the different approaches to access and sample the small intestine *in situ,* different types of samples can be collected. During sampling, a biopsy to investigate the mucosal microbiota or an aspirate to research the luminal microbiota can be obtained, resulting in the exploration of a different community (Donaldson et al., 2016). The microbiota associated with the mucus within an individual are more conserved and less variable compared to the luminal microbiota (Li et al., 2015).

Besides the cross-sectional differences, also longitudinal differences appear. For instance, the community of the small intestine is much more dynamic than the microbial community of the other organs in the gastrointestinal tract, and a lower microbial load (duodenum 10^{3-4} cells/ml, jejunum 10^{4-5} cells/ml, ileum 10^8 cells/mL) compared to the large intestine (10^{11-12} cells/mL) due to the harsh conditions and short transit time (2.1.3) (Hayashi et al., 2005; Walter & Ley, 2011; Wilson, 2004). The different conditions in the three subparts of the small intestine result in different communities for the duodenum, jejunum, and ileum.

Duodenum

In the duodenum, *Streptococcus* and *Prevotella* are frequently observed in both the mucus and the lumen (Table 1) (Li et al., 2015; Nagasue et al., 2022; Seekatz et al., 2019). In particular, it is hypothesized that *Streptococcus* species are favored for their capacity to regulate intracellular pH in the fluctuating pH environment (Seekatz et al., 2019).

Other genera detected in the lumen include *Acinetobacter, Bacteroides, Veillonella, Gemella*, and *Pasteurellaceae*, while in the mucus *Haemophilus, Actinomyces, Gemella, Neisseria, Fusobacterium, Pseudomonas, Veillonella* and *Stenotrophomonas* were discerned, although not consistently across all studies. Differences between the studies could exist in terms of inter-individual variability or sampling method and could explain some of the inconsistencies (Li et al., 2015; Nagasue et al., 2022; Seekatz et al., 2019; Vasapolli et al., 2019).

Jejunum

The jejunal microbiota are more stable than the microbiota in the duodenum and stomach (Seekatz et al., 2019). In the jejunum, *Streptococcus* and *Veillonella* are regularly present in both mucus and lumen, while *Fusobacterium* is detected in both studies investigating the lumen and has also been identified in the mucus (Table 1). Additional genera that can colonize the mucus, include *Prevotella, Rothia, Actinobacillus, Escherichia, Haemophilus, Bacillus, Lactobacillus, Bacteroides, Cytophaga,* while in the lumen *Gemella, Pasteurellaceae, Enterobacteriaceae, Prevotella, Fusobacterium, Escherichia, Klebsiella,* and *Citrobacter* have been detected (Table 1). (Dlugosz et al., 2015; Hayashi et al., 2005; Nagasue et al., 2022; Seekatz et al., 2019; Sundin et al., 2017; Vuik et al., 2019; Wang et al., 2005). Genera like *Clostridium* and *Escherichia* are suggested to be subject-specific (Booijink et al., 2010; van den Bogert, 2013). Yet, the jejunal microbiota are still limited studied, making it difficult to differentiate between contamination and inter-individual variability.

Ileum

Ileostomy effluent is an easy way to sample the ileal lumen and is therefore commonly used. However, Zoetendal et al. (2012) showed that the composition is more comparable with the jejunal composition than the ileal composition. Yet, this was based on one individual. Therefore, the findings of the studies using ileal effluent are classified as proximal ileum samples (Table 1). Limited studies have investigated the bacterial composition of the ileum. In fact, only two studies have examined the lumen bacterial community of the proximal ileum. Both studies reported the presence of *Streptococcus, Veillonella,* and *Enterococcus,* while *Bacteroides, Lactobacillus,* and *Clostridium* cluster I were detected by only one of these studies (Table 1) (Li et al., 2015; Seekatz et al., 2019). Moreover, fluctuations were shown in the microbial composition depending on the carbohydrate intake. Notable, the fluctuations within one day were greater than over different days (Booijink et al., 2010; Van den Bogert et al., 2013; Zoetendal et al., 2012), illustrating the influence of diet. Furthermore, only one study has explored the mucus of the proximal ileum, identifying the presence of *Streptococcus, Bacteroides, Veillonella, Escherichia, Haemophilus,* and *Faecalibacterium* (Nagasue et al., 2022).

The lumen of the distal ileum has been investigated in only one study involving three elderly individuals. This study detected the presence of *Streptococcus, Lactobacillus, Enterococcus, Bacteroides,* and γ-*Pseudomonadota* (Hayashi et al., 2005). In contrast, the mucosa of the distal ileum is more widely explored, though still minimal. *Streptococcus* is the only genus consistently found across all mucosal studies. Additionally, genera such as *Clostridium* cluster XIVa and XI, *Bacteroides*, *Escherichia* or *Shigella, Faecalibacterium* have been detected in two separate studies, while *Clostridium* cluster IX and XIVb, *Blautia, Ruminococcus, Suterella, Fusobacterium, Verrucomicrobia, Actinomyces, Gemella, Granulicatella, Rothia, Atopobium, Lachnoanaerobaculum, Oribacterium, TM7, Solobacterium, Candida, Lactobacillus, Veillonella,* and *Haemophilus* are detected in only one of the conducted studies (Table 1) (Hayashi et al., 2005; Nagasue et al., 2022; Vasapolli et al., 2019; Villmones et al., 2021; Villmones et al., 2018; Wang et al., 2005).

Table 1: Genera found in the mucus and lumen of the duodenum, jejunum, and ileum. 1: (Li et al., 2015) 2: (Nagasue et al., 2022), 3: (Vasapolli et al., 2019), 4: (Seekatz et al., 2019), 5: (Dlugosz et al., 2015), 6:(Wang et al., 2005), 7: (Sundin et al., 2017), 8: (Villmones et al., 2018), 9: (Villmones et al., 2021), 10: (Hayashi et al., 2005), 11: (Booijink et al., 2010), 12 : (Van den Bogert et al., 2013)

	Mucus	Lumen
Duodenum	*Streptococcus* (1, 2, 3)	*Streptococcus* (1, 4)
	Haemophilus (2)	*Acinetobacter* (1)
	Actinomyces (2,3)	*Bacteroides* (1)
	Stenotrophomonas (1)	*Prevotella* (1, 4)

	Prevotella (1, 2, 3) *Veillonella* (3) *Gemella* (3) *Neisseria* (3) *Fusobacterium* (3) *Pseudomonas* (3)	*Veillonella* (4) *Gemella* (4) *Pasteurellaceae* (4)
Jejunum	*Streptococcus* (5, 6) *Veillonella* (5) *Prevotella* (5) *Rothia* (5) *Actinobacillus* (5) *Escherichia* (5) *Fusobacterium* (5, 6) *Haemophilus* (5) *Bacillus* (6) *Lactobacillus* (6) *Clostridium* cluster XI (6) *Clostridium* cluster IX (6) *Bacteroides* (6) *Cytophaga* (6)	*Streptococcus* (4, 7) *Veillonella* (4, 7) *Gemella* (4) *Pasteurellaceae* (4) *Enterobacteriaceae* (4) *Prevotella* (7) *Fusobacterium* (7) *Escherichia* (7) *Klebsiella* (7) *Citrobacter* (7)
Proximal ileum	*Streptococcus* (2) *Veillonella* (2) *Bacteroides* (2) *Escherichia* (2) *Haemophilus* (2) *Fecalibacterium* (2)	*Streptococcus* (11, 12) *Veillonella* (11, 12) *Clostridium* cluster I (11) *Lactobacillus* (12) *Enterococcus* (11, 12) *Bacteroides* (12)
Distal ileum	*Streptococcus* (2, 6, 8, 9) *Clostridium* cluster XIVa (6, 10) *Clostridium* cluster IX (6) *Clostridium* cluster XI (3, 6) *Clostridium* cluster XIVb (6) *Blautia* (3) *Ruminococcus* (3) *Sutterella* (3) β- *Pseudomonata* (6) γ- *Pseudomonata* (6) *Fusobacterium* (6) *Verrucomicrobia* (6) *Actinomyces* (8) *Gemella* (8) *Granulicatella* (8) *Rothia* (8, 9) *Atopobium* (8) *Lachoanaerobaculum* (8)	*Streptococcus* (10) *Lactobacillus* (10) *Enterococcus* (10) *Bacteroides* (10) γ- *Pseudomonata* (10)

	Oribacterium (8) *TM7* (8) *Solobacterium* (8) *Candida* (9) *Lactobacillus* (9) *Bacteroides* (2, 3) *Veillonella* (2) *Escherichia* or *Shigella* (2, 3) *Haemophilus* (2) *Faecalibacterium* (2, 3)

2.1.4.3 *Large intestine*

The bacterial abundance peaks in the colon. Revisited calculations of the bacteria in the colon indicated that 10^{11} to 10^{12} microbial cells/mL are present (Sender et al., 2016). To investigate colonic microbiota, most studies use fecal samples, which are easier and less invasive to collect compared to other sampling strategies. For example, longitudinal studies such as lifeline deep use fecal samples (Scholtens et al., 2015). Investigation of this cohort resulted in the identification of nine core species (defined as species present in 95% of the individuals): *Subdoligranulums p., Alistipes onderdonkii, Alistipes shahii, Alistipes putredinis, Bacteroides uniformis, Eubacterium rectale, Bacteroides vulgatus, Oscillibacter sp.,* and *Faecalibacterium prausnitzii* (Gacesa et al., 2022). Furthermore, by combining different cohorts and global datasets, 14 core genera (genera present in more than 95% of the samples) were identified, namely *Lachnospiraceae, Ruminococcaceae, Bacteroides, Faecalibacterium, Blautia, Roseburia, Erysipelotrichaceae, Coprococcus, Dorea, Clostridiaceae, Hyphomicrobiaceae, Clostridiales, Veillonellaceae,* and *Clostrium* cluster XIVa (Falony et al., 2016). Although stool is easy to sample, it is not fully representative for the gut microbiome. Lately, studies focusing on aspirates, rather than stool samples, manifest. This way of sampling is more representative but is prone to contamination. In the colon *Bacteroides, Caulobacter, Escherichia, Shigella, Parabacteroides, Phenylobacterium, Prevotella, Ruminococcus,* and *Streptococcus* in addition to unclassified genera and other bacteria were identified (Kwon et al., 2021). In the mucus of the colon, genera such as *Butyricicoccus, Ruminococcus, Faecalibacterium and Roseburia* can be found (Nava & Stappenbeck, 2011).

2.1.5 Microbial metabolism

The human genome in itself does not contain the appropriate or sufficient number of genes to perform all necessary digestive processes to break down dietary constituents in the gut. However, the colonization of microbes in the gut indirectly provides humans with a diverse set of functions that lie encoded within the set of microbial genomes, termed the microbiome (Qin et al., 2010). Notably, in the context of food digestion, microbial assets such as carbohydrate-active enzymes (CAZymes) are crucial for breaking down human-indigestible polysaccharides or dietary fiber (Bergman, 1990; Kaoutari et al., 2013).

Through CAZymes and other enzymes, bacteria metabolize nutrients in the gastrointestinal tract, generating metabolites that can be utilized by other bacteria in a process known as cross-feeding, ultimately resulting in the production of metabolites such as organic acids. Bacteria can thrive on carbohydrates, proteins, or lipids (Germerodt et al., 2016). The microbial metabolism concerning each of these three macromolecules will be investigated.

2.1.5.1 Carbohydrate

Mouth bacteria such as *Streptococcus, Actinomyces,* and *Lactobacillus* can ferment carbohydrates from food or salivary mucins covering the oral mucosa. Carbohydrates or sugar alcohols are transported into the bacterial cell and converted into lactate, acetate, ethanol, and formate, among others through various pathways (e.g. glycolysis, Embden-Meyerhof-Parnas pathway) (Takahashi, 2015).

Although the esophagus is often overlooked, it also contains a microbiome that can react to food composition. For example, dietary fiber is associated with a distinct esophageal microbiome with an increase in several Gram-negative bacteria, including *Neisseria, Prevotella,* and *Eikenella* (Nobel et al., 2018).

While the stomach has extensively been investigated for the digestion of food, any microbial process in this part of the gastro-intestinal tract has not yet been elucidated.

As chyme enters the small intestine, pancreatic enzymes will break down the food components down to simple carbohydrates, such as glucose, fructose, mannose, raffinose, L-arabinose, and trehalose, which can be either absorbed by the enterocytes or used by the small intestinal microbiota to produce various metabolites. While absorption at the beginning of the enterocyte involves both human metabolized products and bacterial metabolites, it is hypothesized that the carbohydrate compounds absorbed in the ileum are likely to emanate from bacterial fermentation (Neis et al., 2015; Zoetendal et al., 2012).

Limited information is available about bacterial fermentation in the small intestine. However, the metabolism of commonly identified genera in the small intestine is known. For example, lactic acid bacteria are known for their lactic acid ($C_3H_6O_3$) producing metabolism. Among these, several genera have been located in the small intestine such as *Enterococcus, Lactobacillus,* and *Streptococcus* (König & Fröhlich, 2017). In particular, several *Streptococcus* species have already been identified in the small intestine and described as able to metabolize sugars (e.g. trehalose, raffinose, and L-arabinose) into lactic acid, further metabolized by *Veillonella* species to produce acetic acid (CH_3COOH) and propionic acid ($C_3H_6O_2$) (El Aidy et al., 2015). As well, *Bifidobacteria* are also capable of producing lactic acid as an end-metabolite (König & Fröhlich, 2017). Furthermore, *Escherichia coli* can transform simple sugars into acetate, whereas members of the *Clostridium* cluster XIVa metabolize lactate and acetate into butyrate ($C_4H_8O_2$). Short-chain fatty acids (SCFA) (e.g. acetate and propionate) and organic acids (e.g. lactate, succinate) are also described as metabolization products of the genus *Bacteroides*, with some differences depending on the generation time, incubation period, and fermentable substrates (Kotarski & Salyers, 1981; Rios-Covian et al., 2013; Rios-Covian et al., 2016; Rios-Covian et al., 2015). Similarly, the genus *Prevotella* can produce acetate and succinate even though it is only moderately saccharolytic (Shah et al., 2009).

SCFA, including propionate, acetate, and butyrate are known for their beneficial effect on the host. For example, butyrate is known to decrease inflammation in the small intestine (Wächtershäuser & Stein, 2000). Besides the three most important SCFA, formate (CH_2O_2), valerate ($C_5H_9O_2^-$), and caproate ($CH_3(CH_2)_4COOCH_3$), amongst others are also produced by the small intestinal microbiota (Lim et al., 2005; Zoetendal et al., 2012).

Yet, despite the beneficial effects of the microbiota, resident microbes and host cells compete with each other for nutrients. Therefore, the microbiota require efficient transport systems (e.g. phosphotransferase system), fermentative pathways (e.g. lactate and propionate), and downstream conversion pathways (e.g. pentose phosphate pathways, glycolysis). These systems were more abundant in *Streptococcus* sp. than in *E. coli* and other microbiota, suggesting that the former are well adapted to compete with the host (Zoetendal et al., 2012). Furthermore, the mucosa ileal microbiota show the potential to catabolize complex and diversified plant cell wall polysaccharides from dietary fibers (Patrascu et al., 2017), resistant to the host's metabolization.

While simple carbohydrates are food for the small intestinal microbiota, dietary fiber will act as a nutrient source for the colonic bacteria. Fiber reaching the colon is hydrolyzed by extracellular enzymes of carbohydrate fermenters (e.g. Bacteriodetes, Bacillota, Actinomycetota) to obtain simpler structures and eventually pyruvate or propionate. Pyruvate is taken up by the bacteria and converted to intermediate organic acids such as lactate, formate, acetyl-CoA, and succinate. These are further converted to primarily acetate, propionate, and butyrate by various pathways such as the oxidative decarboxylation of pyruvate in the case of acetate, succinate pathway for propionate formation, and acetyl-coenzyme A pathway for butyrate production (Payling et al., 2020). Of the total polysaccharides reaching the colon, 70-80% w/w are fermented to produce organic acids, primarily in the proximal colon (Macfarlane, Gibson, & Cummings, 1992; Schneeman, 1987).

2.1.5.2 Protein

SCFA in the mouth can also be synthesized through protein fermentation in which proteins and peptides are first broken down through proteases and peptidases after which the amino acids are transaminated. This is accomplished by primary proteolytic bacteria in the oral cavity, including *Actinomyces, Veillonella,* and *Fusobacterium* (Takahashi, 2015).

While in the esaphagus and stomach protein fermentation is not described, in the small intestinal several bacteria metabolize proteins. For example, proteins can be metabolized by bacteria such as *Klebsiella* spp., *Streptococcus* spp., *Escherichia coli, Succinivibrio dextrinosolvens, Anaerovirbio lipolytica,* and *Mitsuokella* spp. (Fan et al., 2017), with the production of metabolites such as SCFA, biogenic amines, and gasses (Neis et al., 2015). In fact, Proteins are suggested to be essential to maintain the ileal bacterial richness, as demonstrated in pigs where protein levels affected the relative abundance of bacteria, with *Clostridium_sensu_stricto_1* decreasing and *Escherichia-Shigella* increasing when the pigs were fed with a protein poor diet containing the same caloric content as the normal protein diet (Fan et al., 2017). However, while proteins seem to be crucial, their availability to the small intestinal microbiota is limited due to competition with the host. Consequently, resident bacteria developed very efficient amino acid metabolism, potentially stimulating *de novo* synthesis of amino acids (Wu, 1998; Zoetendal et al., 2012). Furthermore, metabolites, formed during protein fermentation, differ depending on the amount of protein intake, with a decrease in SCFA and biogenic amines when reducing the intake (Fan et al., 2017).

Although protein fermentation is described in the small intestine, most of the protein fermentation happens in the distal colon, where carbohydrate availability is low, resulting in the production of SCFA, branched-chain fatty acids, biogenic amines, and gasses (Blachier et al., 2007; Macfarlane, Gibson, & Cummings, 1992). Besides the catabolic pathways, *de novo* synthesis of amino acids takes place, which can be used by the host to incorporate into tissue (Neis et al., 2015).

2.1.5.3 Microbial metabolites

Both the microbial protein and carbohydrate fermentation result in short-chain fatty acid production (SCFA). In the oral cavity, concentrations of SCFA are 6.3-16.2 mM for acetate, 1.2-3.1 mM for propionate, 0.0-0.04 mM for butyrate, 2.3-6.3 mM for lactate, 0.0-1.5 mM for succinate, 10.3-17.9 mM for formate (HCO_2), and 0.0-0.9 mM for isovalerate (Lu et al., 2014).

In the small intestine, the concentration of the organic acids in the small intestine has only been investigated by limited studies (Cummings et al., 1987; Zoetendal et al., 2012), with no data yet existing concerning the duodenum. In the jejunum, only acetate and lactate are described, while in the ileum a more diverse panel of organic acids has been detected (Table 2) (Zoetendal et al., 2012). Yet, these concentration varies based on the study population and type of samples. For example, In sudden death victims, SCFA concentrations of 13 ± 6 mmol/kg were found in the ileum (Cummings et al., 1987), while in ileostomy patients a concentration between 51.9 and 119 mM (Zoetendal et al., 2012).

Table 2: Organic acid composition detected in sudden death victims (mmol/kg) or ileostomy (mM) effluent in the different compartments of the small intestine (Cummings et al., 1987; Zoetendal et al., 2012). N.d. = no data

		Sudden death victims		Ileostomy effluent
Organic acid	**Duodenum**	**Jejunum**	**Ileum**	**Ileum**
Acetate	n.d.	0.6 ± 0.6 mmol/kg	7.9 ± 4.1 mmol/kg	53.8-41.7 mM
Propionate	n.d.	0 mmol/kg	1.5 ± 1.0 mmol/kg	2.7-3.9 mM
Isobutyrate	n.d.	0 mmol/kg	0.3 ± 0.2 mmol/kg	n.d.
Butyrate	n.d.	0 mmol/kg	2.3 ± 1.3 mmol/kg	17.5-6.3 mM
Isovalerate	n.d.	0 mmol/kg	0.1 ± 0.1 mmol/kg	n.d.
Valerate	n.d.	0 mmol/kg	0.2 ± 0.1 mmol/kg	n.d.
Isocaproate	n.d.	0 mmol/kg	0.1 ± 0.1 mmol/kg	n.d.
Caproate	n.d.	0 mmol/kg	0. ± 0.2 mmol/kg	n.d.
Lactate	n.d.	2.0 ± 1.2 mmol/kg	13.5 ± 5.5 mmol/kg	11 – 11.6 mM

Formate	n.d.	n.d.	n.d.	26-7.8 mM

The total concentration of SCFA in the proximal colon is 70-140 mM and 20-70 mM in the distal colon (Topping & Clifton, 2001). Typically, acetate, propionate, and butyrate are found in the feces in a molar ratio of 60:25:15 (Barret et al., 2018), while branched-chain fatty acid concentration in the proximal colon is on average 4.6 mmol/kg and 6.3 mmol/kg in the distal colon (Macfarlane, Gibson, Beatty, et al., 1992).

2.1.5.4 Lipid

Lipid digestion primarily happens in the small intestine through bile salt emulsification, facilitating solubilization and absorption (El Aidy et al., 2015). Primary bile acids, synthesized in the liver, are reabsorbed for 95% in the ileum and recirculate to the liver, a process known as enterohepatic circulation (ZR, 1990). However, a portion of the bile acids can undergo microbial conversion, namely (i) hydrolysis, which results in deconjugation of the amino acid side chain, (ii) 7α/β-dehydroxylation, which converts primary bile acids into secondary bile acids, and (iii) oxidation or epimerization of hydroxy groups which generates isobile salts. This happens partly in the ileum where deconjugation and oxidation of the hydroxy group takes place (Begley et al., 2005; ZR, 1990), but also in the colon, where the bile acids can be further modified. Subsequently, these modified bile acids can eventually be recirculated to the liver or excreted from the body. Notably, bile salts have antimicrobial properties, particularly the unconjugated form of bile acids (Begley et al., 2005; Tian et al., 2020). Moreover, the secondary bile acids produced by bacterial metabolism mediate microbial-host communication by activating host nuclear receptors such as FXR (Farnesoid-X-receptor), which control several metabolic pathways (Claudel et al., 2005; Hylemon et al., 2009).

2.2 Modeling the small intestinal microbiota *in vitro*

As mentioned, the community of the small intestine is less characterized than the community of the large intestine partly due to the relative inaccessibility of the small intestine compared to the large intestine (Kastl Jr et al., 2020). Several studies made use of animal models such as rats or mice. Nevertheless, these differ in anatomy and microbial community from humans (Kastl Jr et al., 2020; von Martels et al., 2017) hence limiting the translatability to human physiology. To overcome this problem, *in vitro* models can be employed.

Compared to *in vivo* approaches, *in vitro* models have fewer ethical restraints and limitations. More importantly, *In vitro* models enable to work in a controlled and reproducible environment, hence reducing confounding factors, more frequent sampling and thus allowing mechanistic and time-resolved analysis. Therefore, to better describe the small intestinal ecology, a physiological-relevant *in vitro* model for the small intestinal microbiota is crucial (Kastl Jr et al., 2020; von Martels et al., 2017).

Several small intestinal microbiota models exist ranging from simple batch fermentation models to more complex continuous models based on the TNO gastric and small Intestinal Model (TIM-1), The Smallest Intestine *in vitro* model (TSI), the Simulator of the Human Intestinal Microbial Ecosystem (SHIME) and mucosal-SHIME (M-SHIME) (Cieplak et al., 2018; Deyaert et al., 2023; Minekus et al., 1995; Roussel et al., 2020; Stolaki et al., 2019; Williams et al., 2015).

In the process of designing a model, there are several important considerations to take into account. Firstly, a gastrointestinal tract model can be (i) static, so keeping the physicochemical parameters constant, or (ii) dynamic, hence changing parameters during the experiment. A second important aspect is the number of compartments. A batch fermentation model typically consists of one compartment. In contrast, the TIM and SHIME are multicompartment models, allowing the simulation of different sections or the gastrointestinal tract or replicates. In fact, in each compartment, parameters, such as pH, retention time, medium, and/or microbial inoculation, must be considered and can be set based on physiological features (Dixit et al., 2023).

2.2.1 Batch fermentation models

Batch fermentation models consist of one vessel, which can simulate any part of the gastrointestinal tract. These models are usually run for a short period (up to 72h) due to nutrient depletion and growth inhibition caused by metabolite accumulation (Williams et al., 2015). They are commonly used to assess the effect of a product on the diversity and physiology of the microbiota, inter-individual variability, different doses of a certain bioactive, and to discover underlying pathways (Thuenemann et al., 2015). Since this model is only suitable for short incubations and is less physiologically relevant than continuous models, no further focus will be placed on this type of model.

2.2.2 Continuous and semi-continuous models

Continuous models offer a more representative environment compared to batch fermentation models. Moreover, these models allow a deeper study of the gut microbiota and their effect on, for example, certain food compounds (Venema & Van den Abbeele, 2013). In the following part, several small intestinal continuous models will be discussed with their obtained results e.g. bacterial composition and organic acid composition.

2.2.2.1 *In vitro* model based on TIM-1

The TIM-1 is a dynamic *in vitro* model that mimics the stomach, duodenum, jejunum, and ileum. This model simulates peristaltic movement, in contrast to the Smallest Intestinal *in vitro* model and the Simulator of the Human Intestinal Microbial Ecosystem discussed below (see 2.2.2.2 and 2.2.2.3) (Guzman-Rodriguez et al., 2018). To simulate peristalsis, each compartment is composed of a flexible inner wall and an outer wall separated by water. The flexible inner wall of the vessels can be squeezed and relaxed with 3 cycles per minute in the stomach and 6 cycles per minute in the small intestine parts. In addition, both the stomach and the small intestinal compartments are squeezed together 6 times per minute. Masticated food mixed with saliva enters the stomach. The model receives 0.25 ml/min pancreatic juice, 0.5 ml/min biliary, and 0.5 ml/min gastric secretions. The jejunum and ileum are connected to a membrane (pore size 10 kDa) allowing for dialysis of water-soluble molecules, while lipophilic products are removed through a 50 nm filter. Temperature, pH, and volume in the system are controlled. However, The current system is not inoculated with microbiota and is then only employed to simulate the digestion of nutrients in the lumen of the gastrointestinal tract (Minekus et al., 1995; Thuenemann, 2015).

Based on the TIM-1 system, Stolaki et al. (2019) developed a dynamic *in vitro* model that simulates the ileal microbiota (Figure 4). This model consists of two reactors with flexible walls designed to replicate the conditions in the ileum. By mimicking the peristaltic movement of the ileum, the contents of the vessels are mixed. Furthermore, growth medium is added (0.5 mL/min) and an overflow mechanism is kept in place to maintain a consistent volume of 100 mL throughout the simulation. The pH is controlled at 7.2 and a dialysis system with pore size of 10 kDa is included in the model to prevent the accumulation of microbial products and to maintain appropriate concentrations of metabolites such as glucose and bile acids. The amount of filtration was checked using glucose and bile acids as markers, obtaining 96% filtration of the initial glucose and a concentration of bile acids between 5 and 15 mM in the duodenum, 10 mM in the jejunum, and 2-4 mM in the ileum, in line with literature data (Minekus et al., 1995). To keep an anaerobic environment, the system is flushed with N_2. Additionally, to recapitulate the *in vivo* transit of 3-4h (Davis et al., 1986), a liquid flow rate of 0.5 ml/min is set and results in a residence time of 3.5h (Stolaki et al., 2019).

Lastly, to include representative small intestine microbiota, ileostomy and feces were tested as inoculum for the system. Although the composition of the *in vitro* system is very similar to the *in vivo* situation, some differences occurred, with an increase in Pseudomonadota, Actinomycetota, and Bacteroidota and a decrease in Bacilli, Clostridium clusters IV and XIVa. Both ileostomy and fecal inoculation ensured compositional stability after approximately 10 days. The stable community of both inoculation methods was dominated by Pseudomonadota, Bacilli, Clostridium cluster XIVa, Bacteroidota, and Actinomycetota. In contrast, functional stability was only reached for the fecal inoculum, while not achieved using an ileostomy inoculum. The stable microbiota originating from the feces after 7 days, resulted in the production of 15.3±0.5 mM acetate, 5.3±0.2 mM propionate, and 1.9±0.1 mM butyrate, along with 0.5±0.1 mM lactate (Stolaki et al., 2019). The

ileostomy inoculum did not result in functional stability for SCFA concentrations, with after 14 days, 15.9±0.2 mM acetate, 8.2±1.6 mM propionate, and 2.0±0.2 mM butyrate were produced. In contrast, stable concentrations of 5.4±0.9 mM lactate were obtained throughout the entire run (Stolaki et al., 2019).

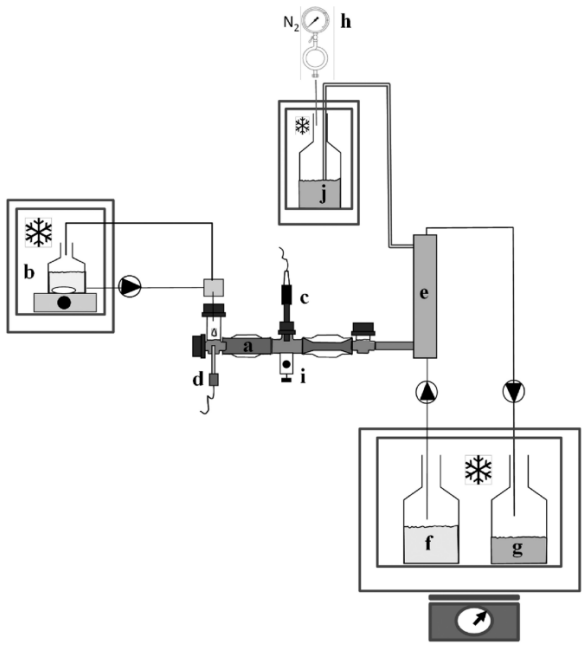

Figure 4: The adapted TIM-1 model (a) with medium in a cooling chamber (b) (7 °C), a pH meter (c) and pH-dependent NaOH dosage (d), a hollow fiber membrane (e) and nitrogen supply (h) can be sampled through sampling port (i), Efflux is collected in a bottle (j). Dialysis fluid (f) and a flask for metabolites and digestion products (g) are placed in a cooling chamber (7°C) on a weighing scale (Stolaki et al., 2019).

2.2.2.2 The Smallest Intestine *in vitro* model

The Smallest Intestine *in vitro* model (TSI) consists of five pH-controlled vessels in a PVC composite climate box, each with a working volume of 12 ml consecutively mimicking the duodenum, jejunum, and ileum in the same vessel at 37 °C (Figure 5) (Cieplak et al., 2018). Stirrers are added to the reactors to ensure the mixing of the food bolus. In addition, the oxygen level in the PVC chambers is controlled by flushing with N_2 (Cieplak et al., 2018). A pH is maintained within the vessels of 6.5-6.8 for the duodenum, 6.8-7.2 for the jejunum, and 7.2 for the ileum (Cieplak et al., 2018).

In the duodenal phase, feed, water, pancreatic juice, and bile salts are introduced. During the jejunal phase, absorption of nutrients and bile salts is simulated by transfer through a dialysis cassette with a pore size of 10 kDa. However, just like the dialysis unit of TIM-1, this cassette only simulates passive absorption. In contrast, *in vivo,* some molecules are better absorbed than others due to specific transporters (Cragg et al., 2005; Suzuki & Sugiyama, 2000).

TSI is inoculated in the ileal phase with a consortium of 7 strains: *E. coli* DSM 1058, *Streptococcus salivarius* DSM 20560, *Streptococcus luteinensis* DSM 15350, *Enterococcus fecalis* DSM 20478, *Bacteroides fragilis* DSM 2151, *Veillonella parvula* DSM 2008 and *Flavonifractor plautii* DSM 6740. By using a defined community, the model can be standardized (Cieplak et al., 2018). This model mainly focusses on the behavior of bioactive compounds and probiotics throughout the small intestine, while less attention is placed on microbial behavior. Yet, the five vessels could enable biological replicates for up to five individuals in parallel to capture the inter-individual variability.

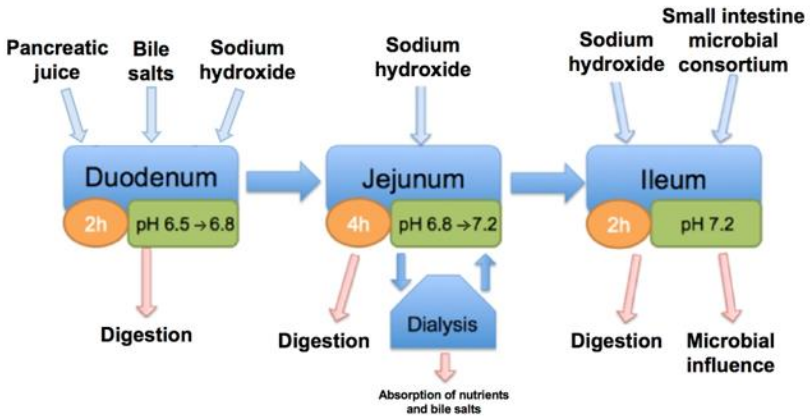

Figure 5: Schematic overview of the Smallest Intestine in vitro model (Cieplak et al., 2018).

2.2.2.3 The Simulator of the Human Intestinal Microbial Ecosystem

The Simulator of the Human Intestinal Microbial Ecosystem (SHIME) is a dynamic model simulating the human gut (Figure 6). The set-up can depend on the research question but classically consists of 5 vessels simulating specific sections of the gastrointestinal tract, including the stomach, small intestine, ascending colon, transverse colon, and descending colon, maintained at 37°C. Each colon vessel has a controlled pH between 5.6 and 5.9 for the ascending colon, 6.15 and 6.4 for the transverse colon, and 6.6 and 6.9 for the descending colon, while a residence time of 20h is maintained for the ascending colon, 32h for the transverse colon, and 24h for the descending colon and a volume of 500mL for the ascending colon, 800mL for the transverse colon, and 600mL for the descending colon. The environment inside the fermentation vessels is kept anaerobic by flushing the headspace with N_2 (Van den Abbeele et al., 2010).

The liquid in the compartment-, feed-, and pancreatic juice vessels are transferred through peristaltic pumps. Three times a day, 140mL of SHIME feed is introduced into the stomach, while 60mL of pancreatic juice, containing bile salts and pancreatin is pumped into the small intestinal vessel (Van den Abbeele et al., 2010).

The colon vessels are inoculated with a fresh fecal sample to introduce the microbiota, maintaining the inter-individual variability (Van den Abbeele et al., 2013). As such, this model can simulate the gastrointestinal tract and, after a stabilization period of around two weeks (Molly et al., 1993), can be maintained for a long period.

This model does not include a dialysis membrane to ensure physiological concentrations of metabolites, yet it has a medium deprived of nutrients normally absorbed in the small intestine.

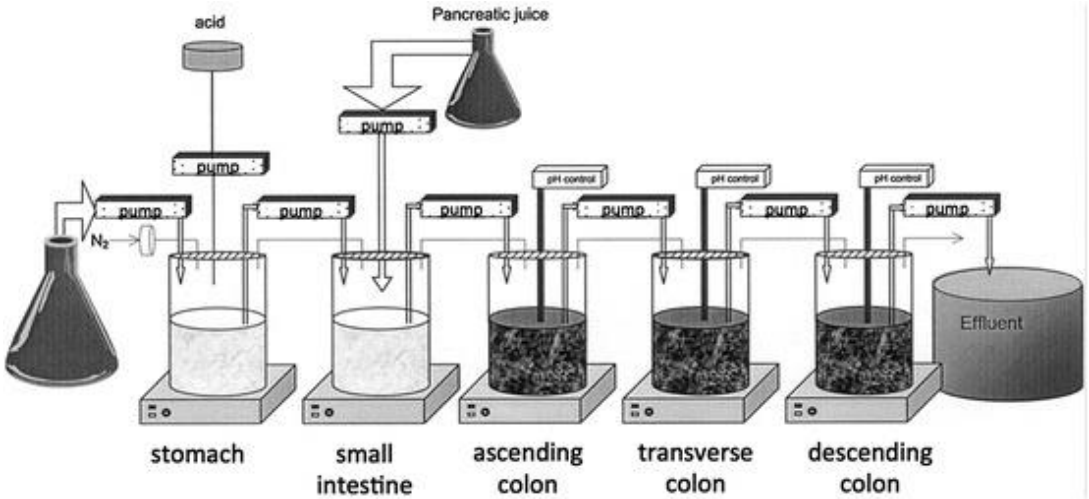

Figure 6: Schematic overview of the SHIME model (Van de Wiele et al., 2015).

Recently, Deyaert et al. (2023) adapted the SHIME to create an *in vitro* model for the ileal microbiota. For this aim, several strategies were tested for the inoculation process, including ileostomy effluents, fecal sample and a synthetic community of 12 bacterial species (*Streptococcus bovis* LMG 8518, *Streptococcus intermedius* LMG 17840, *Ligilactobacillus salivarius* LMG 9477, *Limosilactobacillus reuteri* LMG 9213, *Enterococcus faecalis* LMG7937, *Enterococcus faecium* DSM 20477, *Veillonella parvula* LMG 30945, *Veillonella dispar* DSM 20735, *Blautia obeum* DSM 25238, *Faecalibacterium prausnitzii* DSM 17677, *Clostridium nexile* LMG 28906, *Prevotella melaninogenica* LMG 28911). It was determined that the inoculation with the synthetic community and a retention time of 4h, most closely represented the *in vivo* human condition. Moreover, to reduce the high bacterial load observed in an initial model, the ileal medium with reduced nutritional load (30% of simple sugars, yeast extract, special peptone, cysteine-HCl, and mucin compared to the normal SHIME medium) was used. Additionally, the mucosal aspect was also integrated into the SHIME, increasing the relevance of the model. While for the colon the conventional mucin-covered microcosms were used, for the ileum mucin-alginate beads were implemented. Furthermore, to improve the sterility, the sampling of the beads in the vessel and the addition of fresh beads occurs via the inlet port with a 50 mL syringe with a catheter tip. As a result, the bacterial community consists mainly of genera of the synthetic consortium. The ileal lumen and mucus were dominated by *Streptococcus*, *Veillonella*, and *Enterococcus*, although in a different abundance. Moreover, a bacterial load of 2.53-7.58*10^8 cells/mL was described in the lumen, and concentrations of acetate, propionate, and butyrate were present in a ratio of 50/49/1 for donor 1 and 54/45/2 for donor 2, while the total concentrations were 13.5 ± 0.7 mM and 13.9 ± 0.5 mM.

Another *in vitro* model based on the SHIME for the small intestinal microbiota was created by Roussel et al. (2020). The system was operated for six donors and consisted of a combined stomach/duodenum-jejunum, ileum, and ascending colon vessels. The mucosal environment was recreated in the ileal vessels by adding mucin-agar coated microcosms using type III porcine mucin agar. A transit time of 3h for the ileal vessel and 20h for the ascending colon vessel was maintained. At the start of the SHIME run, fecal slurry was added to the ascending colon and two times (day 3 and 8) during the SHIME run, a retrograde inoculation (ascending colon to ileum) was performed. The nutritional SHIME medium was enriched with simple sugars. After a stabilization period of 7 days, a diverse microbial community was observed. In particular, the ileum genera such as *Klebsiella, Enterobacteriaceae, Anaerovibrio, Veillonella, Mitsuokella,* and *Bacteroides* were present, while the ascending colon microbiota was mainly characterized by *Succinivibrio, Lachnoclostridium,* and *Bacteroides*.

2.2.3 Model overview

Based on the specific technical features, each *in vitro* model mimics the gastrointestinal tract differently (Table 3), resulting in diverse advantages and disadvantages (Table 4). For example, TSI works with small volumes, short runs, and a standardized inoculum, making it relatively high throughput compared to other models. However, these advantages make the model less physiologically relevant and do not allow to capture the inter-individual variability. In contrast, the other three models have low throughput but result in a more physiologically relevant model. In particular, the SHIME models incorporate a mucosal aspect and mimic a larger part of the gut, but this is associated with higher costs. Additionally, this model does not simulate nutrient absorption in the gut, whereas the TSI and *in vitro* model based on TIM-1 involve a dialysis component for water-soluble compounds. Furthermore, the latter simulates also peristalsis, the mixing of food with saliva, as well as the absorption of lipid-soluble components.

Table 3: The inoculation strategy, simulated gut compartments, transit time, and pH of each small intestinal bacterial in vitro model with TIM-1 = TNO GastroIntestinal Model, TSI = The Smallest intestinal model, M-SHIME = Mucosal Simulator of the Human Intestinal Microbial Ecosystem

System type	Simulated gut compartments	Inoculation strategy small intestine	Transit time	pH	Reference
***In vitro* model based on TIM-1**	Stomach to ileum	Ileostomy effluent or fecal inoculum	3.5h	7.2	(Stolaki et al., 2019)

TSI	Duodenum to ileum	Synthetic consortium (*E. coli* DSM 1058, *Streptococcus salivarius* DSM 20560, *Streptococcus luteinensis* DSM 15350, *Enterococcus fecalis* DSM 20478, *Bacteroides fragilis* DSM 2151, *Veillonella parvula* DSM 2008 and *Flavonifractor plautii* DSM 6740)	Duodenum: 2h Jejunum: 4h Ileum: 2h	Duodenum: 6.5-6.8 Jejunum: 6.8-7.2 Ileum: 7.2	(Cieplak et al., 2018)
M-SHIME	Stomach to ascending colon	Retrograde inoculation from the colon vessel to the ileum vessel. Colon was inoculated with feces.	Stomach: 1h Duodenum-jejunum: 2h30 Ileum: 3h Colon: 20h	Stomach: 2 Duodenum-jejunum: 5 Ileum: 6 Colon: 6.2-6.4	(Roussel et al., 2020)
M-SHIME	Ileum to distal colon	Synthetic consortium (*Streptococcus bovis* LMG 8518, *Streptococcus intermedius* LMG 17840, *Ligilactobacillus salivarius* LMG 9477, *Limosilactobacillus reuteri* LMG 9213, *Enterococcus faecalis* LMG7937, *Enterococcus faecium* DSM 20477, *Veillonella parvula* LMG 30945, *Veillonella dispar* DSM 20735, *Blautia obeum* DSM 25238, *Faecalibacterium prausnitzii* DSM 17677, *Clostridium nexile* LMG 28906, *Prevotella melaninogenica* LMG 28911)	Ileum: 4h Colon: 20h	Ileum: 7.05-7.35 Colon: 6.15-6.40	(Deyaert et al., 2023)

Table 4: Advantages and disadvantages of the discussed small intestinal bacterial in vitro models with TIM-1 = TNO Gastrointestinal Model, TSI = The Smallest intestinal model, M-SHIME = Mucosal Simulator of the Human Intestinal Microbial Ecosystem

Parameters	*In vitro* model based on TIM-1 (Stolaki et al., 2019)	TSI (Cieplak et al., 2018)	M-SHIME (Deyaert et al., 2023)	M-SHIME (Roussel et al., 2020)
Peristalsis	X			
High throughput		X		
Standardized inoculum		X	X	
Mucosal environment			X	X
Saliva and fat-soluble components	X			
Limited compartments	X	X		
Complex/realistic	X		X	X
Inter-individual variability	X			X
Absorption simulated	X	X		
Expensive	X		X	X

To be able to study the small intestinal microbiota, in every *in vitro* model it is essential to define the best inoculation strategy and inoculum. So far this has been done with synthetic communities, fecal communities of one or more donors, or ileostomy effluent (Cieplak et al., 2018; Deyaert et al., 2023; Rajilic-Stojanovic et al., 2010; Roussel et al., 2020; Stolaki et al., 2019). While synthetic communities have the advantage of being standardized and reproducible (Cieplak et al., 2018),

the microbial richness, interactions, and biodiversity are reduced, along with the inter-individual variability (Biagini et al., 2023).

Conversely, Fecal samples and ileostomy effluents account for inter-individual differences, yet disadvantages exist as well. For example, fecal samples primarily represent the luminal, rather than the mucosal microbiota (Rumney & Rowland, 1992), and the distal (colon), rather than the proximal (small intestine) gastrointestinal tract (Chung et al., 2016). In fact, unlike colonic microbiota, which are specialized in complex carbohydrate degradation, the ileal microbiota have a fast uptake and conversion of nutrients, making a fecal inoculum less ideal for accurately recapitulating the functional complexity of ileal microbiota (Chung et al., 2016; Zoetendal et al., 2012). In addition, it can be difficult to maintain cell densities, microbial profiles of food mucus-associated, and gut-lumen bacterial populations (Fehlbaum et al., 2015). Although fecal samples of multiple donors could be added to improve reproducibility, Rajilic-Stojanovic et al. (2010) suggested that pooled fecal samples alter the interactions between bacteria favoring certain genera, resulting in an unrepresentative microbial composition, with associated alterations in functionalities. Comparable with the fecal samples, ileostomy effluents might not be reproducible since they contain a distinct microbial community composition, as seen in the study of Deyaert et al. (2023).

3 OBJECTIVES

The last decades of scientific research have seen a growing awareness and interest in understanding the role of gut microbiota in health and disease. While most studies focus on the fecal microbiota to understand colon microbial processes that modulate host health, far less emphasis has been placed on the small intestinal microbiota. This segment of the gut is in close contact with the immune system through the gut-associated lymphoid tissue and Peyer's patches (Ahluwalia et al., 2017; Collins et al., 2017; Garabedian et al., 1997; Hillman et al., 2017). Not surprisingly, shifts in the small intestinal bacteria are implicated with the outgrowth of enteropathogens, small intestinal bacterial overgrowth, and coeliac disease, making it a crucial part of the gut to study. However, since sampling is invasive and prone to contamination, only limited insight into the composition, metabolites, and dynamics of the small intestinal bacteria is available. Therefore, in this study an *in vitro* model will be developed, based on the SHIME, to study the small intestinal bacteria, enabling a mechanistic understanding of these bacteria. By inoculating the small intestinal SHIME with both saliva and feces, a bacterial community will be obtained and validated based on bacterial cell counts, metabolites, and bacterial composition against *in vivo* samples.

Three main research questions were identified:

(i) Are the bacterial cell concentrations comparable to *in vivo* data for the mouth, proximal small intestine, and ileum, and do they match normal colon SHIME bacterial abundances in the proximal and distal colon?
(ii) Are the bacterial metabolites comparable to *in vivo* data and other *in vitro* models for the ileum?
(iii) Is the bacterial composition consistent with *in vivo* literature and donor data and can the system recapitulate inter-individual differences?

4 MATERIAL AND METHODS

4.1 Dialysis absorption efficiency

To assess the absorption efficiency of the dialysis membrane, the SI-M-SHIME medium (Table 5) and each separate component of the SI-M-SHIME medium (Table 6Table 6) were run through the 07 Sureflux Nipro membrane. This was repeated twice for each compound with a new membrane for each repeat. After analysis, starch was omitted from the results due to its high error rate. Similarly, arabic gum was not included since the carbohydrate content of the filtered solution was higher than the ingoing solution.

All compounds were dissolved in distilled water and autoclaved prior dialysis apart from the sugars (glucose, fructose, galactose, mannose, maltose, sucrose, lactose). The SI M-SHIME medium was prepared by combining autoclaved SI M-SHIME medium and filter-sterilized sugars (Table 5). For each compound, 200mL was dialyzed. A dialysis buffer was prepared for (i) both runs and (ii) to wash the membrane prior dialysis (Table 7).

Table 5: SI-SHIME medium of the first donor used in dialysis absorption efficiency experiment.

SI-SHIME medium	(g L^{-1})	Supplier
M-SHIME medium*	10.2	ProDigest, Gent, Belgium.
Starch	4	ProDigest, Gent, Belgium.
Glucose	0.8	Carl Roth, Karlsruhe, Germany
Fructose	0.8	Janssen Chimica, Beerse, Belgium
Galactose	0.4	Carl Roth, Karlsruhe, Germany
Mannose	0.4	Janssen Chimica, Beerse, Belgium
Maltose	0.8	Sigma Aldrich, Hoeilaart, Belgium
Sucrose	0.8	Merck Millipore, Darmstadt, Germany
Lactose	0.8	Carl Roth, Karlsruhe, Germany
*content (g L^{-1}): Arabic gum (1.2), pectin (2), xylan (0.5), glucose (0.4), yeast extract (3), special peptone (1), mucin (2), L-cysteine-HCl (0.5)		

Table 6: Concentration (g L^{-1}) of twelve compounds dialyzed in the dialysis absorption efficiency experiment. Concentrations are based on the concentration of each compound normally present in the proximal small intestine of the SI-SHIME.

Mixture	g L^{-1}	Supplier
Pectin	1.4	Sigma Aldrich, Hoeilaart, Belgium
Xylan	0.35	Sigma Aldrich, Hoeilaart, Belgium
Mucin type II	1.4	Sigma Aldrich, Hoeilaart, Belgium
Starch	2.8	ProDigest, Gent, Belgium.
Glucose	0.85	Sigma Aldrich, Hoeilaart, Belgium
Fructose	0.55	Janssen Chimica, Beerse, Belgium
Galactose	0.3	Carl Roth, Karlsruhe, Germany
Mannose	0.3	Janssen Chimica, Beerse, Belgium
Maltose	0.55	Sigma Aldrich, Hoeilaart, Belgium
Sucrose	0.55	Merck Millipore, Darmstadt, Germany
Lactose	0.55	Carl Roth, Karlsruhe, Germany
SI-SHIME medium	See Table 5	

Table 7: Composition of buffer solution used in the dialysis absorption efficiency experiment.

Buffer	g L^{-1}	Supplier
KH_2PO_4	0.168	Carl Roth, Karlsruhe, Germany
K_2HPO_4	0.86	Carl Roth, Karlsruhe, Germany
NaCl	3.5	Chem-Lab NV, Zedelgem, Belgium
Cysteine HCl	0.3	Calbiochem, Darmstadt, Germany
$CaCl_2.2H_2O$	0.2	Chem-Lab NV, Zedelgem, Belgium

4.1.1 Dialysis membrane operation

Before using the dialysis membrane in the experiment, the serosal side of the membrane was rinsed with 1L dialysis buffer (Table 7) to remove the storage solution (glycerol) (Figure 7). Subsequently, each component was examined separately, passing through the dialysate side of the membrane at a rate of 20 mL/min, and a counter-current dialysis buffer flow at the serosal side of 30 mL/min to filter out the components. This flow is switched compared to the regular application in renal dialysis to prevent clogging of the hollow fibers in the membrane. The mixture outflow was collected in a separate Schott bottle. A 2 mL sample of both the dialyzed component and non-dialyzed component were stored at -20°C for subsequent carbohydrate quantification analysis (method, see 4.1.2).

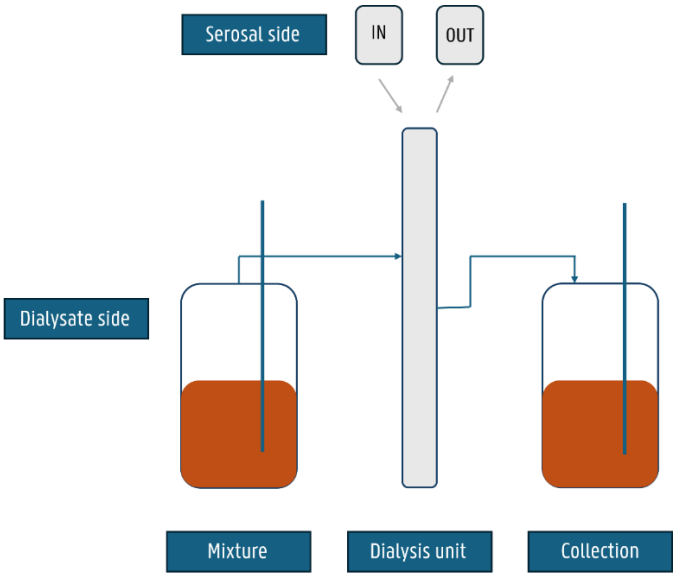

Figure 7: Schematic overview of the dialysis absorption efficiency experiment. At the serosal side, the buffer goes into the dialysis unit and out of the system.

4.1.2 Carbohydrate analysis

A carbohydrate analysis was conducted to test the evolution of the membrane's efficiency in reducing the carbohydrate content over time. The carbohydrate content, measured in glucose equivalents, was detected through acid hydrolysis and spectrophotometry. The reagent was made by dissolving 25 g L^{-1} H_3BO_3 slowly in (98%) H_2SO_4, followed by 5 g L^{-1} L-tryptophan, and mixed for six hours. The final reagent was stored for at least one night in the fridge in the dark and used within a month. Prior analysis samples were diluted, 0.22µm filtered and the reagent acclimatized to room temperature. 2 mL of the reagent was added to 1 mL of sample in a glass vial, closed, shortly vortexed, and incubated for 20 minutes at 100°C in Nanocolor vario 4 heating block (Macherey-nagel, France). Samples were cooled down and afterwards measured by spectrophotometry (ThermoFisher Scientific, Belgium) at 520 nm.

The sample concentrations were quantified by use of an 8-point standard curve ranging from 0 mg glucose/l to 110 mg glucose/l, prepared in Mili-Q water. The SHIME samples were diluted in Mili-Q, aimed to fall within the standard series. SHIME samples of the proximal small intestine and ileum were obtained on days 1, 2, 3, and 4 of the SHIME of the first donor, without changing the membrane (07 Sureflux Nipro, pore size 40 kDa). Each sample was measured in duplicate.

4.2 SI M-SHIME validation experiment

4.2.1 Experimental set-up

The Simulator of the Human Intestinal Microbial Ecosystem (SHIME®) (Molly et al., 1994) was modified to recreate the oral, small intestinal, and colon microbial community *in vitro* (Small intestinal M-SHIME; SI M-SHIME). The configuration consisted of six compartments representing in consecutive order: the mouth, stomach, proximal small intestine (combining the duodenum and jejunum), ileum, proximal and distal colon (Figure 8). In addition, a dialysis membrane (07 Sureflux Nipro, pore size 40 kDa, see 4.1) (Nipro, Mechelen, Belgium) was included between the proximal small intestine and ileum compartments, intended to mimic intestinal absorption, such as the absorption of bile acids and sugars. The intestinal mucus layer was simulated in the proximal small intestine, ileum, and colon compartments by use of carriers (AnoxKaldnes K1 carrier, AnoxKaldnes AB, Lund, Sweden), coated with mucin-agar (Table S 2) (Van den Abbeele et al., 2012). The mucin-agar beads were contained using polyethylene netting in the colon or nylon wire in the proximal small intestine and ileum. In the mouth, hydroxy-apatite discs (HA) (0.5 inch diameter × 0.04–0.06 inch thick) (VWR, Leuven, Belgium) represented the tooth surface. In the mouth, proximal small intestine, and ileum the biofilm carriers (mucin or HA discs) were placed in separate Schott bottles connected to their respective compartments with a (semi-)continuous liquid flow between Schott bottle and compartment (Table 8).

Table 8: Flowrate (mL/min) between the mucin Schott bottles and its respective biofilm compartment.

Compartment	Flowrate (mL/min)
Mouth	3
Proximal small intestine	4
Ileum	4

The double-jacket compartments were continuously stirred and kept at 37°C by connection to a warm water bath. Residence time, pH, and liquid transfer were monitored to maintain the parameters within the defined range (Table 9). The applied parameters were the same for all three donors, except for the stomach liquid transfer which started at pH 3 for donors two and three. The pH was controlled by pH-controllers and kept within range with 0.5M NaOH and 0.5M HCl. Anaerobiosis was maintained in the colon compartments by flushing with N_2 after the inoculation (5 min) and each time when opening the compartments for biofilm sampling (2 min). The mouth and ileum were flushed for 2 min and the proximal small intestine for 1 min during the first run, while the mouth and ileum were flushed for 2 min during the second and third run after inoculation and each biofilm sampling.

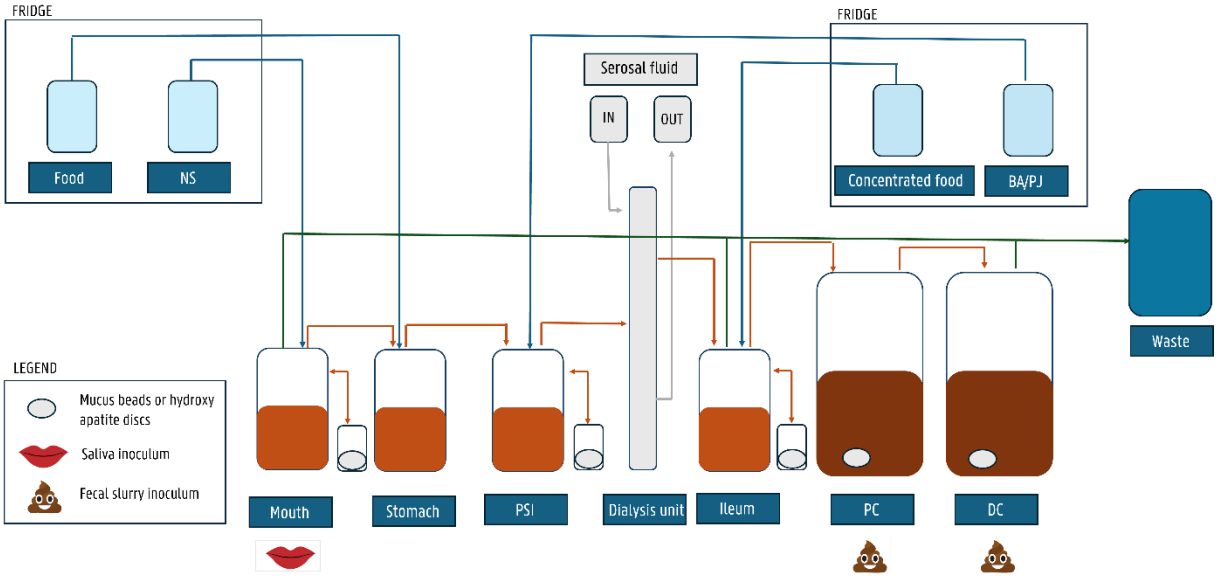

Figure 8: Schematic overview of SI-M-SHIME validation experiment with NS: nutritional saliva, BA/PJ : bile acids and pancreatic juice, PSI: proximal small intestine, PC: proximal colon, distal colon: distal colon. The orange arrows indicate the outflow of the compartments, the blue arrows show the different input flows, and the gray arrows reveal the serosal fluid flow. At the start of the experiment, saliva was used to inoculate the mouth, whereas the fecal slurry inoculated the colon compartments. Each compartment is connected to a base and acid compartment (not shown on figure).

Table 9: Set-up parameters of the SI-M-SHIME

Compartment	Speed (rpm)	pH	Residence time	Volume (mL)	Liquid transfer (mL)	Biofilm
Mouth	150	6.5 – 7.0	12h	150 mL	20	4 HA discs
Stomach	200	Gradual decrease 5 -> 2 Donor 1: Liquid transfer from pH 3.25 Donor 2,3: Liquid transfer from pH 3	1h33min	130 mL feed + 10 mL Mouth + acid	140 + acid	-
Proximal small intestine	150	5.8 – 6.5	+/- 2h (gradual transfer)	200	200	2 x 5 mucin beads
Dialysis membrane	20 mL/min SHIME 30 mL/min serosal	-	11 min flow		200	-
Ileum	150	7.0 – 7.5	+/- 1.5 h	250	200 to Proximal colon 50 to waste	2 x 10 mucin beads
Proximal colon	200	5.6 – 5.9	16h	400	200	4 x 15 mucin beads
Transverse colon	200	6.1 – 6.9	26h	650	200	4 x 15 mucin beads

4.2.2 Inoculation and SI M-SHIME operation

Three SI M-SHIME runs were performed with three different donors. Each SI M-SHIME set-up was inoculated with saliva and feces from the same donor at the start of the experiment. The donor for the first run was a healthy 50 year old male, for the second a 34 year old male, and for the third run a 65 year old male. Each of the donors had no gastrointestinal complaints. The first and second donors tested negative for bowel cancer using a colonoscopy screening. The colonoscopy results for the third donor were not available within the timeframe of this thesis. Additionally, the third donor did use anticoagulant drugs.

Fecal and saliva samples of the first donor were collected one month before colonoscopy and subsequent bowel preparation. The second donor donated the fecal and saliva sample 7 weeks after colonoscopy. The third donor had not yet undergone a colonoscopy. In this thesis, only the results of the first donor are available. The fecal samples were collected in airtight containers comprising an AnaeroGen™ sachet (Oxoid, Hampshire, UK). A fecal slurry was prepared by diluting 20 g feces in 100 mL anaerobic phosphate buffer (8.8 g L^{-1} K_2HPO_4, 6.8 g L^{-1} KH_2PO_4, 1 g L^{-1} Na-thioglycolate) in a stomacher filter bag (63 micron, MLS) (BagPage®, Interscience, Menen, Belgium), and homogenizing for 5 minutes in a Stomacher (LabBlender 400, LEDtechno, Heusden-Zolder, Belgium). The fecal slurry that passed through the BagPage® filter was collected for inoculation. On day 0, the proximal (400 mL M-SHIME medium (Table 10) and 60 mucus beads) and distal colon (650 mL M-SHIME medium and 60 mucin beads) were inoculated with respectively 20 mL and 32.5 mL of the fecal slurry. Saliva was collected by passive drooling, at least 2h after eating or toothbrushing and stored in the fridge until use (maximum 24h). The mouth compartment was inoculated with 1.5 mL saliva of the same donor in 150 mL nutritional saliva medium (Table S 3). The three inoculated compartments were incubated for 42h during the first donor's run, overnight incubated for the second donor, 48h for the mouth and 20h for the colon compartments during the third donor. The incubation included pH controlling but without flow-through. Afterward, the pumps were started and the system could stabilize. The proximal colon established theoretical stability (Van de Wiele et al., 2015) after five days (6 times its residence time). The stable proximal colon was used to inoculate the ileum, an action further referred to as retrograde inoculation. Due to technical problems during the SI-SHIME run of the first donor, which did not ensure the mouth's sterility, the mouth was reinoculated with 1.5 mL defrosted saliva on day 7, which was stored since day 0 at -20 °C.

Table 10: SI M-SHIME medium composition of the first donor.

SI M-SHIME medium	g L^{-1}
M-SHIME*	10.2
Starch	6.0
Glucose	0.8
Fructose	0.8
Galactose	0.4
Mannose	0.4
Maltose	0.8
Sucrose	0.8
Lactose	0.8
* Contains (g L-1): Arabic gum (1.2), pectin (2), xylan (0.5), glucose (0.4), yeast extract (3), special peptone (1), mucin (2), L-cysteine-HCl (0.5)	

Throughout the run, every 8 hours, a new feeding cycle started. During this cycle, SI M-SHIME medium, pancreatic juice and bile acids, saliva medium, dialysis buffer, and 2.5x concentrated M-SHIME medium were introduced throughout the system (Figure 8) (Table S 1, Table S 3, Table S 4, Table S 5, Table S 6). In the second and third run, 20 mL modified Wolin's mineral solution (Table S 7), menadione (K3) (0.1 µg L^{-1}) (Sigma Aldrich, Hoeilaart, Belgium) and cyanocobalamine (B12) (0.05 µg L^{-1}) (Carl Roth, Karlsruhe, Germany) were included into the SI M-SHIME medium, while the added sugars were reduced from

4.8 g L^{-1} to 3 g L^{-1}. The biofilm of the different compartments was sampled and/or replaced regularly. ½ of the mouth discs were brushed every two to three days with phosphate buffer (8.8 g L^{-1} K_2HPO_4 and 6.8 g L^{-1} KH_2PO_4) and halve of the small intestinal and colon beads were changed respectively every two to three and three to four days. The dialysis membrane was changed every two days and operated under the same conditions as explained in 4.1.1. After 16 days the SI M-SHIME was considered stable. The system was run for five additional days, until day 21, except for the second run, which was prematurely ended due to undesirable metabolite concentration and cell counts.

To validate the system, aspirates and biopsies were obtained from the first donor and bacterial DNA was immediately extracted (see 4.3.3).

4.3 Chemical and microbial analysis

Samples from the mouth, proximal small intestine, ileum, proximal colon, and distal colon were collected for further analysis, including cell counts, short chain fatty acids (SCFA), organic acid and ammonium composition as well as 16S rRNA gene amplicon sequencing, dialysis membrane efficiency and carbohydrate quantification. The SHIME was sampled on different days (Figure 9). The samples were stored at -20°C prior analysis except for the cell counting which were measured fresh.

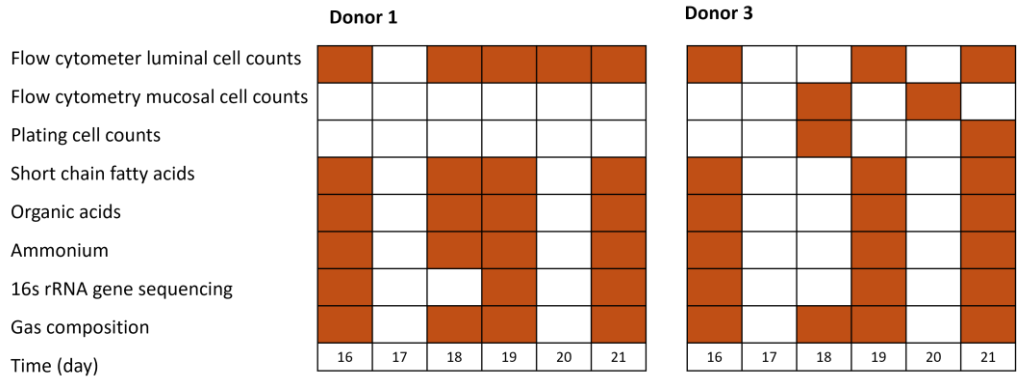

Figure 9: Timeline of the stable days of the different sampling points for different chemical analysis for the different donors. Donor 2 is not included in the plot, since it never reached stability.

4.3.1 Bacterial cell counts

The bacterial cell counts of the lumen and mucus were analyzed by flowcytometry to determine the cell density and the proportion of intact, damaged cells. The fresh luminal samples were diluted in 0.22 µm filtered anaerobic PBS (8.72 g L^{-1} K_2HPO_4, 6.80 g L^{-1} KH_2PO_4, 1.40 g L^{-1} $NaHCO_3$, 0.90 g L^{-1} NaCl, 1.00 g L^{-1} Na-thioglycolate, 1.00 g L^{-1} Cysteine HCl), and generally 10^3 diluted for the mouth, proximal small intestine and ileum and 10^4 mostly for the proximal colon and distal colon to remain within the measuring range. The sampled mucus beads were centrifuged for 5 minutes at low speed to dissociate the mucus from the beads. In general, 0.5g mucus was mixed with 1 mL anaerobic PBS and filtered with pluriStrainer Mini 20 µm (PluriSelect, Germany) prior measuring on the flow cytometer.

Each sample was measured in duplicate. The relevant dilutions were stained separately with two dyes: (i) 1% v/v SYBR® Green I nucleic acid stain (ThermoFisher Scientific, Merelbeke, Belgium) to evaluate the total cell count and, (ii) 1% v/v SYBR® Green propidium iodide (SGPI) (ThermoFisher Scientific, Merelbeke, Belgium) to evaluate the intact cells, also known as life-death staining, but more correctly referred to as intact-damaged staining. The diluted, stained samples were incubated for 20 minutes at 37 °C. Filtered anaerobic PBS was used as a control. The treated samples were examined on a BD Accuri™ $C6^+$ (Biosciences, Erembodegem, Belgium) with autosampler, using a 533/30 filter and >670 filter and operated with FACSflow sheath fluid (BD Biosciences, Belgium). The background was identified by applying 0.22 µm filters on a sample of each compartment. Heath-killed samples were included, to differentiate between intact and damaged cells.

Besides flowcytometry, the cell density obtained with the flow cytometer was compared by plating on days 18 and 21 during the SHIME of the third donor. For this aim, SHIME samples of the proximal small intestine and ileum were diluted to obtain a 10^5 to 10^6 dilution using anaerobic PBS (4.3.1). Each appropriate dilution was prepared in duplicate and plated on BHI agar (Carl Roth, Karlsruhe, Germany). 100µL was plated and thoroughly spread using the spread plate method with a sterile spreader. The plates were incubated for 4 days at 37°C with an air composition of 97.5% N_2 and 2.5% O_2. As a control, non-inoculated plates and plates inoculated with anaerobic PBS were incubated.

4.3.2 Short-chain fatty acid, organic acid, and ammonium composition

Organic acids were analyzed to determine the community stability and metabolic profile, while ammonium was examined as a read-out of the protein fermentation. Short-chain fatty acids (SCFA) (acetate, propionate, isobutyrate, butyrate, isovalerate, valerate, isocaproate, caproate, heptanoate, and octanoate) were determined in undiluted (proximal small intestine and ileum) or two times diluted (saliva, feces, mouth, proximal colon, and distal colon) samples. Dilutions were made in Mili-Q. In short, a 2 mL sample was mixed with 0.4 mL internal standard, 0.4 g NaCl, 0.5 mL 98% H_2SO_4, and 2 mL diethyl ether. The samples were rotated for 2 minutes and subsequently centrifuged for 3 minutes at 3000 rpm. The top layer (ether layer) was transferred to a GC vial and measured by gas chromatography (GC-2014, Shimadzu®, The Netherlands) with a DB-FFAP 123-3232 column (30m x 0.32 mm x 0.25 µm; Agilent, Belgium) and a flame ionization detector (FID).

Organic acids (lactate and formate) were detected on 0.22 µm filtered and diluted samples. Samples of the proximal colon, distal colon, mouth, and fecal slurry were 4 times diluted with Mili-Q, saliva 2 times, whereas the samples of proximal small intestine and ileum were not diluted. The samples were analyzed by ion chromatography using the 930 Compact IC Flex (Metrohm, Switzerland) with an 850 IC conductivity detector and inline bicarbonate removal. A Metrosep Organic acids 250/7.8 column and a Metrosep Organic acids Guard/4.6 guard column were applied.

Ammonium was detected for the colon compartments on 0.22 µm filtered and 10 times in Mili-Q diluted samples. Ammonium was detected by ion chromatography on the 930 Compact IC Flex (Metrohm, Switzerland) with the Metrosep C6-150/4.0 column and C6 Guard/4.0 guard column.

4.3.3 cDNA extraction and 16S rRNA gene amplicon sequencing

DNA was extracted and analyzed to describe the microbial community present in the SI M-SHIME of the first and second donors at specific time points. For this purpose, 1 mL of SHIME sample, fecal, or saliva inoculum was centrifuged for 10 minutes at maximum speed, and the pellets were stored at -20°C until extraction. DNA was extracted using the DNeasy PowerSoilPro Kit (Qiagen, Germany). Beads were transferred to the sample vial, whereafter bead beating was performed (5 cycles of 15" at 4000 rpm and 45" cooldown) with the Powerlyzer 24 Homogenizer (Qiagen, Germany). By adding the different buffers (Table 11) to the homogenized sample, centrifuging, and using a spin column, the DNA was extracted. 400 µL CD1 was supplemented to the sample and 60 µL of CD6 was chosen as volume transferred to the spin column. In-house quality check of the amplification of the extracted DNA was performed by PCR using Taq DNA Polymerase with the PHUSION™ PLUS GREEN PCR MASTER MIX (ThermoFisher Scientific, Vilnius, Lithuania). The obtained PCR product was run on an agarose gel (0.7 g agarose (Invitrogen, Merelbeke, Belgium) in 50 mL diluted TAE buffer (Panreac Applichem, Amsterdam, Netherland) for 20 minutes at 100V and visualized by use of ethidium bromide. The 16S rRNA gene was amplified after DNA extraction. 10 µL of the extracted 16S rRNA gene was sent out for library preparation and sequencing to LGC genomics GmbH (Berling, Germany) using the Illumina MiSeq platform (Illumina, Hayward, CA), as described by De Paepe et al. (2017). The V3 and V4 regions were employed with the primers 27F (5'-AGAGTTTGATCCTGGCTCAG-3') and 1492R (5'-GGTTACCTTGTTACGACTT-3') (Lane, 1991). Negative controls and a mock community in triplicate were included to check the quality of the sequencing run.

Table 11: Different buffer solutions added during the DNA extraction and their effect.

Buffer	Effect
CD1	dissolve humic acids, protect nucleic acid degradation, disperse soil particles
CD2	precipitate non-DNA substances
CD3	aid the binding of DNA to silica of the column
EA and C5	wash the spin column
C6	aid the release of DNA from the spin column

4.3.4 Gas composition

Gas composition was evaluated regularly to check the anaerobic conditions and to have an indication of bacterial metabolic activity. Headspace gas samples from the mouth, proximal small intestine, ileum, proximal colon, and distal colon were analyzed for O_2, N_2, CH_4, CO_2, H_2S, and H_2 with the compact GC 4.0 (Global analyser solutions, Breda, Netherlands). A minimum of 1.5 mL was injected into the GC using a Hamilton NDL KF needle. O_2, N_2, H_2, and CH_4 were measured with a Porabond Q pre-column and a Molsieve 5A column. CO_2 and H_2S were detected with a Rt-QSBond pre-column and column. The concentrations obtained were normalized by dividing with the sum of all gas concentrations. During the second run, CH_4 and H_2S were not checked and therefore the normalization may not be optimal.

4.3.5 Bioinformatics and statistics

The flowcytometric data and Illumina sequencing data were analyzed in R version 4.3.2, while plots were made in R version 4.2.2.

Microbial cell counts obtained through flow cytometry were explored using the Phenoflow package in R (v1.1.2), described by Props et al. (2016).

A community diversity analysis was performed based on the intact flow cytometry data in two fluorescent channels (FL1-H and FL3-H) and two scatter channels (SSC-H and FSC-H), according to Props et al. (2016), using the Phenoflow package (v1.1.2). The data was first transformed using the arcsine hyperbolic function and subsequently normalized by dividing each sample by the maximum SGPI intensity value. Ordination by PCoA for the beta diversity was based on the Bray-Curtis distance metric.

To obtain amplicon sequence variants (ASV), the 16S rRNA gene amplicon sequencing was processed. The demultiplexed, primer-clipped paired-end amplicon data were inferred using the dada2 R package (v1.30.0) following the DADA2 pipeline (Callahan et al., 2016). In short, sequences were quality-filtered, denoised, and merged. Moreover, chimeras were removed, and taxonomy was assigned to amplicon sequence variants (ASV) using a naïve Bayesian classifier (Wang et al., 2007) against the Silva database version 138.1 (McLaren & Callahan, 2021). In the end, 1194 unique ASV for the first donor and 319 for the second donor, each read trimmed at 220 nucleotides, were obtained. Sequences classified as Mitochondria were removed. Unclassified sequences were blasted and removed if human. Furthermore, abundant sequences in the biopsy of the proximal colon only classified on the kingdom level were blasted and were removed since they were classified as eukaryotic DNA.

The absolute microbial composition of the luminal samples of donor one was calculated by combining proportional microbial profiles obtained through 16S rRNA gene amplicon sequencing and total cell counts from flow cytometry total cell counts (SG for the first donor and SGPI for the second donor), to acquire quantitative microbial profiles (QMP) (Props et al., 2016; Vandeputte et al., 2017). The samples of the first donor were rarefied to obtain an even sequencing depth which was used to create a phyloseq object through the Phyloseq package (v1.42.0). For the second donor, the absolute microbial composition was calculated by dividing the number of reads in each sample by the total number of reads in the sample, which was subsequently multiplied by the cell counts.

Furthermore, the ASVs of genera such as *Bacteroides, Enterococcus, Escherichia-Shigella,* and *Streptococcus*, present in the proximal small intestine of the SHIME of the first donor, were plotted in the different compartments of the SHIME.

Microbial variation related to the SHIME compartments was analyzed with principal coordinate analyses (PCoAs) based on the Bray-Curtis difference and visualized on the genus level.

Since the assumptions of parametric tests were not fulfilled for the cell count data, a nonparametric test, namely the Kruskal-Wallis rank sum test was applied, with alpha set at 0.05. A post hoc pairwise comparison with Dunn's test was performed, with a Benjamini-Hochberg correction for multiple testing. For the pairwise comparison, a Wilcoxon test was conducted.

The net daily production of organic acids in the proximal colon and distal colon of the first and third donors was obtained by multiplying the hydraulic residence time in the proximal colon (400mL/600mL/24h) and the distal colon (650mL/600mL/24h) with the difference between the concentrations during the stable period in the compartment and the incoming concentrations, as described by De Paepe et al. (2018). During the SHIME of the second donor, the net daily production was calculated based on days 9, 12, and 13.

During this thesis, ChatGPT was occasionally used to improve sentences.

5 RESULTS

5.1 Carbohydrate absorption dialysis membrane

The absorption capacity of the NIPRO Sureflux 7 membrane was evaluated per component present in the SI M-SHIME medium and for the complete SI M-SHIME medium (*i.e.* a combination of all the components in a premade mix). The absorption was calculated by determining the carbohydrate content in the mixtures before and after dialysis. Acid hydrolysis (4.1.2) was used to convert sugar polymers into sugar monomers. All components for the SI M-SHIME medium were considered, except for starch and arabic gum where experimental errors prohibited further determination of the absorbed fraction.

Based on the medium composition, the theoretical SI M-SHIME medium carbohydrate content was 9.6 g carbohydrates/L (Table 6). Experimentally, the complete SI M-SHIME medium had 6.96 g carbohydrates/L and when combining the values of the separate compounds, except for starch and arabic gum, the SI M-SHIME medium contained 4.38 g carbohydrates/L (Figure 10).

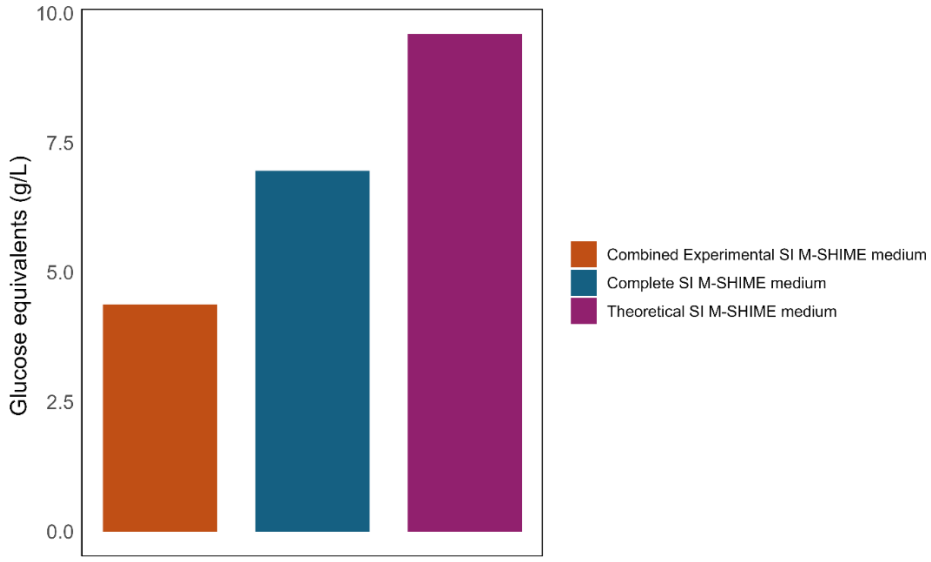

Figure 10: The carbohydrate concentration (g glucose eq. /L) of the SI M-SHIME medium before dialysis, determined in three different ways. (i) "Combined experimental" is experimentally determined by separately analyzing each medium component and adding the determined values together (1.05 g L^{-1} pectin, 0.11 g L^{-1} xylan, 0.31 g L^{-1} mucin type II, 0.80 g L^{-1} glucose, 0.60 g L^{-1} fructose, 0.27 g L^{-1} galactose, 0.26 g L^{-1} mannose, 0.37 g L^{-1} maltose, 0.32 g L^{-1} sucrose, 0.48 g L^{-1} lactose), (ii) "Complete" indicates the experimental determination of the complete SI M-SHIME medium, and (iii) "Theoretical" shows the carbohydrate content of SI M-SHIME medium based on its composition.

After dialysis, the total carbohydrate content removed from the complete SI M-SHIME medium, comprising all the components present in the medium, was 44.4%, whereas the amount removed from the combined experimental SI M-SHIME medium was 56.5% (Figure 11). The individual components were filtered out to a variable degree. Glucose, fructose, galactose, and mannose were absorbed for about 75-80% of the initial carbohydrate content. Xylan was removed for 74.6%, lactose for 61.7%, and mucin type II for 51%. Pectin, maltose, and sucrose were filtered out to a lesser extent with respectively, 28.3%, 23.9%, and 35.6%.

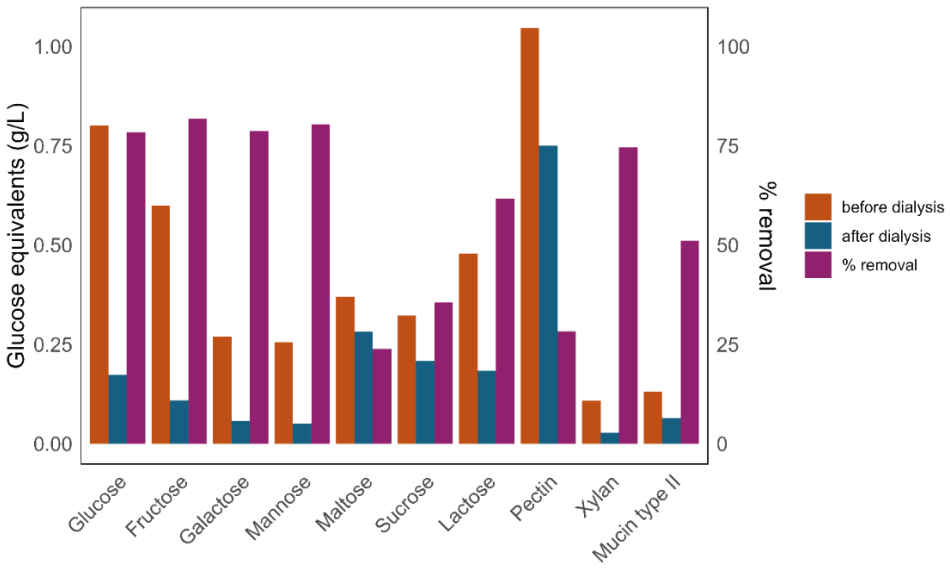

Figure 11: The carbohydrate concentration (mg glucose eq/L) before and after dialysis of the different compounds present in the SI M-SHIME medium ordered on ascending molecular weight. Before and after dialysis are plotted on the left axis, while the % removal is plotted on the right axis.

In addition to examining the dialysis efficiency of the compounds, the dialysis efficiency of the same membrane over time (cycles 1, 4, 6, and 9) during one SHIME run (first donor) was evaluated, based on the carbohydrate content of the proximal small intestine and ileum (Figure 12). The carbohydrate concentration in the proximal small intestine decreased over the first three days before stabilizing. Conversely, the carbohydrate concentration in the ileum rose on the second day compared to the first and then declined. However, the standard error on the ileal concentrations was considerable, particularly on the first day (4.36 ± 1.91 g L^{-1}). The difference between the proximal small intestinal and the ileal concentration initially increased, followed by a subsequent decrease. Furthermore, when calculating the percentages of glucose equivalents in the ileum compared to the proximal small intestine, an initial decrease was observed, followed by an increase (day 1: 48.73%, day 2: 32.63%, day 3: 46.01%, day 4: 49.04%).

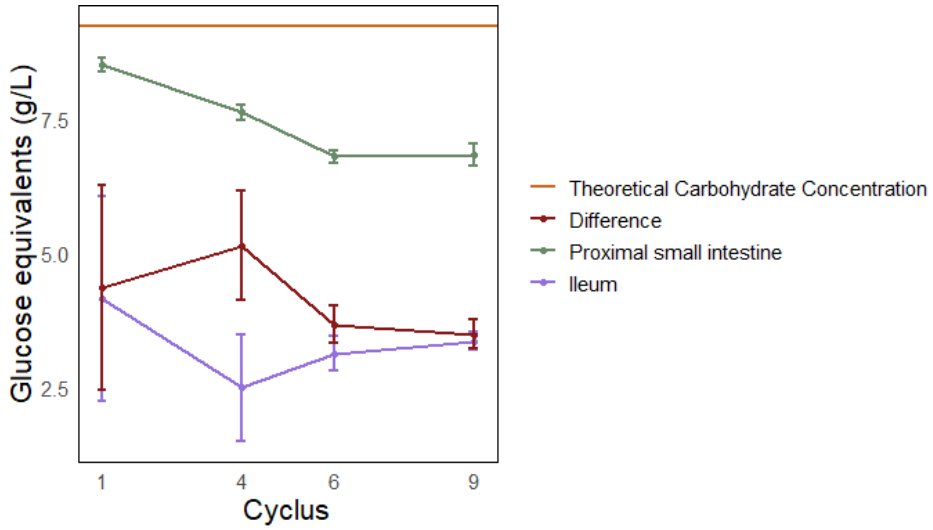

Figure 12: Dialysis efficiency evaluated by the carbohydrate concentration of the proximal small intestine and ileum over four cycles during the SHIME of the first donor (n = 2). The "Theoretical carbohydrate concentration" was calculated based on the SI M-SHIME medium in the proximal small intestine. The "Difference" was determined by subtracting the ileal carbohydrate concentration from the proximal small intestinal concentration.

5.2 SI M-SHIME results

5.2.1 Bacterial cell counts

The bacterial cell counts and viability were regularly quantified by flow cytometry during the SHIME.

In the SHIME of the first donor, the intact cell counts present during the stable period (day 16 to 21) were in the mouth $9.42*10^8 \pm 1.52*10^8$ cells/mL, in the proximal small intestine $7.72*10^7 \pm 2.65*10^7$ cells/mL, in the ileum $5.79* 10^8 \pm 9.80*10^7$ cells/mL, in the proximal colon $6.81*10^8 \pm 2.90*10^7$ cells/mL, and $8.10*10^8 \pm 1.46*10^8$ cells/mL in the distal colon (n = 10) (Figure 13, Table S 8). The intact cell percentage in the mouth was 96.02%, in the proximal small intestine 51.11%, in the ileum 86.69%, in the proximal colon 58.11%, and in the distal colon 76.01%. The bacterial intact cell count in the proximal small intestine was significantly smaller than in the mouth ($p = 2.10*10^{-7}$), ileum (p = 0.0004), proximal colon (p = 0.0060), and distal colon ($p = 8.26*10^{-9}$), the ileum intact cell count was significantly smaller than the distal colon count (p = 0.0038), the mouth intact cell count was significantly smaller than the ileum count (p = 0.0105), and the intact cell count of the proximal colon was significantly smaller than the distal colon count (p = 0.0296).

The SHIME run of the second donor was terminated before reaching stability, meaning no cell counts were acquired during the stable period (Figure 13, Table S 8). Throughout this run, the intact bacterial cell counts increased from mouth to distal colon (day 5 to 19), with a mean of $5.46*10^8 \pm 1.74*10^7$ cells/ mL in the mouth, $3.04*10^8 \pm 1.52*10^8$ cells/mL in the proximal small intestine, $9.98*10^8 \pm 4.46*10^8$ cells/mL in the ileum, $6.60*10^8 \pm 2.62*10^8$ cells/mL in the proximal colon, and $9.95*10^8 \pm 2.34*10^8$ cells/mL in the distal colon. During the SHIME of the second donor, the bacterial cell counts of the proximal small intestine were significantly lower than the distal colon ($p = 3.22*10^{-2}$), ileum (p = 0.0001), and proximal colon (p = 0.0126). The proximal colon cell counts were significantly lower than the distal colon (p = 0.0322), while the mouth cell counts were significantly lower than the distal colon (p = 0.0037) and ileum count (p = 0.0217). The intact cell percentage in the mouth was 92.06%, in the proximal small intestine 40.72%, in the ileum 72.72%, in the proximal colon 35.11%, and in the distal colon 53.88%). The low percentage of intact cells in the proximal colon was one of the reasons for terminating the run of the second donor before reaching the stable phase (Figure S 1). The intact percentage was significantly lower in the mouth (p = 0.01621), proximal small intestine (0.003609), and ileum (p = 0.02365), compared to the same compartment of the first donor (Table S 8).

During the stable period of the SHIME of the third donor an intact cell count of $1.74*10^9 \pm 4.94*10^8$ cells/mL was reached in the mouth, $2.10*10^8 \pm 7.42*10^7$ cells/mL in the proximal small intestine, $1.17*10^9 \pm 2.32*10^8$ in the ileum, $8.31*10^8 \pm 3.17*10^8$ cells/mL in the proximal colon and $1.18*10^9 \pm 2.79*10^8$ cells/mL in the distal colon (Figure 13). The percentage of intact cells was 97.58% in the mouth, 50.74% in the proximal small intestine, 89.63% in the ileum, 39.95% in the proximal colon, and 64.09% in the distal colon. The mouth intact bacterial concentration was significantly higher than in the proximal small intestine (p = 0.0002) and in the proximal colon (0.0263).

The mucus bacterial cell counts were determined for the proximal small intestine and the ileum of the second and third donors by flow cytometry. For the second donor on day 16, an intact bacterial cell count of $3.70*10^8 \pm 3.99*10^7$ cells/g was reached in the proximal small intestine, while $5.48*10^9 \pm 2.46*10^8$ cells/g in the ileum. For the third donor, the mucus counts were evaluated on multiple days (days 18 and 20) (Table 13). When comparing the luminal and mucosal counts of the third donor, the lumen bacterial cell counts are significantly higher compared to the mucus, while in the proximal small intestine

and the ileum of the second donor, the mucosal cell counts are not significantly different from those in the lumen (Table 12).

Table 12: Mucosal (cells/g) and luminal (cells/mL) counts in the proximal small intestine and the ileum of the second and third donors. The mean and standard deviation was calculated on day 16, with two replicates (n = 2) for the second donor, while over day 18 and 20, with each time two replicates (n = 4) for the third donor.

		Mucus		Lumen	
Donor	**Compartment**	Mean (cells/g)	Standard deviation	Mean (cells/mL)	Standard deviation
Donor 2	**Proximal small intestine**	3.70E+08	3.99E+07	4,27E+08	7,70E+07
	Ileum	5.48E+09	2.46E+08	6,69E+08	6,47E+06
Donor 3	**Proximal small intestine**	1.67E+08	9.92E+07	2.38E+08	7.75E+07
	Ileum	1.49E+09	1.45E+08	1.22E+09	2.77E+08

Furthermore, luminal intact cell counts obtained with flow cytometry and plating were compared during the SHIME of the third donor. In the proximal small intestine, the plating counts (Table 14) were significantly lower compared to the flow cytometry counts, while the ileum plating and flow cytometry counts were not significantly different.

Table 13: Intact luminal flow cytometry and plating counts in the proximal small intestine and the ileum of the third donor. The mean and standard deviation were calculated over days 18 and 21, with each time 2 replicates (n = 4).

	Flow cytometry		Plating		
Compartment	Mean (cells/mL)	Standard deviation	Mean (cells/mL)	Standard deviation	P value
Proximal small intestine	1.62E+08	1.11E+07	1.07E+08	3.60E+07	0.02857
Ileum	1.06E+09	2.39E+07	9.33E+08	2.73E+08	0.8000

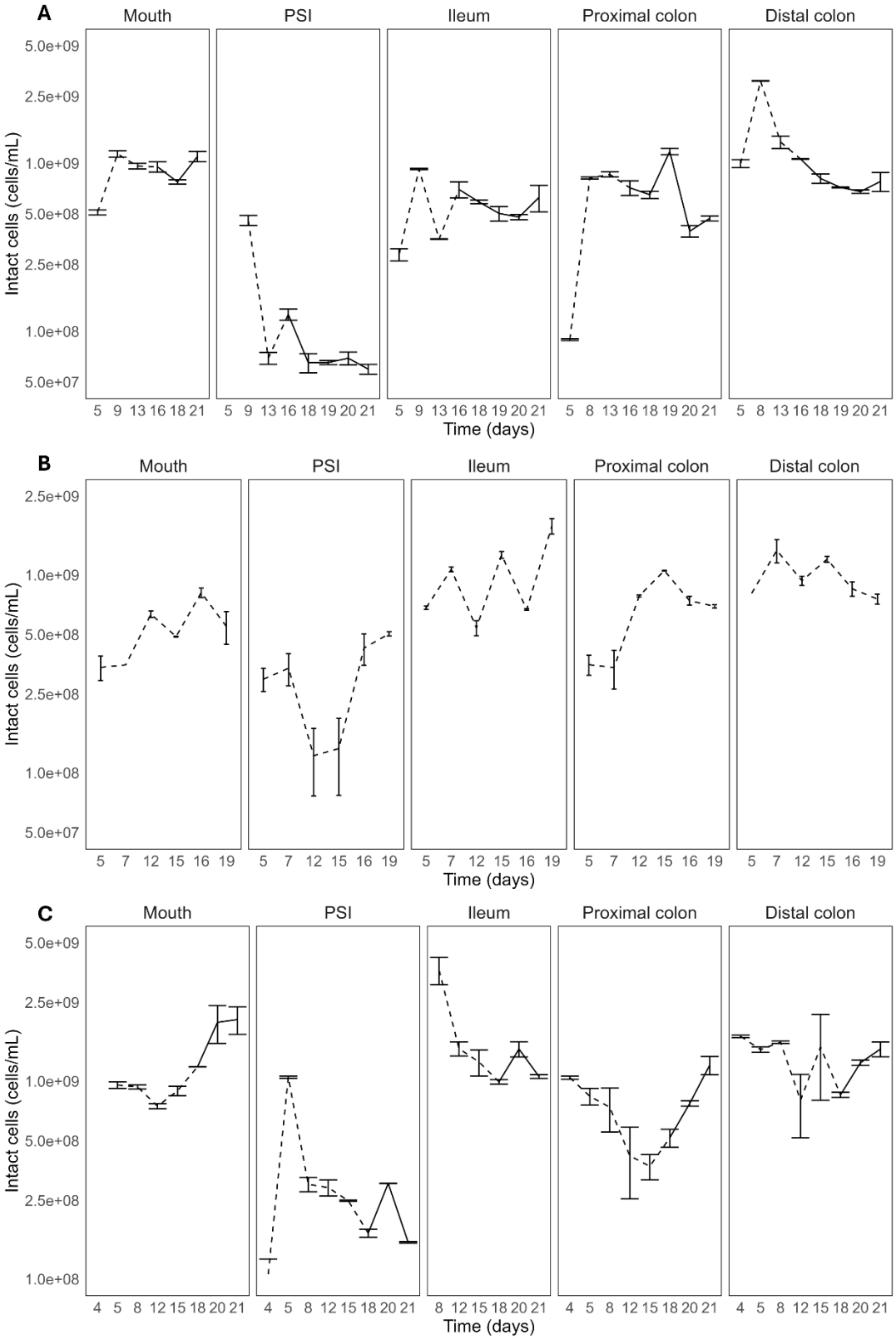

*Figure 13: Mean bacterial intact cell counts (cells/mL) of **A** the first donor, **B** the second donor, and **C** the third donor, separated by compartment, determined by flow cytometry and SGPI staining. Means and standard deviations are calculated based on two technical replicates (n = 2). PSI stands for proximal small intestine.* Stable days are indicated by a dashed line, the non-stable phase is indicated by a full line.

5.2.2 Organic acid profiles

The organic acids were measured to identify the bacterial metabolic activity in each SHIME compartment. For the first donor, the mean was calculated over four stable days, while for the third donor, three stable days were considered. For the second donor, since the run was terminated before the stable phases, the organic acid profile represents the concentration on the days before stability (days 9 and 12 for the mouth, proximal small intestine, and ileum, and days 9, 12, and 13 for the proximal colon and distal colon). The organic acid concentrations in the upper digestive tract (mouth, proximal small intestine, and ileum) are shown as concentrations measured in each compartment (Figure 14), while the values of the colon compartments are reported as net daily production (Figure 15). The net daily production represents what is produced in a compartment in one day, by taking into account the residence time and the in- and outflow of the compartment.

Throughout the different compartments, acetate was the predominant organic acid except in the proximal colon of the second donor where propionate was more abundant. Furthermore, the organic acid profile of the first donor exhibited greater diversity and yielded a higher total amount of organic acids compared to that of the second and third donors.

In the mouth compartment of the first donor, acetate (24.14 ± 1.29 mM) predominated, followed by propionate (6.54 ± 0.34 mM) and butyrate (1.51 ± 0.51 mM) (Figure 14, Table S 9). Lactate was detected in low quantities (0.003 ± 0.003 mM). Similarly, acetate (2.91 ± 0.45 mM) was the primary component in the second donor, closely trailed by propionate (2.31 ± 0.54 mM) (Figure 14). Notably, no butyrate was detected. In the mouth of the third donor, acetate (5.98 ± 0.49 mM), propionate (5.29 ± 0.18 mM), and butyrate (3.55 ± 0.22 mM) were most abundant. Lactate (0.11 ± 0.10 mM) and formate (0.36 ± 0.13 mM) were also present, though in lower concentration compared to the other organic acids present. The organic acid profile varied among the three donors. The first donor exhibited a more diverse pattern and higher total amount of organic acids compared to the third and especially the second donor (35.46 mM, 5.95 mM, and 17.61 mM for the first, second, and third donor, respectively). Acetate was predominantly detected in all three donors, with the concentration of the first donor being ten times that of the second donor and five times the concentration of the third donor (Figure 14). Propionate was also abundant in the first and third donors, with nearly triple the concentration in the first donor compared to the second donor. Notably, the mouth of the first donor contained minimal lactate, in contrast to the second (0.33 ± 0.20 mM) and third donor, but did contain valerate and a more diverse array of branched short-chain fatty acids (BCFA), which were not detected in the simulated mouth of the second and third donors.

The metabolic profile of the simulated proximal small intestine from the first donor was primarily characterized by acetate (4.41 ± 0.93 mM) and lactate (2.03 ± 0.12 mM) (Figure 14). In contrast, the proximal small intestine of the second donor predominantly contained acetate (2.57 ± 0.18 mM) and formate (2.27 ± 0.24 mM) (Figure 14, Table S 9). Similarly, the third donor exhibited a predominance of acetate (2.81 ± 0.19 mM), lactate (2.46 ± 0.39 mM), and formate (1.07 ± 0.33 mM). The total organic acid concentration in the proximal small intestine of the first donor was 8.52 mM, 6.31 mM for the second donor, and 6.94 mM for the third donor, indicating a similar overall concentration among the donors, but with a more diverse profile observed in the first donor (Figure 14). Notably, the proximal small intestine of the first donor and third donor contained BCFA (the first donor: 0.40 ± 0.01 mM, donor 3: 0.11 ± 0.007 mM) and butyrate (the first donor: 0.13 ± 0.03 mM, donor 3: 0.22 ± 0.01 mM), which were not found in the proximal small intestine of the second donor.

In the ileum of the first donor, the most prominent organic acids were acetate (11.01 ± 2.14 mM), formate (7.51 ± 1.33 mM), and lactate (3.41 ±1.35 mM) (Figure 14, Table S 9). Similarly, in the second donor, acetate (5.73 ± 0.78 mM), formate (5.98 ± 1.08 mM), and lactate (2.06 ± 0.06 mM) were the most abundant (Figure 14). The ileum of the third donor exhibited mainly acetate (7.93 ± 1.46 mM), formate (6.63 ± 0.43 mM), lactate (5.17 ± 1.46 mM), and propionate (1.35 ± 0.29 mM). Acetate, lactate, and formate were predominant in the ileum of all donors, with the highest concentrations observed in the first donor (Figure 14). This pattern extends to the total organic acid concentration in the donors, with the first donor showing the highest concentration and most diverse range of organic acids (23.73 mM) compared to the second (14.25 mM) and third (21.22 mM).

In the proximal colon, acetate, propionate, and butyrate were daily net produced with acetate 38.50 ± 2.92 mM, propionate 15.20 ± 0.73 mM, and butyrate 12.07 ± 1.88 mM for the first donor (Figure 15, Table S 10). Additionally, isobutyrate,

isovalerate, and valerate were net-produced, while formate, lactate, and isocaproate were net-consumed (Figure 15). For the second donor, unexpectedly low concentrations of butyrate were obtained. More in particular, the net daily production ratio of acetate was 23.34 ± 4.51 mM, for propionate 20.94 ± 4.48 mM, and butyrate 0.41 ± 0.44 mM (Figure 15), which triggered us to stop the experiment as the butyrate-producing functionality was almost completely lost. Furthermore, lactate and isovalerate were net daily produced, while formate and caproate were net daily consumed. In the third donor, acetate, propionate, and butyrate were primarily net produced, with a concentration of 25.35 ± 0.59 mM for acetate, 21.41 ± 0.84 mM for propionate, and 11.12 ± 1.37 mM for butyrate (Figure 15). Moreover, isobutyrate, isovalerate, and valerate were net-produced, whereas lactate and formate were net-consumed. Overall, the organic acid composition in the proximal colon of the second donor was less diverse compared to donor three and especially one. Furthermore, the second donor exhibited almost no butyrate compared to the other two donors.

In the distal colon of the first donor, formate, lactate, propionate, butyrate, and isocaproate were net-consumed to produce mainly acetate (5.25 ± 3.28 mM) and caproate (3.88 ± 2.06 mM), along with isobutyrate, isovalerate, valerate, caproate, heptanoate, and octanoate (Figure 15,Table S 10). All measured organic acids were net-produced or consumed by the distal colonic bacteria of the first donor. In contrast, only lactate and formate were net-consumed in the distal colon of the second donor, mainly resulting in the formation of acetate (38.92 ± 4.13 mM), propionate (28.74 ± 4.58 mM), but also some isobutyrate, butyrate, isovalerate, and valerate (Figure 15). In the distal colon of the third donor primarily acetate (33.83 ± 2.72 mM), propionate (23.14 ± 2.03 mM), and butyrate (14.14 ± 1.13 mM) were net obtained, with additional net production of isobutyrate, isovalerate, and valerate (Figure 15). Lactate and formate were net-consumed in the distal colon of the third donor. Consistent with the earlier compartments, the first donor displayed the most diverse organic acid profile, while donors two and three exhibited similar organic acids.

Overall, the net daily concentration of organic acids in the proximal colon exceeded that of the distal colon. In the proximal colon of the first donor, a total of 71.95 mM was net-produced, compared to 9.24 mM in the distal colon. Similarly, the second donor exhibited 59.81 mM in the proximal colon and 25.49 mM in the distal colon. In the case of the third donor, 58.72 mM of organic acids were net-produced in the proximal colon, while only 12.09 mM were net-consumed in the distal colon (Figure 15, Table S 10).

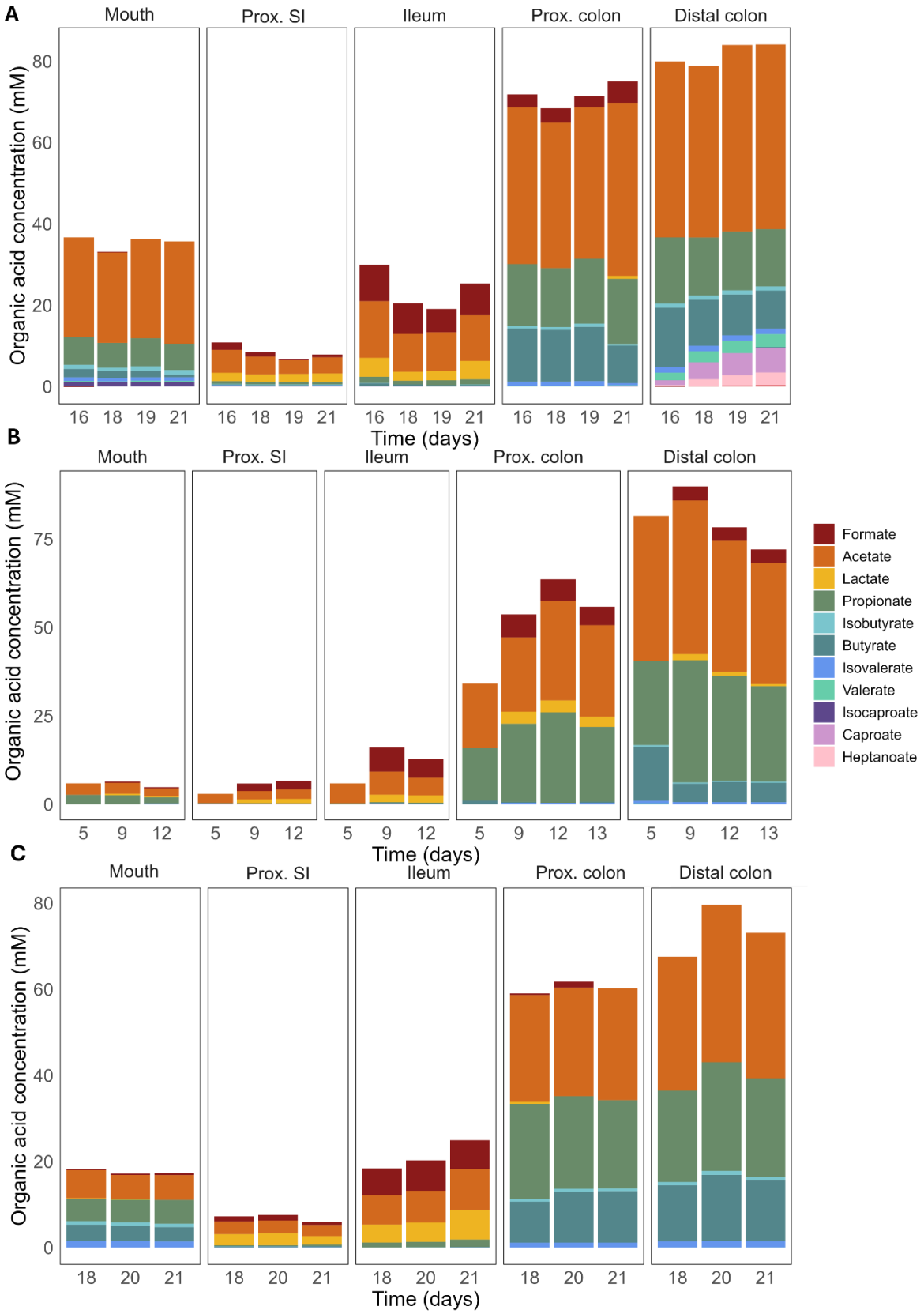

*Figure 14: Organic acids concentration (mM) during the SHIME run of **A** the first donor, **B** the second donor, and **C** the third donor, per compartment and day. Prox. SI indicates the proximal small intestine and Prox. colon the proximal colon.*

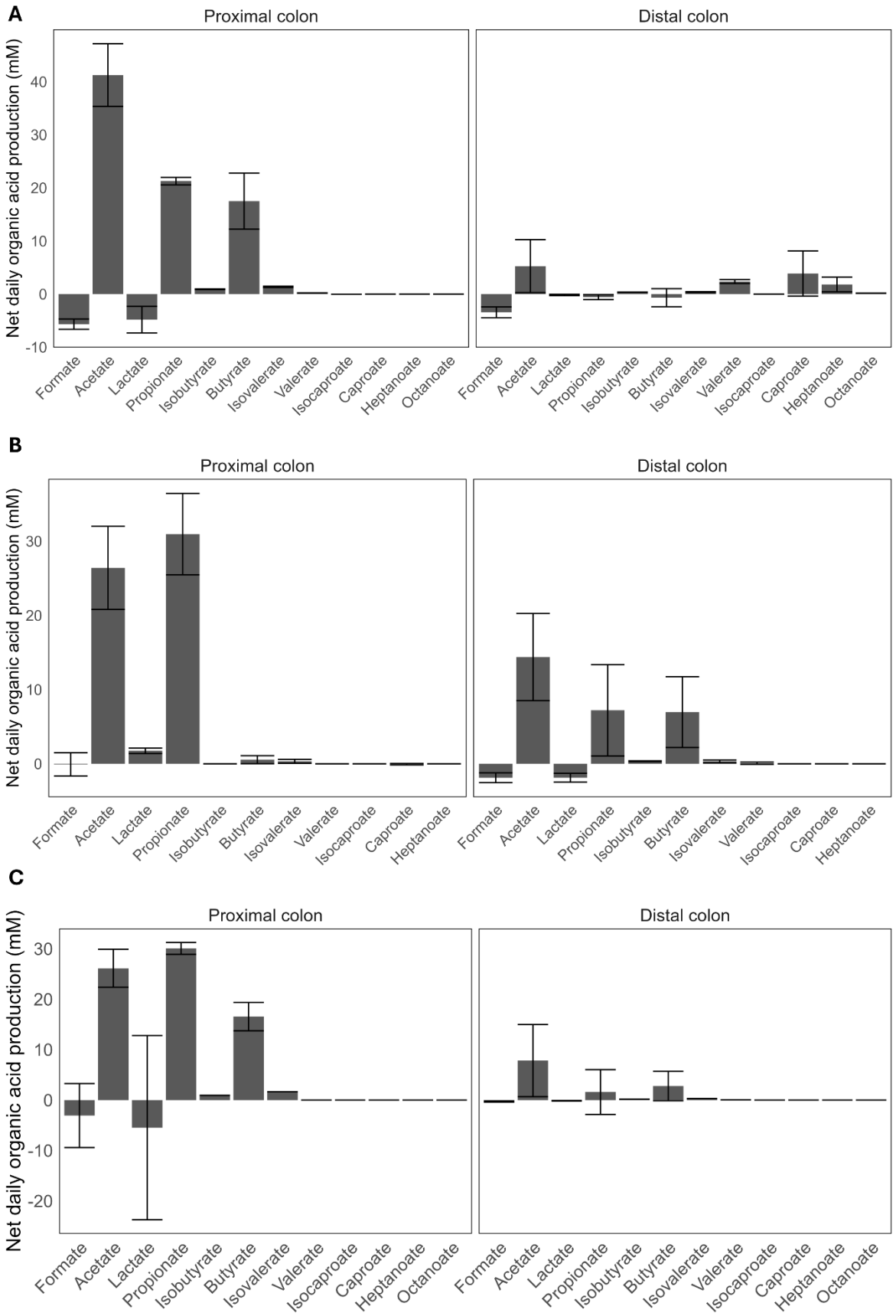

*Figure 15: Daily net organic acid production in the proximal colon and distal colon during the stable days of **A** day 16, 18, 19, and 21 for the first donor (n = 4), **B** day 9, 12, and 13 for the second donor (n = 3), **C** day 18, 19, and 21 for the third donor (n = 3).*

5.2.3 Ammonium concentration

The NH_4^+ concentration during the stable days of the first donor was higher in the distal colon (26.00 ± 1.41 mM), compared to the proximal colon (15.92 ± 0.89 mM) (Figure 16). Similarly, the ammonium concentration was higher for the distal colon (20.90 ± 0.65 mM) than in the proximal colon (9.93 ± 2.20 mM) of the third donor. The lowest concentration of ammonium in the third donor was detected in the ileum (4.09 ± 0.50 mM) (only measured for the third donor).

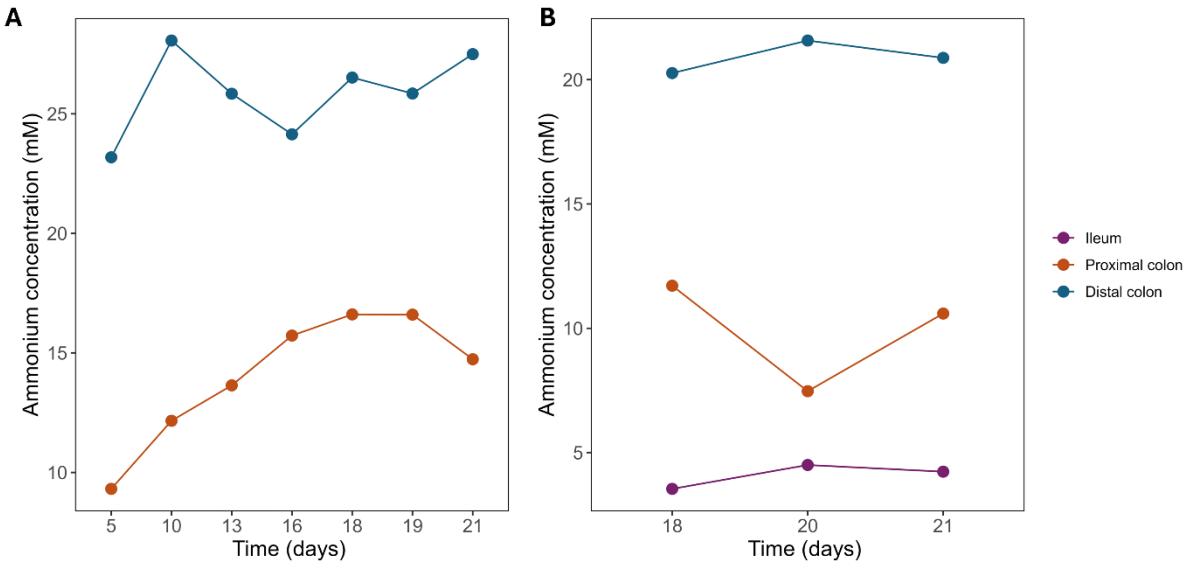

*Figure 16: Ammonium concentration of **A** the first donor and **B** the third donor in the proximal colon and distal colon of the SHIME run of the second donor.*

5.2.4 Gas composition

The O_2 content in the proximal small intestine during the stable SHIME of the first donor (15.56 ± 4.19%) was higher than for the second (4.08 ± 4.76%) and third donor (5.06 ± 2.25%) (Figure 17, Figure 18, Figure 19). Similarly, the ileum of the first donor (12.24 ± 6.11%) contained a higher level of O_2 than the second (3.44 ± 4.00%) and third donor (2.56 ± 1.54%). The CO_2 concentration was the highest in the proximal colon (the first donor: 45.35 ± 15.85%, the second donor: 34.15 ± 11.09%, third donor: 30.69 ± 8.68%) and distal colon (the first donor: 31.34 ± 13.28%, the second donor: 34.18 ± 23.80%, donor 3: 24.42 ± 3.71%), compared to the other compartments. The H_2 concentration was the highest of all compartments in the proximal colon in the first (13.40 ± 6.29%) and third donor (3.08 ± 1.75%), while in the second donor, the distal colon (7.54 ± 2.72%) displayed the highest concentration of H_2, compared to all compartments.

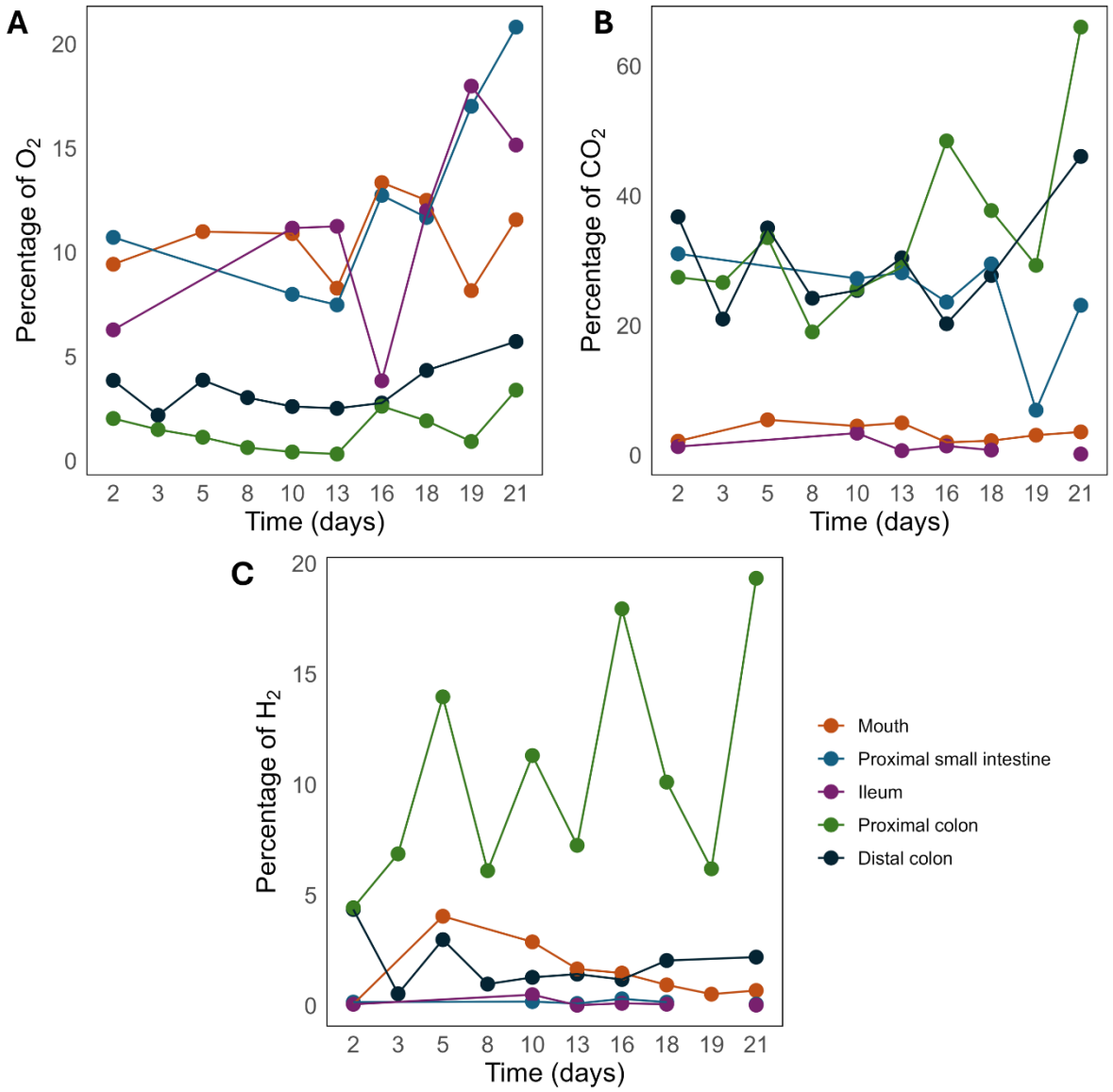

*Figure 17: **A** O_2, **B** CO_2 and **C** H_2 composition in the different SI-M-SHIME compartments during the SHIME of the first donor.*

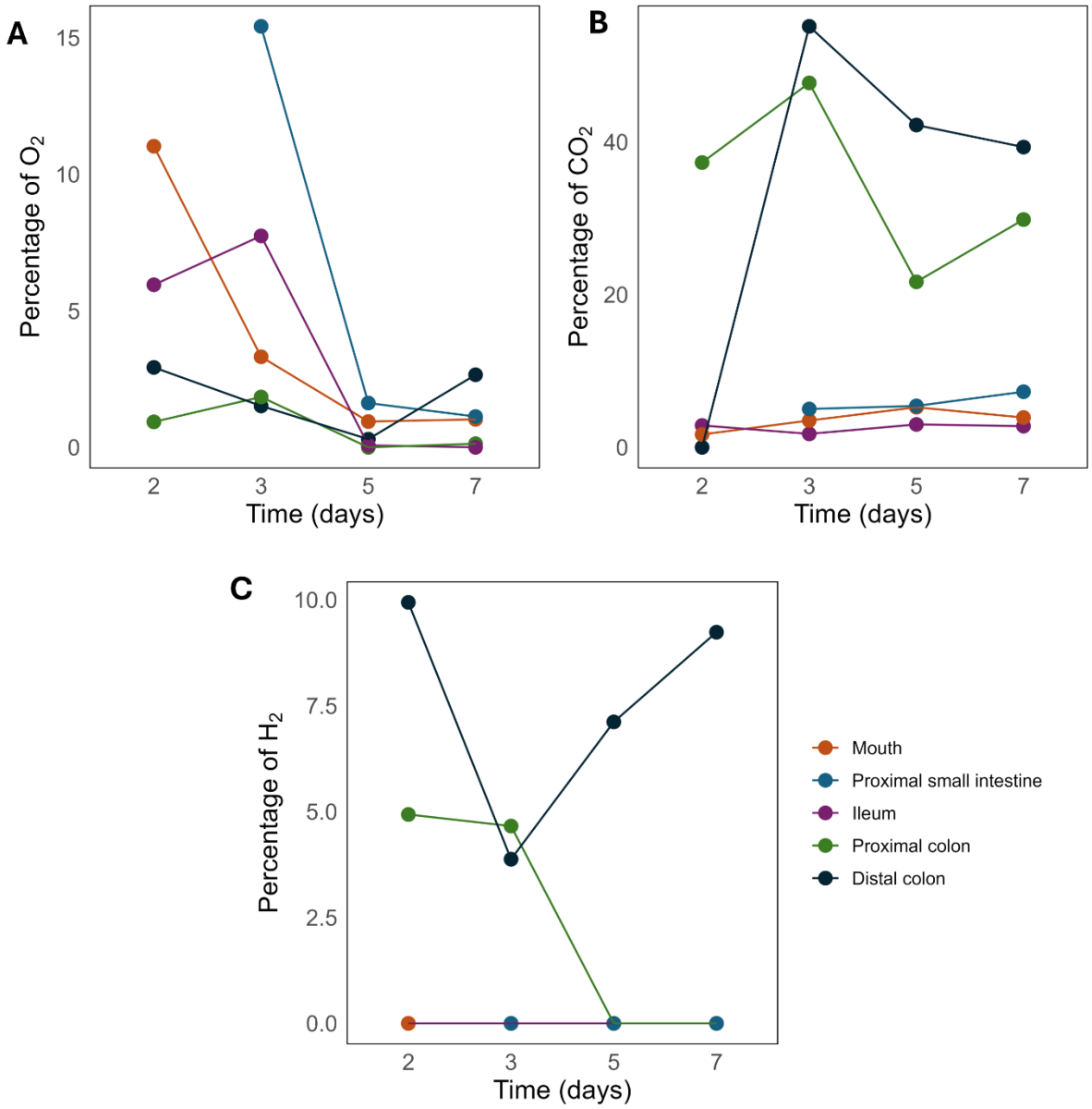

*Figure 18: **A** O_2, **B** CO_2 and **C** H_2 composition in the different SI-M-SHIME compartments during the SHIME of the second donor.*

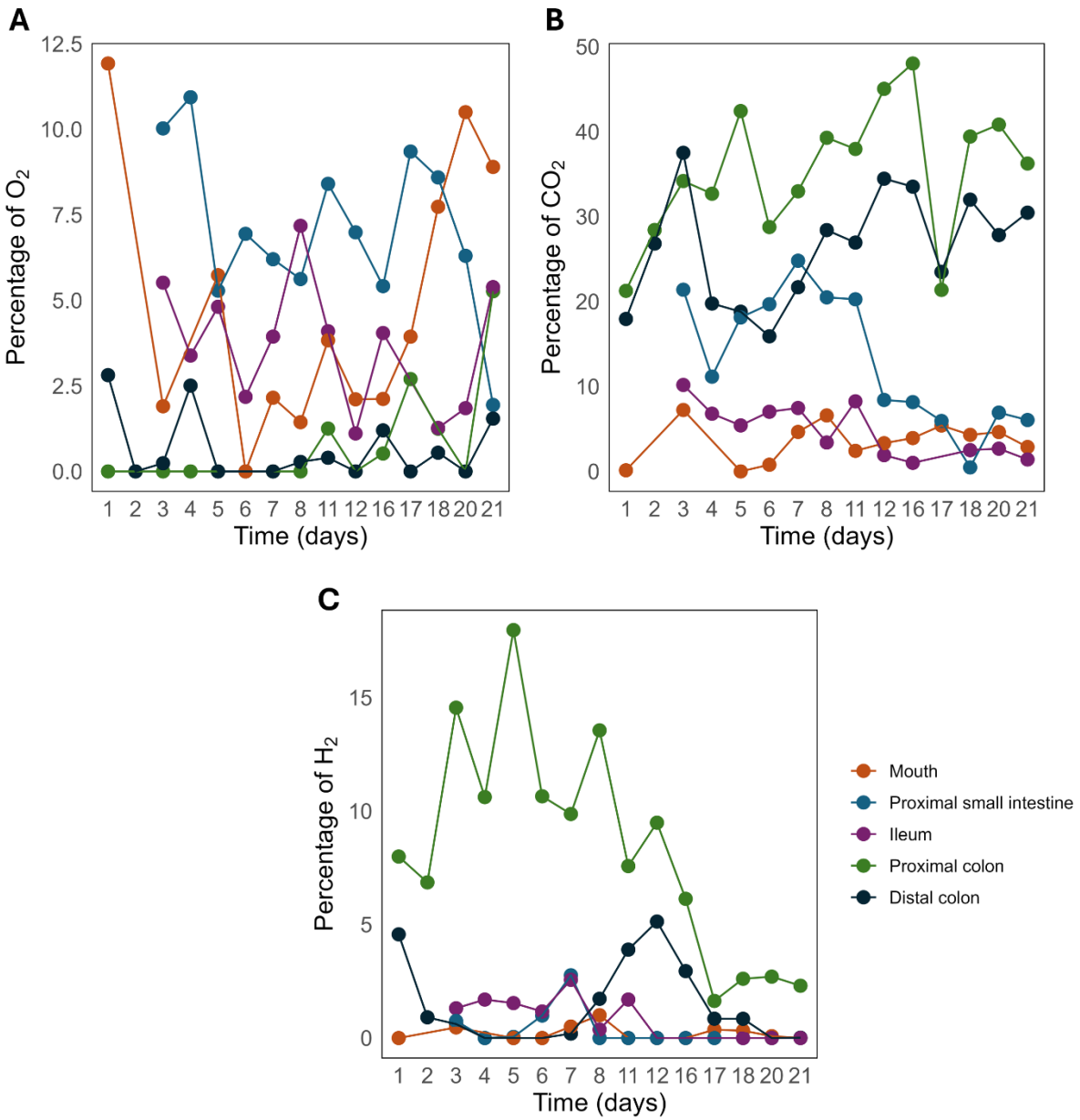

*Figure 19: **A** O2 ,**B** CO2,and **C** H2 composition in the different SI-M-SHIME compartments during the SHIME of the second donor.*

5.2.5 The bacterial composition of the first donor is more diverse compared to the second donor.

The microbial community of the first and second donors was assessed to get a better understanding of the bacterial community in the SI-M-SHIME compartments. For the third donor, the results could not be acquired in the timeframe of this thesis. Absolute bacterial abundance values were obtained for the lumen by combining flow cytometry total cell counts and relative bacterial community composition (see 4.3.5). Relative abundances were obtained for the mucus. The reported relative or absolute abundances of the first donor are the mean of the stable day samples (lumen n = 3 and mucus n = 2), while for the second donor only day 12 was investigated.

First the *in vitro* and *in vivo* bacterial community results of the first donor will be discussed, followed by the investigation of potential sources of contamination. At last, *in vitro* results of the second donor were examined.

5.2.5.1 *In vitro* bacterial community of the first donor

A principal coordinate analysis (PCoA) of the first donor showed the saliva microbiome to be closer to the mouth compartment compared to other compartments (Figure 20) reflecting the bacterial composition that contained similar genera (Figure 21). In the saliva of the first donor, *Streptococcus* ($1.66*10^8$ ± cells/mL) was most prominent, followed by *Actinomyces* ($1.06*10^8$ cells/mL), *Veillonella* ($4.58*10^7$ cells/mL), *Rothia* ($3.57*10^7$ cells/mL), *Leptotrichia* ($2.10*10^7$ cells/mL), and *Prevotella* ($2.20*10^7$ cells/mL) (Figure 21). The salivary genera were mostly conserved in the mouth compartment, although in a different absolute abundance. Genera that were conserved include, *Streptococcus* ($8.07*10^8$ ± $4.38* 10^8$ cells/mL), *Veillonella* ($1.29*10^8$ ± $7.91*10^7$ cells/mL), *Leptotrichia* ($2.59*10^7$ ± $2.87*10^7$ cells/mL), *Actinomyces* ($4.71*10^7$ ± $7.81*10^7$ cells/mL), and *Prevotella* ($1.17*10^7$ ± $3.89*10^6$ cells/mL), while *Rothia* was no longer present. Other species, with an abundance above 10^7 cells/mL in the mouth compartment include *Solobacterium* ($4.25*10^7$ ± $6.54*10^7$ cells/mL), *Granulicatella* ($2.56*10^7$ ± $2.48*10^7$ cells/mL), *Peptostreptococcus* ($1.69*10^7$ ± $8.25*10^6$ cells/mL), and *Fusobacterium* ($8.57*10^7$ ± $2.19*10^7$ cells/mL). These also occurred in the saliva inoculum sample, although in smaller numbers, except for *Peptostreptococcus* which was not detected (Table S 11)

The lumen of the proximal small intestine of the first donor maintained the presence of *Escherichia-Shigella* ($1.66*10^8$ ± $7.03*10^7$ cells/mL) (Figure 21). Notably, on day 5, this genus was not yet present. During the stable days, genera in the proximal small intestine also include *Streptococcus* ($2.3*10^7$ ± $1.18*10^7$ cells/mL), *Solobacterium* (3.36 $*10^6$ ± $5.81*10^6$ cells/mL), *Actinomyces* ($1.98*10^6$ $3.44*10^6$ cells/mL), *Veillonella* ($1.83*10^6$ ± $3.17*10^6$ cells/mL), *Levilactobacillus* ($1.69*10^7$ ± $5.99*10^6$ cells/mL), and *Bacillus* ($1.07*10^6$ ± $6.99*10^5$ cells/mL). On day 5, *Clostridium sensu stricto 1* was very abundant ($6.46*10^7$ cells/mL) in the lumen, whereas it was not present during the stable period. The proximal small intestine mucosal community resembled the luminal community. The mucus of the proximal small intestine was characterized predominantly by the presence of *Escherichia-Shigella* (67.70 ± 6.86%), *Bacteroides* (14.01 ± 1.15%), *Clostridium sensu stricto 1* (1.00 ± 0.95%), and *Levilactobacillus* (15.00 ± 8.88%). Yet, some differences can be discerned based on the relative abundance such as a higher abundance in the mucus of the genera *Bacteroides* and *Clostridium sensu stricto 1,* while *Streptococcus* (0.24 ± 0.17%) was less present, compared to the lumen.

The ileal lumen was mainly colonized by *Escherichia-Shigella* ($6.01*10^8$ ± $9.84*10^7$ cells/mL), *Enterococcus* ($5.99*10^7$ ± $3.36*10^7$ cells/mL), *Levilactobacillus* ($3.19*10^7$ ± $1.49*10^7$ cells/mL), *Bacteroides* ($2.21*10^7$ ± $1.47*10^6$ cells/mL), *Clostridium sensu stricto 1* ($1.52*10^7$ ± $1.95*10^7$ cells/mL), and *Bifidobacterium* ($1.08*10^7$ ± $6.57*10^6$ cells/mL) (Figure 21). The ileum mucosal composition was comparable with the luminal composition, although the genera *Bacteroides* (16.87 ± 9.48%), *Clostridium sensu stricto 1* (12.53 ± 4.47%), *Lachnoclostridium* (1.81 ± 0.42%), and *Veillonella* (1.03 ± 0.83%) were more abundant in the mucus, whereas *Levilactobacillus* (0.48 ± 0.05%) was less abundant compared to the lumen (Figure 21). Notably, on the day of the retrograde inoculation (day 5), prior the inoculation of the ileum, *Clostridium sensu stricto 1* ($2.94*10^8$ cells/mL), *Streptococcus* ($4.35*10^7$ cells/mL), and *Bacillus* ($1.56*10^7$ cells/mL) genera were more abundant in the lumen, compared to the stable days, while *Bacteroides* was only detected in very low amounts in the relative abundances (0.01%).

Similarly to the other compartments, in the lumen of the proximal colon, *Escherichia-Shigella* ($7.50*10^8$ ± $2.85*10^8$ cells/mL) was the most abundant genus (Figure 21). The proximal colon was characterized by the presence of *Lachnoclostridium* ($2.88*10^8$ ± $2.28*10^8$ cells/mL), *Bacteroides* ($2.54*10^8$ cells/mL), *Bifidobacterium* ($9.88*10^7$ cells/mL), *Agathobacter* ($1.68*10^7$ cells/mL), *Bilophila* ($1.11*10^7$ cells/mL), *Blautia* ($3.22*10^7$ ± $1.34*10^7$ cells/mL), *Collinsella* ($4.45*10^7$ ± $1.61*10^7$ cells/mL), *Enterococcus* ($6.43*10^7$ ± $5.51*10^6$ cells/mL), *Faecalibacterium* ($3.89*10^7$ ± $4.67*10^7$ cells/mL), *Lachnospiraceae ND3007 group* ($1.56*10^7$ ± $1.05*10^7$ cells/mL), *Roseburia* ($5.61*10^7$ ± $2.38*10^7$ cells/mL), and *Veillonella* ($1.08*10^7$ ± $2.52*10^6$ cells/mL). On the day of the retrograde inoculation, *Bifidobacterium* ($1.49*10^9$ cells/mL) and *Streptococcus* ($6.31*10^7$ cells/mL) were more prominent compared to the stable phase, and *Escherichia-Shigella* and *Bacteroides* were not yet detected. The mucosal part of the proximal colon clustered with the luminal part, as seen in the PCoA, revealing the similarity in composition between the mucosal part and the lumen (Figure 20). The main differences between the mucus and lumen of the proximal colon were less *Lachnoclostridium* (3.96 ± 1.32%), and more *Veillonella* (4.68 ± 0.11%), and *Bifidobacterium* (14.23 ± 3.28%) in the proximal colon mucus.

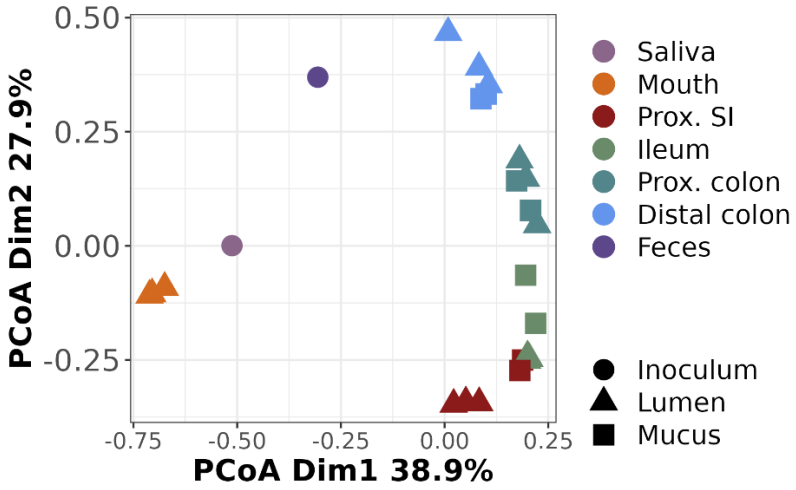

Figure 20: Principle coordinate analysis of the bacterial composition of the different compartments of the first donor and second donor. Prox. SI stands for proximal small intestine and Prox. colon for proximal colon

In the distal colon, *Escherichia-Shigella* ($3.31*10^8 \pm 1.46*10^8$ cells/mL) was present, although not as prominent as in the three preceding compartments (Figure 21). Besides, *Bacteroides* ($3.00*10^8 \pm 4.87*10^7$ cells/mL), *Faecalibacterium* ($1.47*10^8 \pm 7.66*10^7$ cells/mL), *Lachnoclostridium* ($2.04*10^8 \pm 1.43*10^7$ cells/mL), *Agathobacter* ($1.17*10^7 \pm 1.85*10^6$ cells/mL), *Bifidobacterium* ($2.42*10^7 \pm 2.29*10^6$ cells/mL), *Blautia* ($8.40*10^7 \pm 3.03*10^7$ cells/mL), *Bilophila* ($1.75*10^7 \pm 4.25*10^6$ cells/mL), *Collinsella* ($2.87*10^7 \pm 5.14*10^6$ cells/mL), *Enterococcus* ($1.36*10^7 \pm 6.74*10^6$ cells/mL), *Lachnospiraceae ND3007 group* ($3.87*10^7 \pm 1.08*10^7$ cells/mL), *Parabacteroides* ($1.46*10^7 \pm 4.75*10^6$ cells/mL), *Roseburia* ($3.55*10^7 \pm 2.39*10^7$ cells/mL), and *Subdoligranulum* ($7.65*10^7 \pm 3.87*10^7$ cells/mL) were detected. On the day of the retrograde inoculation, more *Bifidobacterium* ($4.20*10^8$ cells/mL) was present, while less *Escherichia-Shigella* ($1.37*10^6$ cells/mL) was present. In the mucus, similarly to the proximal colon, less *Lachnoclostridium* (6.35 ± 1.67%), *Faecalibacterium* (1.71 ± 0.64%), and *Blautia* (2.24 ± 0.15%) were present compared to the lumen, while more *Enterococcus* (10.52 ± 1.35%) species occurred.

The PCoA revealed that the feces of the first donor were more similar to the distal colon (Figure 20). Genera that were abundant in both the feces and distal colon comprised *Subdoligranulum* (feces: $3.40*10^9$ cells/mL, distal colon: $7.65*10^7$ cells/mL), *Faecalibacterium* (feces: $1.05*10^9$ cells/mL, distal colon: $1.47*10^8$ cells/mL), *Collinsella* (feces: $4.44*10^9$ cells/mL, distal colon: $2.87*10^7$ cells/mL), *Blautia* (feces: $2.03*10^9$ cells/mL, distal colon: $8.40*10^7$ cells/mL), *Bifidobacterium* (feces: $8.01*10^8$ cells/mL, distal colon: $2.42*10^7$ cells/mL), *Bacteroides* (feces: $4.29*10^8$ cells/mL, $3.00*10^8$ cells/mL). Genera which were abundant in the feces and in low abundance in the distal colon (< 10^7 cells/mL) include *Methanobrevibacter* (feces: $2.52*10^9$ cells/mL, distal colon: $3.05*10^5$ cells/mL), *Coprococcus* (feces: $1.3*10^9$ cells/mL, distal colon: $6.10*10^5$ cells/mL), *Christensenellaceae* R-7 group (feces: $1.12*10^9$ cells/mL, distal colon: $2.13*10^6$ cells/mL), *Akkermansia* (feces: $1.43*10^9$ cells/mL, distal colon: $6.86*10^6$ cells/mL), and *Prevotella* (feces: $1.79*10^9$ cells/mL, $1.22*10^6$ cells/mL). Genera that were abundant in the feces, but not detected in the distal colon, comprise *Romboutsia* ($2.21*10^9$ cells/mL), *Clostridium sensu stricto 1* ($1.17*10^9$ cells/mL), and CAG-352 ($9.98*10^8$ cells/mL), which is part of the Ruminococcaceae family (Figure 21, Table S 11).

Notably, *Enterococcus* and *Bacillus* were identified in the distal colon but were not identified in the donor's feces. Moreover, these genera were not yet detected on day 5 *in vitro* and were also not discovered in the donor's saliva. *Actinomyces* ($6.10*10^5 \pm 2.64*10^5$ cells/mL), *Solobacterium* ($1.52*10^5 \pm 2.64*10^5$), and *Veillonella* ($1.52*10^5 \pm 2.64*10^5$ cells/mL) were present in the distal colon, although in low abundance, and were solely detected in the donor's saliva and in the mouth compartment.

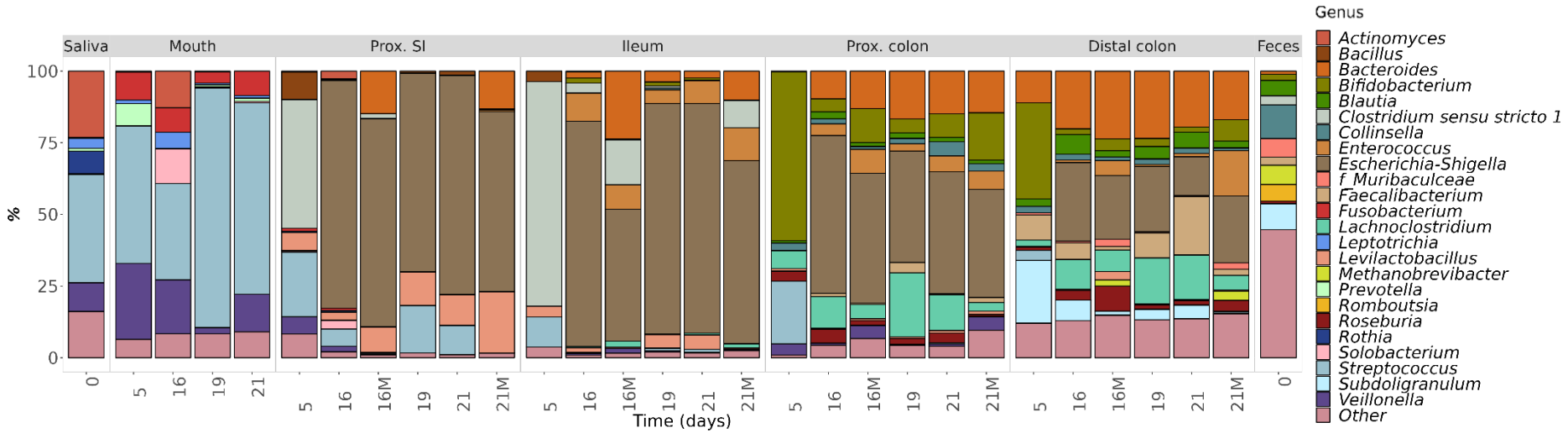

Figure 21: Proportional bacterial composition based on 16S rRNA gene amplicon sequencing in the different SHIME compartments of the first donor. On the x-axis the days were displayed, and the M represents the mucosal sample of the day, Prox. SI stands for proximal small intestine and Prox. colon for proximal colon. The ASV of Muribaculaceae could not be classified on genus level, therefore f_Muribaculaceae stands for the family of Muribaculaceae.

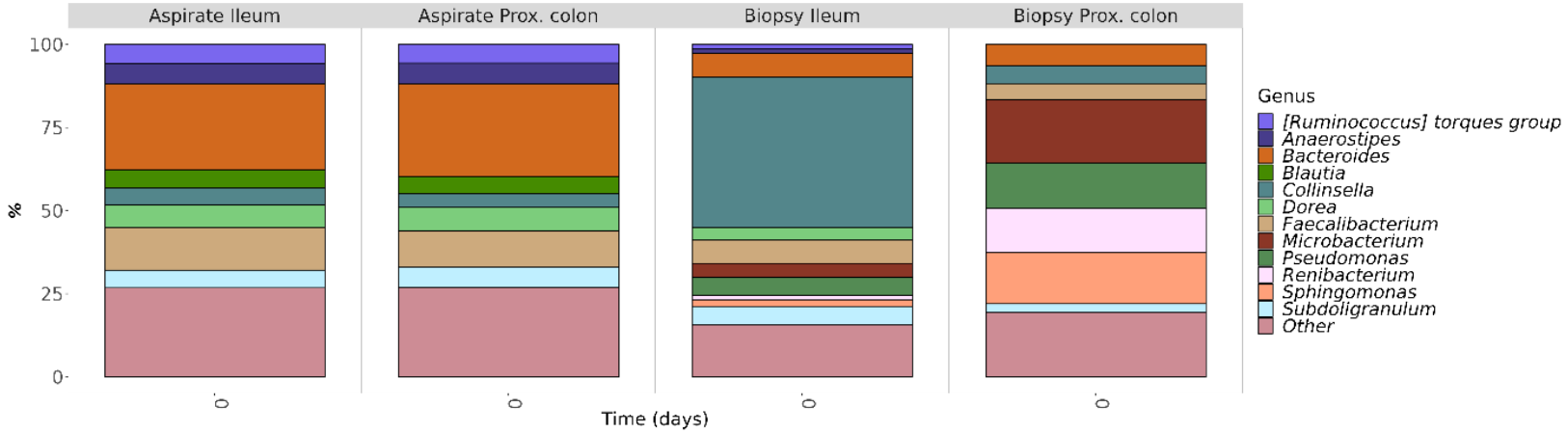

Figure 22: Proportional bacterial composition of the aspirates and biopsies from the first donor. Prox. colon stands for proximal colon.

5.2.5.2 *In vivo* bacterial results of the first donor

For the validation of the SI-M-SHIME, a biopsy and aspirate from both the ileum and proximal colon were obtained. The composition of the ileal and proximal colon aspirate was very similar and mainly consisted of *Bacteroides* (ileum: 25.98%, proximal colon: 27.93%) (Figure 22). Other species identified were *Subdoligranulum* (ileum: 5.37%, proximal colon: 6.09%), *Faecalibacterium* (ileum: 12.72%, proximal colon: 10.93%), *Dorea* (ileum: 6.80%, proximal colon: 6.97%), *Collinsella* (ileum: 5.23%, proximal colon: 4.14%), *Blautia* (ileum: 5.39%, proximal colon: 5.22%), *Anaerostipes* (ileum: 5.96%, proximal colon: 6.22%), and *[Ruminococcus] torques group* (ileum:5.81%, proximal colon: 5.56%). The biopsy of the ileum mainly showed *Collinsella* (40.90%), but also *Subdoligranulum* (4.95%), *Sphingomonas* (1.68%), *Renibacterium* (1.31%), *Pseudomonas* (4.86%), *Microbacterium* (3.83%), *Faecalibacterium* (6.26%), *Dorea* (3.45%), *Bacteroides* (6.35%), *Anaerostipes* (1.12%), and *[Ruminococcus] torques group* (1.31%). After filtering the human ASVs, the biopsy of the proximal colon mainly returned *Subdoligranulum* (2.65%), *Sphinogomonas* (15.53%), *Renibacterium* (13.26%), *Pseudomonas* (13.64%), *Microbacterium* (18.94%), *Faecalibacterium* (4.92%), *Collinsella* (5.30%), and *Bacteroides* (6.44%).

5.2.5.3 Origin of genera present in the SHIME system of the first donor

For the DNA extraction process and sequencing several blanks were included as controls. The blanks were mainly characterized by the presence of *Microbacterium*, *Renibacterium*, and *Sphingomonas.* In the first blank, also *Pseudomonas* was detected (Figure 23).

The ASVs of *Streptococcus*, *Enterococcus*, *Bacteroides*, and *Escherichia-Shigella* present in the proximal small intestine were plotted across all compartments and the inputs of the SHIME (Figure 24). Looking at the ASVs of *Streptococcus* present in the proximal small intestine, these are likely derived from the mouth compartment. Only one ASV of *Enterococcus* was identified in the proximal small intestine, which was also found in both the proximal colon and ileum. While 43 distinct *Bacteroides* ASVs were present throughout the SHIME, only 5 were present in the proximal small intestine. These 5 were also detected in the ileum, proximal colon, and distal colon. Two different *Escherichia-Shigella* ASVs were discovered in the proximal small intestine. These two were also abundantly present in the ileum, proximal colon, and distal colon. However, the most prevalent ASV was also detected in the SHIME feed, included as a control, for the run of the first donor. This may be indicative of contamination.

Several ASVs present in the mouth compartment across all investigated days were also found in the lumen or mucus of the subsequent compartments. ASVs belonging to the genera *Actinomyces*, *Clostridium* sensu stricto 1, *Granulicatella*, *Streptococcus*, *Solobacterium*, and *Veillonella* were detected in all subsequent compartments. *Peptostreptococcus* and *Prevotella* were exclusively found in the proximal small intestine and the ileum, while *Leptotrichia* was identified in the latter two compartments as well as the proximal colon. *Fusobacterium* were observed in the proximal small intestine, ileum, and distal colon.

To investigate the influence of the retrograde inoculation, ASVs present in the proximal colon on the day of the retrograde inoculation (day 5) were examined to see if they were also present in the preceding compartments during the stable days. Genera present in the proximal colon on day 5, which were found in the proximal small intestine during the stable days but not in the mouth compartment, included *Levilactobacillus* and *Escherichia-Shigella*. For the ileum, *Agathobacter*, *Bacteroides*, *Bifidobacterium*, *Blautia*, *Collinsella*, *Escherichia-Shigella*, *Lachnoclostridium*, *Lachnospiraceae* ND3007 group, *Levilactobacillus*, and *Roseburia*, which were found in the proximal colon on day 5, were also detected on the stable days. Although no ASVs from *Enterococcus* and *Bacteroides* in the proximal colon were present at the time of the retrograde inoculation, ASVs of *Enterococcus* present in the proximal colon after day 5 were found in the ileum, while *Bacteroides* were found in both the proximal small intestine and ileum. The *Bacteroides* identified after the retrograde inoculation in the small intestinal compartments was also detected in the feces of the donor.

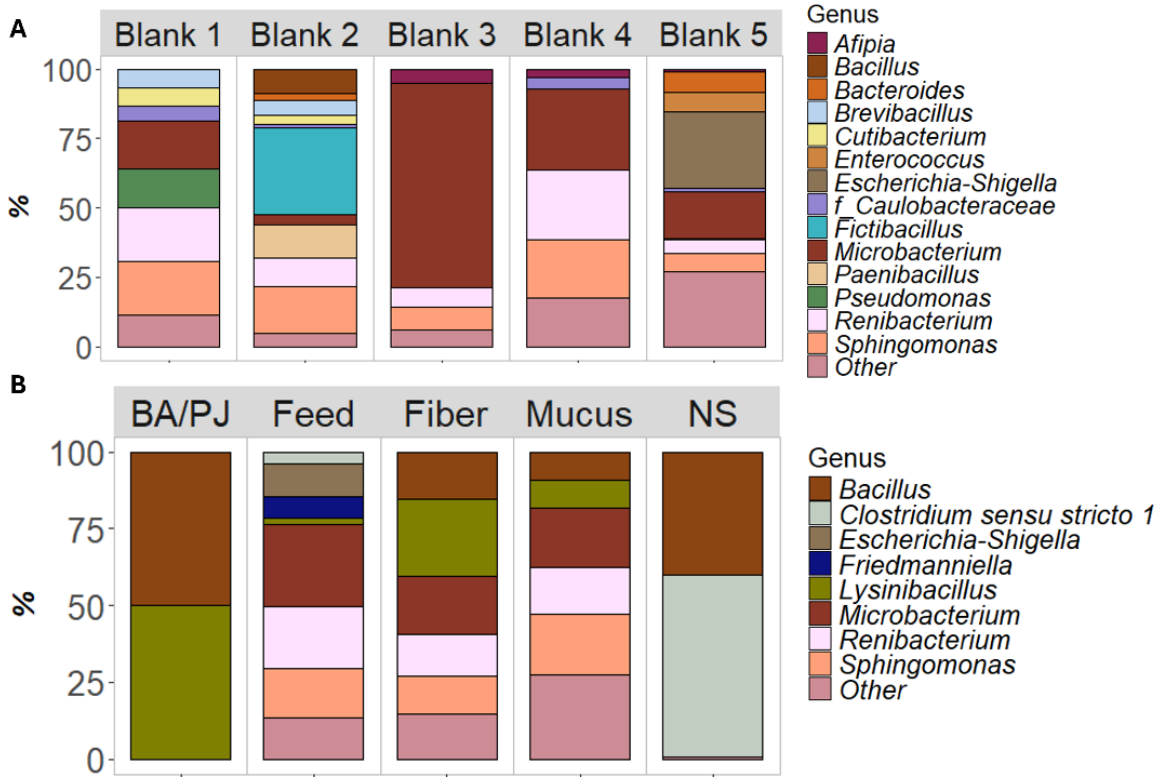

*Figure 23: **A** Blanks added during extraction and PCR of the SHIME of the first donor and **B** extracted inputs of the SHIME with BA/PJ = Bile acids and pancreatic juice, SI M-SHIME Feed, Concentrated SI SHIME Fiber medium, mucus extracted from the small intestinal beads, and NS = Nutritional saliva. The ASV of Caulobacteraceae could not be classified on genus level, therefore f_Caulobacteraceae stands for the family of Caulobacteraceae.*

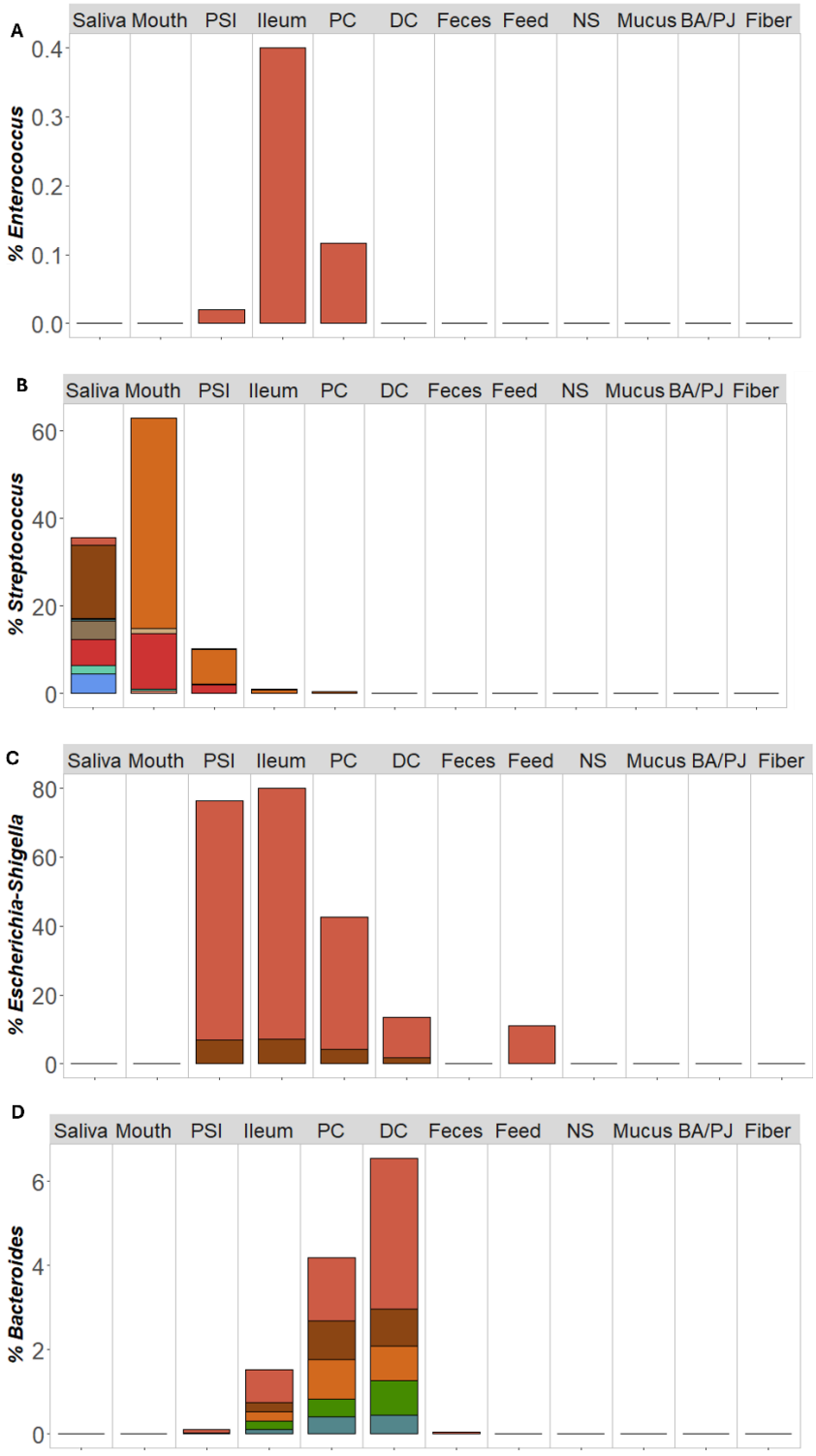

*Figure 24: The different ASVs of **A** Streptococcus, **B** Enterococcus, **C** Escherichia-Shigella, and **D** Bacteroides in the lumen of the compartments during day 21 (PSI = proximal small intestine, PC = proximal colon, DC = distal colon), saliva, feces, feed, nutritional saliva (NS), mucus of the small intestine (mucus), Bile acids and pancreatic juice (BA/PJ), and fiber solution (Fiber) added to the SHIME of the first donor. Each ASV within a genus is indicated with another color.*

5.2.5.4 *In vitro* bacterial community of the second donor

As the SHIME of the second donor was terminated earlier due to unexpectedly low butyrate levels in the proximal colon, only DNA samples from one day (day 12) and the inocula (saliva and feces) were extracted and sequenced.

In the mouth, proximal small intestine, and ileum the dominant genus observed was *Serratia* (Figure 25). This genus was also identified in the proximal colon and distal colon, although less prevalent. Notably, this genus was not detected in either saliva or feces.

The bacterial community of the saliva mainly consisted of *Actinomyces* ($1.7*10^7$ cells/mL), *Prevotella_7* ($1.38*10^7$ cells/mL), *Rothia* ($2.12*10^7$ cells/mL), *Streptococcus* ($3.47*10^7$ cells/mL), and *Veillonella* ($1.11*10^7$ cells/mL) (Figure 25). In contrast, the mouth compartment contained only limited genera with mainly *Serratia* ($6.34*10^8$ cells/mL), *Acinetobacter* ($5.65*10^7$ cells/mL), and *Fontibacillus* ($1.24*10^7$ cells/mL), none of which were detected in the saliva of the donor. Similar to the saliva of the donor, the mouth compartment presented *Streptococcus* ($5.03*10^4$ cells/mL) and *Veillonella* ($1.75*10^6$ cells/mL) but did not contain *Rothia, Actinomyces,* and *Prevotella.*

The proximal small intestine of the second donor encompassed mainly *Serratia* ($5.73*10^8$ cells/mL) and *Enterococcus* ($6.51*10^7$ cells/mL) (Figure 25). Similar to the proximal small intestine, the ileum was inhabited by *Serratia* ($4.93*10^8$ cells/mL), *Enterococcus* ($2.56*10^8$ cells/mL), and *Acinetobacter* ($1.03*10^7$ cells/mL).

The proximal colon was mainly colonized by *Megamonas* ($7.82*10^8$ cells/mL), *Bacteroides* ($3.40*10^8$ cells/mL), *Serratia* ($2.99*10^8$ cells/mL), *Enterococcus* ($1.79*10^8$ cells/mL), and *Bacteroides* ($3.40*10^8$ cells/mL) (Figure 25). Although *Serratia* is abundant, it likely did not grow in this compartment. This is because the ileal fluid (200 mL), which contained the bacterial cells from the ileal lumen, was transferred to the proximal colon, resulting in a total volume of 400 mL. Therefore, a dilution factor of two must be considered. The proximal colon counts were lower than twice the ileal counts.

On the PCoA plot, the distal colon and proximal colon were in close proximity, which was also perceived in a similar bacterial composition (Figure 25, Figure 26). The distal colon included mainly *Megamonas* ($7.03*10^8$ cells/mL), *Enterococcus* ($3.29*10^8$ cells/mL), and *Bacteroides* ($3.65*10^8$ cells/mL).

The feces of the donor was mainly inhabited by *Bifidobacterium* ($7.17*10^9$ cells/mL), *Collinsella* ($2.74*10^9$ cells/mL), *Faecalibacterium* ($2.12*10^9$ cells/mL), *Blautia* ($2.27*10^9$ cells/mL), *Bacteroides* ($9.98*10^8$ cells/mL), *Alistipes* ($7.81*10^8$ cells/mL), *Ruminococcus* ($7.20*10^8$ cells/mL), and *Megamonas* ($3.84*10^8$ cells/mL) (Figure 25). Although *Faecalibacterium* and *Ruminococcus* were prominent in the feces, they were not identified in the distal colon of the second donor. Notably, the feces and saliva of the second donor contained fewer ASVs compared to the first donor.

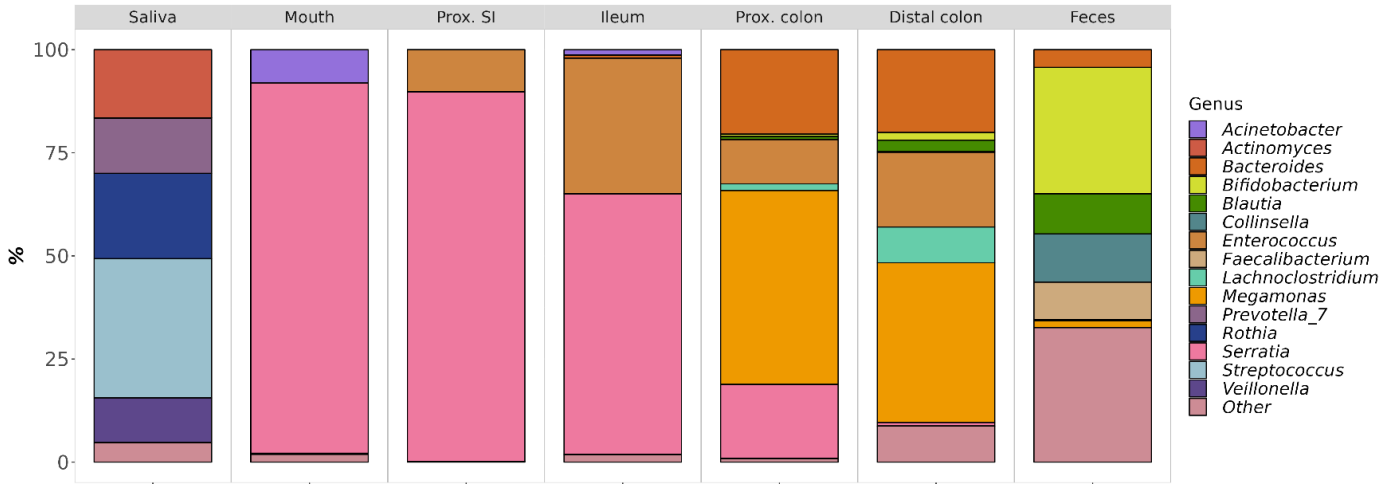

Figure 25: Proportional bacterial composition based on 16S rRNA gene amplicon sequencing in the different SHIME compartments on day 12 of the second donor. Prox. SI stands for proximal small intestine and Prox. colon for proximal colon.

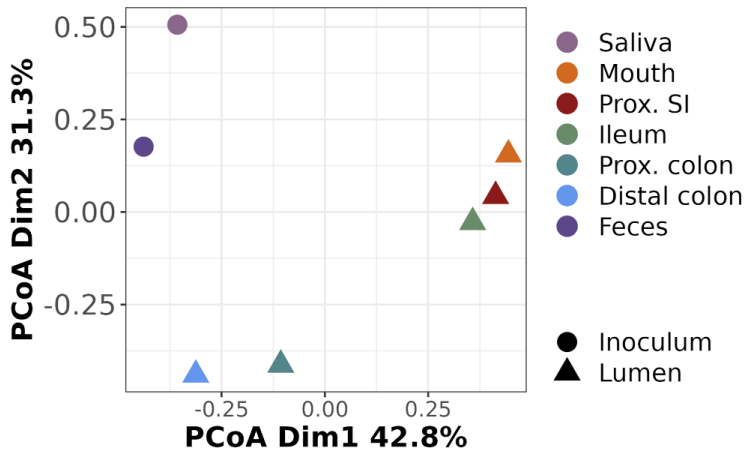

Figure 26: Principle coordinate analysis of the bacterial composition of the different compartments of the second donor. Prox. SI stands for proximal small intestine and Prox. colon for proximal colon.

5.2.6 Phenotypic diversity

Although specific information regarding the bacterial composition of the third donor is lacking, insights into the bacterial community can be obtained from the phenotypic characteristics detected *via* flow cytometry. To this end, the phenotypic diversity was calculated, using two fluorescence and two scatter signals, across the three donors. The intact cell population flow cytometry data from day 21 for the first and third donors were analyzed, while for the second donor, day 12 was considered.

The mouth of the third donor exhibited the highest phenotypic diversity across all donors and compartments, contrasting with the lower diversity observed in the second and first donors (Figure 27). Among the proximal small intestine, the diversity was more similar between donors, with the third donor having the highest diversity, while the first donor had the lowest diversity. The second donor displayed the lowest phenotypic diversity in the last three compartments. In the ileum, the third donor had the highest diversity, while in the proximal and distal colon, the second donor had the highest. Beta diversity analysis showed no clear clustering, although the distal colon compartments oriented together (Figure 28).

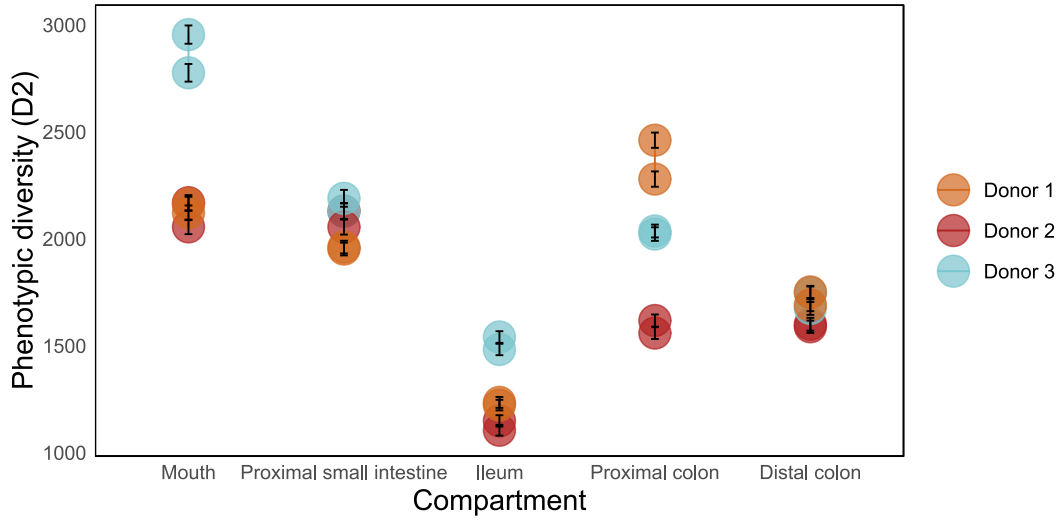

Figure 27: Phenotypic diversity of the three donors for the different compartments. Day 21 is considered for the first and third donors, while day 12 for the second donor, with two technical replicates.

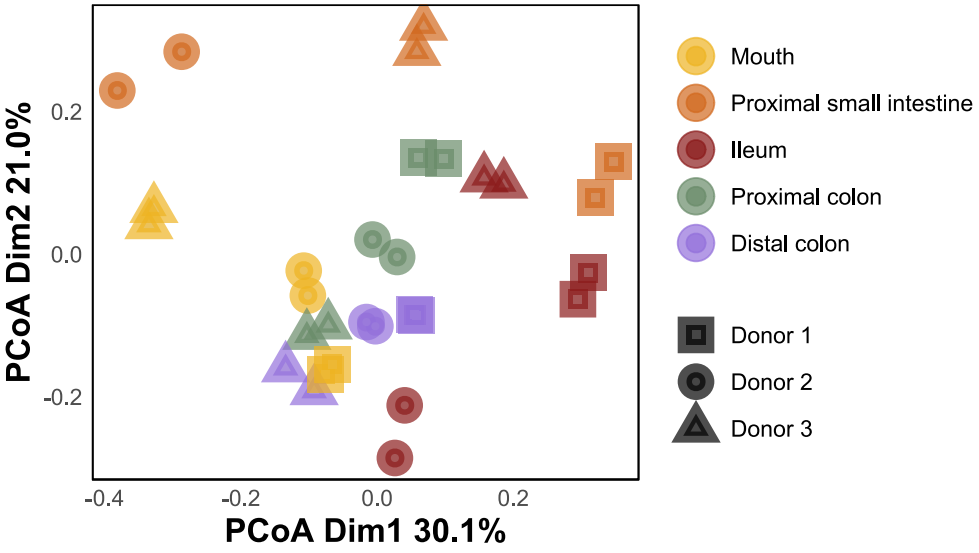

Figure 28: Community beta diversity of the three donors for the different compartments.

6 DISCUSSION

In this thesis, an *in vitro* model was developed and validated to mimic the human small intestine and its resident microbiota. To achieve this, the SHIME gastrointestinal model, created by Molly et al. (1993), was adapted. Three small intestinal M-SHIMEs (SI M-SHIME) were run with three different donors. The *in vitro* samples were evaluated for metabolite production, bacterial cell counts, and bacterial composition. To validate the model, the microbial community *in vitro* of the first and second donors was compared with literature *in vivo* data and *in vivo* gastrointestinal samples for the first donor. Moreover, additional experiments were conducted to improve the model, such as membrane efficiency to filter out the sugars.

6.1 The Small Intestinal M-SHIME can recapitulate genera found *in vivo*

6.1.1 Validation of the system by comparison to literature data

The mouth compartment is representative compared to literature, except for the lack of Rothia detection.

The mouth compartment of the first donor exhibited genera such as *Streptococcus, Veillonella, Leptotrichia,* and *Prevotella,* which are recognized as part of the human mouth core microbiome (Bik et al., 2010; Chen & Jiang, 2014). The genera *Granulicatella, Fusobacterium, Gemella*, *Solobacterium, Haemophilus, Treponema, Catonella, Actinomyces, Selenomonas,* and *Peptostreptococcus,* identified in our system, are not typically part of this core microbiome, but have been documented in the subgingival plaque, saliva, gingival crevicular fluid and/ or dorsal surface of the tongue (Liu et al., 2012; Liu et al., 2020). Although *Rothia* is a frequently mentioned genus of the oral cavity and was present in the saliva of the first donor, it was not detected in the mouth compartment. The growth of *Rothia* may have been limited by the absence of simulated surfaces like the dorsal tongue or buccal membrane, potentially leading to its displacement by other competing genera. Additionally, the oxygen levels of approximately 10% in the mouth compartment might be insufficient for the aerobic genus *Rothia* (Fatahi-Bafghi, 2021). Nevertheless, the mouth compartment contained hydroxyapatite discs to promote biofilm development in which *Rothia* is suggested to be involved (Uchibori et al., 2013). The absence of certain micronutrients might also explain the lack of *Rothia.* For example, molybdenum is a cofactor for nitrate-reductase enzymes, which might be necessary for the nitrate-reducing bacterium *Rothia* (B. Rosier et al., 2020; B. T. Rosier et al., 2020). Furthermore, nitrate is absent in the nutritional saliva in the SI M-SHIME, even though *in vivo* salivary nitrate concentrations of 0.1 to 0.5 mM in fasting conditions have been reported, while 5 to 8 mM in fed conditions (Lundberg & Govoni, 2004). Therefore, the lack of nitrate and molybdenum in the nutritional saliva might limit the nitrate reductive metabolism of *Rothia*, potentially restricting its growth. Furthermore, several species of this genus have been found to encode the siderophore enterobactin, which can bind Fe^{3+}, Mg^{2+}, and Zn^{2+}. This may indicate the importance of supplementing various metallic ions (Uranga et al., 2020), which is confirmed by a study indicating that in order to grow *R. mucilaginosa,* six metal ions (Fe^{3+}, Mn^{2+}, Zn^{2+}, Co^{2+}, Cu^{2+}, Fe^{2+}) needed to be supplemented to the RPMI medium (Leonidou et al., 2024). While in our medium hemin is present, containing Fe^{3+}, the addition of the Mn^{2+}, Zn^{2+}, Co^{2+}, Cu^{2+}, Fe^{2+} might improve *Rothia* growth. The nutritional saliva medium added in the SI M-SHIME is vitamin-deprived, except for menadione. In contrast, the RPMI medium used in the previously mentioned study contained several vitamins. While the specific vitamin requirements of *Rothia* are not well understood, this deficiency might be a contributor to the lack of *Rothia.*

While the mouth compartment of the first donor harbored a diverse community, the second donor predominantly hosted *Serratia* and *Acinetobacter,* both of which have been observed *in vivo* in the oral cavity, yet in lower amounts (Barbosa et al., 2006; Souto et al., 2014). Nonetheless, the limited diversity is likely attributed to the overgrowth of *Serratia,* a recognized human pathogen (Mahlen, 2011). The phenotypic fingerprinting also revealed a less diverse community, with the second donor exhibiting the lowest diversity compared to the other two donors. Similarly to the first donor, *Rothia* was not identified in the mouth compartment of the second donor, though it remains uncertain whether the lack of detection is due to the absence of biofilm surfaces, oxygen, nutrient deficiencies, or the dominance of *Serratia.*

Overgrowth of *Escherichia-shigella in vitro* in donor 1 and overgrowth of Serratia in donor 2

The proximal small intestine and the ileum of the first donor were primarily colonized by *Escherichia-Shigella.* Its prevalence extended to the proximal colon and was also detected in the distal colon. This genus has been isolated from the jejunal mucosa (Dlugosz et al., 2015), but is not seen in high amounts in the *in vivo* sample. Some species among this genus have been associated with dysbiosis in diseases such as SIBO and liver cirrhosis (Baltazar-Díaz et al., 2022; Barlow et al., 2021). Thus, its overgrowth might suggest a possible dysbiotic state within the proximal small intestinal compartment of the first donor. The donor did not report any gastrointestinal complaints and this genus was not as abundant in the aspirate of the ileum. This may suggest that the abundance of this genera is linked to the *in vitro* conditions. As this genus was also detected in the feed, its origin may be environmental. Alternatively, it could have been present in the saliva or feces of the donor, but being under the detection limit of Illumina sequencing. Besides its origin, the observed overgrowth of this genus *in vitro* could be attributed to the elevated levels of oxygen and sugar concentration, as *Escherichia-Shigella* is a facultative anaerobic microorganism capable of thriving in environments rich in oxygen and sugars (Strockbine & Maurelli, 2015). For this reason, the oxygen- and sugar content during the SHIME run of the second and third donors were lowered. Indeed, in the SHIME of the second donor, *Escherichia-Shigella* was not detected. Yet, the genus *Serratia,* another facultative anaerobic microorganism (Olajide & LaPointe, 2022), dominated nearly 90% of the system during this SHIME experiment, potentially outcompeting *Escherichia-Shigella*. In this view, no real conclusion of the effect of the lowered sugar and oxygen content on the growth of *Escherichia-Shigella* can be made when comparing sequencing data from the first and the second SHIME runs. Notably, *Serratia* was not detected in the saliva and feces of the donor. A SHIME from pig samples (SPIME) performed in the lab previously to the described SHIME of donor 2 showed a low presence of Serratia (data not shown). As such, it is plausible to think that its presence may be attributed to residual *Serratia* in the vessels from this previous SPIME. Several bacteria from the *Serratia* genus are nosocomial pathogens, responsible for hospital-acquired infections (Haddy et al., 1996; Penna et al., 2001). Nevertheless, the reason for its dominance remains uncertain. Potentially, the residual cleaning solution hindered the initial establishment of the saliva genera. This, combined with the presence of *Serratia,* may have allowed *Serratia* to dominate.

Most proximal small intestinal genera have been identified in the proximal small intestine *in vivo*.

Additionally to *Escherichia-Shigella*, *Streptococcus,* and *Veillonella,* which were present in the SHIME of the first donor, have been observed inhabiting the lumen of the duodenum and jejunum *in vivo* (Li et al., 2015; Nagasue et al., 2022; Seekatz et al., 2019). In contrast, genera such as *Solobacterium, Actinomyces, Levilactobacillus,* and *Bacillus*, which were prevalent *in vitro*, have not yet been recovered from the duodenal and jejunal lumen. Nevertheless, *Levilactobacillus, Bacillus,* and *Actinomyces* have been identified in the duodenal and/ or jejunal mucus *in vivo*, while *Solobacterium* has been detected in the ileal mucus *in vivo* (Nagasue et al., 2022; Vasapolli et al., 2019; Villmones et al., 2018; Wang et al., 2005).

In the SHIME of the second donor, *Acinetobacter* was notably abundant and has been isolated from the duodenal lumen *in vivo,* whereas *Serratia* has not been found in the small intestine *in vivo* (Li et al., 2015; Nagasue et al., 2022; Seekatz et al., 2019). Nonetheless, the community lacks diversity, as mentioned before, probably due to the overgrowth of *Serratia*, which hindered the establishment of a diverse community. Despite the overgrowth of *Serratia*, phenotypic diversity analysis of days sequencing indicates that the second donor had the highest diversity. These apparent diverging results in sequencing and flow cytometry-based phenotypic diversity may arise from genera taking on multiple phenotypic forms (Props et al., 2016). Additionally, Illumina sequencing was based on the total bacterial population, while the phenotypic diversity was based on the intact bacterial population. In this regard, it is worth noting that 16S rRNA sequencing might yield biased results due to multiple copies of this gene in the genome, which is associated with fast-growing species when exposed to complex mediums (Klappenbach et al., 2000). While it is possible to adjust for copy-number variations, these tools still perform poorly (Louca et al., 2018). Lastly, by sequencing the sorted live fraction of the bacterial population instead of the total population, part of the described results could be associated with the damaged bacterial fraction. To overcome this, sequencing on a live bacterial subpopulation that has been sorted out with flow cytometry-assisted single cell sorting is currently being implemented in the laboratory.

The ileum luminal environment is representative of the *in vivo* environment.

The ileum compartment of the first donor exhibited the presence of *Enterococcus* and *Bacteroides*, both isolated *in vivo*. These genera were also found in the ileum of the second donor *in vitro*. Notably, *Enterococcus* was not detected in the saliva and feces of both donors. *Enterococcus* might have been under the detection limit of the 16S rRNA gene Illumina sequencing in the fecal sample, since this genus has been consistently identified *in vivo (Booijink et al., 2010; Hayashi et al., 2005; Van den Bogert et al., 2013)* and in *in vitro* models in the ileal lumen (Deyaert et al., 2023). This may indicate that *Enterococcus* can thrive in the ileal environment. Contamination of this genus cannot be ruled out. However, this seems rather unlikely since this genus was not detected in the blanks. *Levilactobacillus,* previously identified in the ileal lumen *in vivo,* was also detected in the ileal lumen *in vitro*. However, it was not detected in the fecal sample or saliva, suggesting that it remained under the detection limit of Illumina sequencing. Additionally, *Clostridium* sensu stricto 1 and *Bifidobacterium* were identified in the SHIME of the first donor. Although these genera are not yet observed *in vivo* in the ileum, they have been detected *in vivo* in the colon. Notably, *Acinetobacter*, a genus previously identified *in vivo,* was present in the SHIME of the second donor (Dlugosz et al., 2015; Hayashi et al., 2005; Nagasue et al., 2022; Rivière et al., 2016; Seekatz et al., 2019; Sundin et al., 2017; Vuik et al., 2019; Wan et al., 2022; Wang et al., 2005).

The colon luminal community is representative of the *in vivo* environment.

The proximal colon and distal colon of the first donor exhibited various genera such as *Bacteroides, Blautia, Roseburia,* and *Veillonella,* aligning with the core microbiome of the colon described in literature (Falony et al., 2016). Additionally, other genera common in the colon *in vivo* such as *Escherichia-Shigella, Lachnoclostridium,* and *Bifidobacterium* were detected. Although similarities existed between the proximal colon and distal colon, discrepancies in abundance were noted: *Subdoligranulum* and *Faecalibacterium* were more prevalent in the distal colon, while *Lachnospiraceae* ND3007 group and *Bifidobacterium* were more abundant in the proximal colon.

In contrast, the proximal colon and distal colon of the second donor were characterized by a distinct taxonomic profile. The colon compartments were primarily dominated by *Megamonas, Enterococcus, Lachnoclostridium, Bifidobacterium,* and *Serratia,* none of which are part of the core microbiome, but have been detected in feces *in vivo* (Falony et al., 2016). Notably, *Serratia* was transferred during each SHIME cycle but did not proliferate in the proximal colon.

The mucosal bacterial composition differed from the luminal composition

In addition to the luminal bacteria, mucosal bacteria play a crucial role in our body, with observable differences between these niches *in vivo* (Sommer & Bäckhed, 2016). Therefore, mucin agar beads were incorporated into the SI M-SHIME to simulate the intestinal mucus. The use of mucin beads *in vitro* has been noted in previous models by Deyaert et al. (2023) and Roussel et al. (2020). In this thesis, differences between both niches were also evident.

The mucus of the proximal small intestine and ileum of the first donor generally exhibited higher levels of *Bacteroides* and *Clostridium* sensu stricto 1, but lower levels of *Streptococcus* compared to the lumen. Additionally, the ileum displayed elevated levels of *Lachnoclostridium* and *Veillonella* within the mucus compared to the lumen. Moving to the lower digestive tract, increased amounts of *Enterococcus* and *Bifidobacterium,* alongside decreased levels of *Lachnoclostridium,* were observed in the colon mucus compared to the lumen. Furthermore, the mucus of the proximal colon contained higher levels of *Veillonella* and *Bifidobacterium*. Conversely, lower levels of *Blautia* and *Faecalibacterium* were identified in the distal colon mucus than in the lumen. Several of these genera, including *Bacteroides* and *Clostridium* sensu stricto 1, are known to degrade mucus and were also more abundant in the mucosal niche of the SHIME (Calvigioni et al., 2023; Hayase et al., 2022; Raimondi et al., 2021). In contrast, mucus degraders such as *Lachnoclostridium, Blautia,* and *Faecalibacterium,* were detected in lower abundance in the mucus (Calvigioni et al., 2023; Glover et al., 2022; Raimondi et al., 2021). This may suggest a preference for the luminal habitat with mucus degradation only occurring in nutrient-deprived conditions. Interestingly, the abundance of *Bifidobacterium,* primarily found in the mucus of the large intestine, positively correlates with mucus growth rates in mice (Schroeder et al., 2018). Although the mucus growth rate was not tested in the SHIME, *Bifidobacterium* was more abundant in the mucus than the lumen of the colon.

6.1.2 Validation based on donor *in vivo* data

Validation by comparing the donor saliva sample with the mouth compartment revealed a similar community.

The saliva sample from the first donor exhibited a composition in the mouth compartment that partially mirrored the donor's saliva, though with variations in abundance. This shift resulted in *Actinomyces* and *Rothia,* which became more prevalent in the saliva, while *Peptostreptococcus* and *Solobacterium* became more abundant in the mouth compartment. Before inoculating, the saliva is collected into an Eppendorf tube which is subsequently refrigerated. Therefore, the saliva composition may have been altered by the prolonged exposure to oxygen. This likely favored aerobic bacteria such as *Actinomyces* and *Rothia* over obligate anaerobic genera such as *Peptostreptococcus* and *Solobacterium* in the saliva. In contrast, in the mouth compartment *in vitro*, oxygen levels were lower, potentially causing *Peptostreptococcus* and *Solobacterium* to flourish (Fatahi-Bafghi, 2021; Kageyama & Benno, 2015; Sharma et al., 2018; Song & Finegold, 2011). The storage method may have introduced a bias when comparing the mouth compartment *in vitro* with the saliva. Similarly, *Actinomyces* and *Rothia* were abundant in the saliva of the second donor, although a direct comparison with the mouth compartment was deemed unrepresentative due to the overgrowth of *Serratia*.

The aspirates were likely contaminated with colonic bacteria, while the low biomass biopsies contained sequencing contaminants.

In the first donor, the aspirate of the ileum exhibited a distinct composition compared to the lumen of the ileum compartment, characterized by the presence of *Subdoligranulum, Faecalibacterium, Dorea, Collinsella, Blautia, Anaerostipes,* and *Ruminococcus torques* group *in vivo*. These genera are commonly found in the large intestine and were likely introduced by colonic bacteria contamination during the sampling process, as suggested by the nearly identical bacterial compositions between the ileal aspirate and colon (Figure 22). Moreover, the biopsy of the ileum differed from the ileal mucus in the SHIME, in which mainly *Collinsella* was detected, alongside other genera such as *Ruminococcus torques group, Anaerostipes, Bacteroides, Dorea, Faecalibacterium,* and *Subdoligranulum.* Similar genera were present in the biopsy and aspirate including *Ruminococcus torques* group, *Anaerostipes, Bacteroides, Collinsella, Dorea,* and *Faecalibacterium.* However, as established before, these genera are more related to the colon microbiota, suggesting that the biopsy was possibly contaminated during the sampling procedure. Indeed, to access the sampling site and after sampling, the scope must pass through the anal canal and colon, making it susceptible to contamination with colonic bacteria. Moreover, biopsy samples are usually considered low biomass samples. Therefore, taxa found in the blanks are regularly suggested in literature to be DNA sequencing contaminants. These taxa include *Microbacterium, Renibacterium, Spinghomonas,* and *Pseudomonas* (Salter et al., 2014). Thus, it is evident, as previously mentioned (2.1.4.2) that *in vivo* sampling is prone to contamination, complicating the comparison between the SHIME community and the donor's samples. Besides contamination, it is important to consider bowel preparation as a potential source of bacterial community shifts. This preparation, used to empty the colon, has been shown to alter colonic bacteria composition (Nagata et al., 2019). Although not yet investigated, such shifts might also occur in the ileal community. Still, bias introduced due to bowel preparation is probably insignificant compared to the contamination likely seen in the aspirate and biopsies of the first donor.

The aspirate from the proximal colon of the first donor displayed differing genera abundances compared to the proximal colon compartment of the SHIME, with *Subdoligranulum, Dorea,* and *Anaerostipes* present in the aspirate, but not detected in the SHIME compartment, while present in the distal colon of the SHIME. Considering the contamination of the ileal aspirate, it is not unlikely that contamination occurred with the distal colonic microbiota. Additionally, the biopsy of the proximal colon exhibited a community characterized by *Faecalibacterium, Bacteroides, Collinsella,* and *Subdoligranulum*, taxa inhabiting the mucus of the proximal colon *in vitro,* although more abundantly present in the distal colon of the SHIME.

The distal colon compartment retained inter-individual differences.

The distal colon *in vitro* of the first donor exhibited similar genera as the fecal sample, though with varying abundances, a pattern also observed *in vivo* (Kwon et al., 2021). Notably, *Escherichia-Shigella, Enterococcus, Bacteroides,* and *Rombautsia*

showed increased prevalence in intestinal samples compared to feces (Shalon et al., 2023). This mirrored the findings of this study, except for *Romboutsia,* which was detected in feces but was not detected in the distal colon. Furthermore, genera such as *Clostridium* sensu stricto 1 and CAG-352 were identified in the feces but did not colonize the distal colon. The feces predominantly contained *Subdoligranulum, Collinsella, Blautia, Bifidobacterium,* and *Faecalibacterium.* Notably, the aspirate of the proximal colon also exhibited these genera, except for *Bifidobacterium,* suggesting contamination of the aspirate with distal colonic bacteria.

Surprisingly, the fecal composition of the second donor exhibited a closer resemblance to saliva than the colon compartments of the SHIME, based on the PCoA (Figure 26), suggesting a notable difference between feces and colon compartments. Although this is against expectations, as previously mentioned, the SHIME of the second donor experienced overgrowth of *Serratia*, resulting in a distinct composition in the colon. Genera identified in the feces include *Alistipes, Bacteroides, Bifidobacterium, Blautia, Collinsella, Faecalibacterium, Megamonas,* and *Ruminococcus*, while the distal colon of the second donor harbored *Megamonas, Bifidobacterium, Blautia,* and *Bacteroides,* although in different abundances as the feces. Despite the distinct abundances, the majority of genera found in the feces are preserved in the colon compartments. This preservation, including genera such as *Megamonas,* proves that the SI M-SHIME allows for the preservation of an individual's unique microbial signature (Van den Abbeele et al., 2010).

6.1.3 Origin of the bacteria present in the SHIME

Each SHIME run encompassed a compartment representing the mouth, stomach, proximal small intestine, ileum, proximal colon, and distal colon, simulating the entire gastrointestinal tract. As such this represents a novel *in vitro* model, never described before in literature. This configuration diverged from other small intestinal *in vitro* models previously described by incorporating salivary bacteria in a mouth compartment (Cieplak et al., 2018; Deyaert et al., 2023; Roussel et al., 2020; Stolaki et al., 2019). In this way, the oral-gut transmission could be simulated in the model (Schmidt et al., 2019).

Indeed, oral-gut transmission was clear in our system, as genera such as *Actinomyces, Clostridium* sensu stricto 1, *Granulicatella, Streptococcus,* and *Veillonella* were transmitted through the entire SHIME. Genera such as *Peptostreptococcus* and *Prevotella* were solely identified in the small intestinal compartments. They likely became outcompeted in the subsequent compartments, leading to a lack of detection in the colon compartments. Similarly, Schmidt et al. (2019) observed that *Prevotella*, initially present in the saliva was not transmitted to the feces of all patients.

The *Fusobacterium* ASVs, present in the mouth compartment, were also detected in the distal colon, but not in the proximal colon. Furthermore, these ASVs were not identified in the feces of the donor, nor the extraction/sequencing blanks. This indicates that these genera remained under the detection limit of Illumina sequencing in the proximal colon and/or feces. The oral-gut transmission was also clear in the second donor, with *Serratia* being transmitted throughout the entire system.

In addition to the salivary bacteria of the donor, the *in vitro* model was also inoculated in the ileum compartments by the proximal colon, referred to as retrograde inoculation, introducing crucial genera. As expected, genera such as *Blautia,* and *Levilactobacillus* were introduced in the ileum. Additionally, *Bacteroides* was present in the ileum. This genus was not yet detected in the proximal colon on day 5 nor in the saliva of the donor. Since this genus was present in the feces of the donor, it was likely introduced in the ileum during the retrograde inoculation, while remaining under the Illumina detection limit in the proximal colon on day 5. Surprisingly, *Bacteroides* was also present in the proximal small intestine, probably originating from the proximal colon due to cross-contamination during manipulation, as it was not identified in the mouth compartment. Similarly, although *Enterococcus* was not yet detected in the proximal colon on day 5, the proximal colon likely serves as the source of the small intestinal *Enterococcus*. Furthermore, *Bifidobacterium* was introduced. This genus has not yet been described in the ileum *in vivo*, but has been detected in the *in vitro* ileum compartment of Stolaki et al. (2019).

6.2 The dialysis membrane filters fibers next to the sugars.

To recreate bile acid and sugar absorption, a dialysis membrane was implemented between the proximal small intestine and ileum. The dialysis membrane should be able to remove most sugars and bile acids since the concentration of these components is known to differ between the proximal small intestine and ileum. For example, primary bile acids are reabsorbed for 95% in the ileum *in vivo* (ZR, 1990), with about 0.5 g/day escaping the enterohepatic circulation (Chiang & Ferrell, 2018). Beside their role in lipid digestion, these bile acids possess antibacterial properties, thereby contributing to the suppression of the resident bacterial populations (Di Ciaula et al., 2018). Unlike sugars and bile acids, the membrane should not remove the fiber and mucin since these are not absorbed in the small intestine and should arrive in the colon to be fermented by the bacteria (Wang et al., 2019). Hence, incorporating a dialysis membrane in the SHIME set-up allows the simulation of nutrient absorption. While previous studies employed for this purpose membranes with a pore size of 10 kDa (Cieplak et al., 2018; Stolaki et al., 2019), the membrane incorporated in the described SHIME set-up was the dialysis membrane 07 Sureflux Nipro with pore size 40 kDa. (Cieplak et al., 2018; Stolaki et al., 2019). Considering the larger pore size utilized in the SI M-SHIME experiment, a separate experiment was conducted to assess the extent to which the components of the SHIME medium were absorbed by the membrane.

Results indicated that sugars such as glucose, fructose, galactose, mannose are filtered out by approximately 80%, lactose by around 60%, and maltose and sucrose by approximately 30%. Additionally, some fibers were also removed, mostly xylan and mucin type II. While the removal of xylan was expected due to its low molecular weight being smaller (Durruty et al., 2017) than the membrane's cutoff, it was surprising that mucin type II, with a higher molecular weight (Schömig et al., 2016), was partially retained as well. Moreover, pectin was partly removed, although to a lesser extent. Based on this data, it was decided to supplement the ileum compartment with extra concentrated SI-SHIME medium to ensure sufficient fiber availability for bacterial fermentation in the colon.

Although the protein retraction was not assessed, it is suspected that these are also partly filtered out considering the low molecular weight of peptone (< 1 kDa) (Davami et al., 2015). Consequently, additional proteins were introduced into the ileum. To test the ingoing and filtered protein solutions, the Lowry method, a similar method as used for the carbohydrates, could be implemented (Lowry et al., 1951).

The theoretical glucose equivalents present SI M-SHIME medium were 1.4 times more than the experimental value, suggesting that the method underestimates the carbohydrate content. This is likely because not all carbohydrates were completely broken down into their respective monosaccharide. Relative values are in this case more reliable.

In addition to assessing the dialysis efficiency of the separate compounds in the SI M-SHIME medium, the efficiency of the membrane over time was also evaluated. Initially, unexpectedly, the efficiency appears to increase. However, this may be due to a lack of accuracy in this method, as seen in the high standard errors. Conversely, the efficiency seems to increase afterward, suggesting although the method is not very accurate, that the efficiency does decrease over four days. During the experiments, the membrane was changed every other day, yet based on these results we cannot conclude whether it is possible to extend the use of one membrane.

6.3 The bacterial load in the proximal small intestinal compartment was higher than *in vivo* reported values, while the bacterial load of the other compartments was within expected values.

The bacterial load in our model is similar to the *in vivo* values in the case of the mouth and ileum and compared to normal colonic cell counts in the SHIME for the proximal colon and distal colon (Minnebo, De Paepe, et al., 2023; Minnebo, Delbaere, et al., 2023; Walter & Ley, 2011). However, the proximal small intestine had a bacterial load with 3-5 orders of magnitudes higher compared to *in vivo* data in the first donor.

Considering that most of the studies on small intestinal microbiota employed plating techniques instead of flow cytometry for cell counting, plating was performed to check the comparability with the flow cytometry data. In fact, not all bacteria

can be cultured, a phenomenon referred to as the "great plate count" anomaly, which states that only 1% of the bacteria can be cultured on plates (Staley & Konopka, 1985). Additionally, plating selects for the fast growers (Hugenholtz, 2002), which could result in lower counts when compared to flow cytometry data. An experiment was therefore conducted to assess the comparability of cell counts obtained via flow cytometry and plating techniques for SHIME samples collected simultaneously. During this experiment, the cell counts for both techniques fell within the same order of magnitude, except for the proximal small intestinal cell counts, which were significantly lower when using plating. The viable counts obtained with plating also were lower compared to flow cytometry in another study (Chen & Li, 2005).

Although a difference was observed between the plating and flow cytometry counts, this cannot explain the difference of 10^3 to 10^5 of the proximal small intestine *in vitro* compared to *in vivo.* A similar situation was seen in the ileal *in vitro* model of Deyaert et al. (2023). Deyaert et al. (2023) found an ileal concentration that was too high (10^9 cells/mL) when using the normal ileal nutritional medium. Upon reduction of the simple sugars, yeast extract, special peptone, cysteine-HCl, and mucin with 70%, a typical bacterial load on the order of 10^8 cells/mL was detected in the ileum. Therefore, the sugar content was 1.6 times lower. Furthermore, since the stomach pH results in a lot of damaged/dead bacterial cells, which are transferred to the small intestine, decreasing the stomach pH or elongating the retention time at the lower pH of the stomach, could be an alternative strategy to lower the cell count. In literature it is reported that the pH drops to 1.5-2 after food entrance in *in vivo* conditions (Barret et al., 2018; Malagelada et al., 1976). In the SHIME of the first donor, the stomach pH gradually decreased from 5 to 2, with liquid transfer to the proximal small intestine starting from pH 3.25. During the run of the second and third donors, liquid transfer started at pH 3 to increase the selection pressure on the microbial population and hence further decrease the bacteria load in the proximal small intestine. However, the proximal small intestine bacterial load of the second and third donors was still an order of 10^3 to 10^5 too high compared to the *in vivo* data (Walter & Ley, 2011). The stomach empties its contents in the proximal small intestine. *In vivo,* this happens as a plug-flow system, resulting in a concentration gradient of nutrients, bile acids, and pH in the small intestine (Li & Kong, 2022). In contrast, the SI M-SHIME is a semi-continuous system, leading to one concentration for the proximal small intestine. The lack of a gradient may lead to a high concentration of nutrients in this compartment, as well as the lack of a bile acid profile as observed *in vivo,* allowing an outgrowth of the bacteria. Furthermore, it is noted that during the migrating motor complex, the loose mucus layer and its associated bacteria move towards the distal colon (Johansson et al., 2013), a process not simulated in the SI M-SHIME.

In the small intestine, various mechanisms regulate bacterial load, offering opportunities for optimization or future incorporation into the SI M-SHIME. For instance, IgA, present in the small intestine, and lysozymes, produced in the mouth, both possess antibacterial properties and could potentially be integrated (Pabst, 2012; Vila et al., 2019). Nevertheless, IgA is an antibody that binds antigens present on the bacterial surface, hence, because of its specificity, a mixture of IgA representative for the *in vivo* environment should be considered. As well, IgA-bacterial interaction is individual-specific, which hinders the application of IgA in the SHIME model (Huus et al., 2021). Another important factor controlling the microbial load *in vivo* are bile acids, naturally occurring in the small intestine and having an antibacterial effect (Di Ciaula et al., 2018). In our system 4.6 mM bile acids were present. *In vivo* values around 10 mM have been identified, suggesting that the bile acid concentration could be increased (Hofmann & Eckmann, 2006; Kalantzi et al., 2006). At last, since 9L of fluids pass daily through the small intestine (Wilson, 2004), it could be interesting to account for this in the SI M-SHIME model by diluting the fluid transfer from the mouth to the stomach.

For the second donor, more damaged cells were observed in all compartments, except for the mouth and proximal small intestine, compared to the first donor, while in the third donor, this trend was observed across all compartments. This is especially the case for the proximal colon where 10% more intact cells are found during the run of the first donor and third donor. Still, the proximal colon of the latter two donors has a high damaged cell count. The low intact ratio in both donors could be explained by the sudden pH drop from the ileum to the proximal colon or the ileal microbiota coming into a well-established microbial network in the proximal colon that outcompeted them. The lower intact ratio for the second donor is probably due to the overgrowth of *Serratia,* which did not allow for a well-established cross-feeding network.

6.4 The organic acid profiles of the first and third donors were representative of the *in vivo* environment

6.4.1 The metabolite composition of the mouth compartment contained lower levels of lactate and formate compared to *in vivo*, along with higher levels of butyrate.

The organic acid composition in the mouth compartments of all three donors differed from the *in vivo* conditions. Generally, lactate and particularly formate concentrations were lower *in vitro.* Moreover, for the first donor, the acetate, propionate, and butyrate levels were higher *in vitro*. Lactate can undergo conversion into formate, acetate, propionate, and eventually, butyrate given a sufficient timeframe (Lu et al., 2014; Takahashi, 2015). This suggests that the retention time in the mouth compartment was too long, allowing mouth bacteria to further metabolize the lactate into other metabolites. Indeed, in the third donor butyrate was also elevated *in vitro.* Interestingly, no butyrate was detected in the mouth compartment of the second donor. Nevertheless, lactate and formate concentrations were lower in the second donor *in vitro* and the organic acid profile was less diverse compared to the first and third donors. This could be attributed to *Serratia* overgrowth, as it is known to produce lactate and acetate (Solé et al., 2000), in combination with *Acinetobacter* which thrives on lactate and acetate (Towner, 1992). This overgrowth may have disrupted the establishment of a well-functioning cross-feeding network.

Organic acid profiles have been proposed as non-invasive markers for dysbiosis (Sagar et al., 2015), as demonstrated in the mouth of the second donor, where lower levels of acetate, formate, and lactate were detected. In contrast, in a healthy mouth, the predominance of formate is expected, along with the presence of lactate, acetate, propionate, and minimal to no isovalerate and butyrate (Lu et al., 2014).

6.4.2 The small intestinal compartments were characterized by rapid carbohydrate fermentation.

Organic acid concentrations in the proximal small intestine were relatively low across all three donors compared to the colon compartments. This is anticipated given that bacterial fermentation is less pronounced in the proximal small intestine due to a shorter residence time (proximal small intestine: 2h, proximal colon: 16h, distal colon: 26h). The primary metabolites formed in all three donors are acetate, lactate, and formate, alongside less abundant organic acids. A study examining the organic acid composition of the proximal small intestine identified only acetate and lactate, while formate was not investigated. Nevertheless, this was observed in sudden-death victims, necessitating cautious interpretation (Cummings et al., 1987). Lactate production is associated with rapid carbohydrate fermentation (Clausen & Mortensen, 1997), a characteristic feature of the proximal small intestine (Zoetendal et al., 2012).

The proximal small intestine of the first donor exhibited a more diverse composition compared to the other two donors. This was mirrored in bacterial composition, with the presence in the first donor of *Streptococcus* and *Levilactobacillus,* known lactate producers, alongside *Veillonella,* which can metabolize lactate to acetate and propionate (El Aidy et al., 2015). Furthermore, the proximal small intestine of the first donor showed an overgrowth of *Escherichia-Shigella*, coupled with a decrease in *Clostridium* sensu stricto 1 compared to day 5. This pattern is in line with observations in the pig ileum, where an increase in *Escherichia-Shigella* along with a decrease in *Clostridium* sensu stricto 1 under limited protein intake was seen (Fan et al., 2017). Therefore, elevated oxygen levels, high sugar content, and insufficient protein intake emerge as potential factors driving *Escherichia-Shigella* overgrowth.

The less diverse metabolite composition in the proximal small intestine of the second donor is likely due to the overgrowth of *Serratia* in combination with mainly *Enterococcus,* primarily producing acetate and formate, and to a lesser extent, lactate (Ramsey et al., 2014).

The ileal concentrations for all three donors surpassed the concentrations in the proximal small intestine, particularly with higher levels of lactate, acetate, and formate, consistent with *in vivo* findings (Cummings et al., 1987; Zoetendal et al., 2012). However, the total organic acid concentration observed *in vivo* nearly doubled the ileal concentrations in the SHIME of the

first and third donors, while almost tripling the concentrations of the second donor. However, these *in vivo* data result from the analysis of ileostomy effluent (Zoetendal et al., 2012), hence, caution is advised in interpreting these data.

In vitro, acetate concentrations in the first donor were slightly lower than those reported by Stolaki et al. (2019) but almost doubled those measured by Deyaert et al. (2023) and in ileostomy effluent *in vivo* (Zoetendal et al., 2012), which exhibited values more similar to the third donor. Conversely, acetate concentration in the second donor was slightly lower than that of the third donor. *In vivo,* propionate values doubled those found in the first and third donor and were four times higher compared to the second donor. Similarly, values reported in other *in vitro* systems were almost four times the values of the first and third donor (Deyaert et al., 2023; Stolaki et al., 2019; Zoetendal et al., 2012).

Butyrate levels in the second donor were three times lower than in the first donor and twice lower compared to the third donor. For all donors, butyrate levels were 130 to 160 times lower compared to *in vivo* values (Zoetendal et al., 2012). *In vitro* concentrations of butyrate were more comparable to other models, although still lower (Deyaert et al., 2023; Stolaki et al., 2019). Lactate composition was similar across donors, but exceeded other *in vitro* models and lower than *in vivo* data (Stolaki et al., 2019; Zoetendal et al., 2012).

Several primary fermenters such as *Levilactobacillus, Bacteroides,* and *Bifidobacterium* were present in the ileum compartment of the first donor, accounting for lactate production. This lactate could be metabolized to acetate and propionate by *Bacteroides* species and butyrate by the *Clostridium* sensu stricto 1 (Appert et al., 2020; König & Fröhlich, 2017; Kotarski & Salyers, 1981; Rios-Covian et al., 2013; Rios-Covian et al., 2016; Rios-Covian et al., 2015). In contrast, the SHIME of the second donor exhibited a much less diverse profile of organic acids, likely related to the overgrowth of *Serratia*.

6.4.3 The proximal colon was characterized by saccharolytic fermentation, while the distal colon by proteolytic fermentation.

In the first donor, the highest concentration of H_2, a well-known end product of carbohydrate fermentation, was observed in the proximal colon, along with elevated organic acid levels, which is characteristic of saccharolytic fermentation (Blachier et al., 2007; Clausen & Mortensen, 1997; Macfarlane, Gibson, & Cummings, 1992; Schneeman, 1987). However, the organic acid concentration in the proximal colon exceeded expectations, potentially due to the concentrated medium introduced into the ileum and the high sugar content of the medium. An excess of nutrients could account for the heightened concentrations of organic acids and H_2 in the proximal colon. In contrast, the distal colon exhibited lower concentrations of organic acids than anticipated. Instead, the distal colon presented elevated concentrations of ammonia and an increase in SCFA such as caproate, valerate, isovalerate, and isobutyrate. These metabolites are indicative of protein fermentation (Clausen & Mortensen, 1997; Macfarlane & Macfarlane, 2012; Mafra et al., 2013). The low organic acid profile in the distal colon likely stemmed from the depletion of the fibers in the proximal colon.

In the SHIME of the second and third donor, the sugar content of the feed was reduced by 1.6 times, aiming for a decrease in organic acid content in the proximal colon and an increase in daily net produced organic acids in the distal colon. As expected, organic acid content in the proximal colon of the second donor decreased by 0.13 times and 0.19 for the third donor. Additionally, the distal colon of the second donor exhibited an almost threefold increase in concentration compared to the first donor, while the third donor's organic acid content was 1.3 times that of the first donor. The H_2 levels for the second and third donors decreased nearly two times. However, similar to the other compartments, the results of the second donor may not be fully representative due to the overgrowth of *Serratia* in the proximal colon. The H_2 concentration in the proximal colon of the second donor initially mirrored the pattern observed in the first donor for the first three days, after which no more H_2 was detected. This may suggest that *Serratia* from then on dominated the system. Moreover, lactate was present and no butyrate was detected, indicating an incomplete cross-feeding network and potential dysbiosis (Flint et al., 2015; Flint et al., 2012). The distal colon of the second donor showed almost no increase in branched short-chain fatty acids, caproate, and valerate, indicating inadequate protein fermentation. Conversely, bacteria in the distal colon of the third

donor metabolized the lactate and formate to produce, amongst other compounds, isovalerate, isobutyrate, and valerate, although to a lesser extent than observed in the first donor.

7 CONCLUSION

This thesis has developed and validated an *in vitro* model for small intestinal bacteria by comparing it with *in vivo* data. The *in vitro* model was constructed based on the well-studied colon M-SHIME (Simulator of Human Intestinal Microbial Ecosystem), incorporating compartments for the mouth, proximal small intestine (comprising the duodenum and jejunum), ileum, proximal colon, and distal colon. The system was inoculated with fecal bacteria in the colonic compartments and salivary bacteria in the mouth compartment. The mouth semi-continuously inoculates the system during each feeding cycle, three times a day. Beside the inoculation of the mouth, the ileum was also inoculated with a proximal colon suspension on day 5, referred to as retrograde inoculation. Additionally, a dialysis membrane between the proximal small intestine and ileum mimicked intestinal absorption, while hydroxy apatite discs in the mouth simulated teeth, and mucus beads in the proximal small intestine, ileum, and colon compartments replicated the mucosal environment. The obtained read-outs (bacterial cell counts, metabolites, community) were validated against *in vivo* and *in vitro* data.

As expected, during the SI M-SHIME of the first donor, the semi-continuous inoculation of mouth bacteria *in vitro* introduced *Streptococcus, Veillonella* into the small intestinal compartments, complemented by a retrograde inoculation, which introduced genera such as *Bacteroides* and *Enterococcus* into the ileum, creating a representative community. Furthermore, differences between the mucus and lumen were observed in the first donor with an expected increase in *Bacteroides, Lachnoclostridium,* and *Clostridium* sensu stricto 1 in the mucus of the small intestinal compartments compared to the lumen, since these are known mucus degraders. At last, individual microbial signatures were maintained in the model.

The luminal cell counts in the small intestinal M-SHIME recapitulated the expected profile, except for the proximal small intestinal cell counts, which were an order of 10^3 to 10^5 higher than reported *in vivo* data.

The bacteria in the SHIME metabolized feed, thereby creating a unique metabolite profile in each compartment. The small intestine was characterized by the presence of lactate, which is expected due to its short transit time, leading to rapid carbohydrate fermentation. Furthermore, saccharolytic fermentation predominated the proximal colon, while proteolytic fermentation was evident in the distal colon.

Therefore, we can conclude that the small intestinal M-SHIME is validated based on *in vivo* and *in vitro* data, mimics the small intestinal bacteria well, and serves as a promising *in vitro* model for studying the small intestinal bacteria. In the future, this model holds the potential for investigating microbial dynamics in health and disease, as well as exploring drug-microbiome interactions.

However, this model has several limitations. The proximal small intestinal cell counts are too high. Furthermore, it lacks the inclusion of the human immune system, which plays an important role in shaping the bacterial community. Moreover, while absorption is simulated after the proximal small intestine, the continuous intestinal wall absorption is not, potentially impacting metabolite concentrations and bacterial metabolism. Lastly, the absence of peristalsis, although the system is continuously mixed, is another notable deviation from *in vivo* physiology.

8 FUTURE PERSPECTIVES

Moving forward, there are still opportunities to further improve the small intestinal M-SHIME and conduct a more thorough analysis of the collected data.

Firstly, the proximal small intestine bacterial cell counts can be further optimized. This could involve incorporating antibacterial compounds like lysozymes in the mouth and optimizing the bile acid concentration. Furthermore, adjusting the stomach pH to lower the bacterial cell counts, without killing all bacteria could be explored. Alternatively, introducing a higher dilution factor when transferring the mouth contents to the stomach may help lower the microbial levels.

At present, the assessment of bacterial functionality in the SHIME relies on analyzing the organic acid and gas composition as well as the ammonium concentration. However, a more thorough analysis of the community functionality could provide deeper insights into gene expression. This can be achieved through functional metagenomics using RNA sequencing. Furthermore, co-functional network could be utilized, in which sequencing data is converted to gene functional information (Shim et al., 2017).

Literature indicates that different niches in the oral cavity may host distinct bacterial communities (Mager et al., 2003). Similarly, in our mouth compartment, two niches are present: the lumen and the hydroxyapatite discs. Therefore, exploring the community on the hydroxyapatite discs, which simulate the tooth surface, may be interesting.

The small intestinal harbors a very dynamic community, characterized by a higher variability within a day compared to variations within a month (Booijink et al., 2010). Consequently, exploring the dynamics of a community during a day could be an interesting opportunity to get a better understanding of the evolution during and after feeding cycles.

Validation of the obtained data involves comparison with existing literature as well as samples from donors, such as aspirates and biopsies. However, contamination risks during these operations are very likely, as suggested by the similar composition of the ileal and proximal colon aspirate. Besides, biopsies may carry luminal bacteria. Thus, adopting a more “sterile” sampling method would enhance accuracy and enable a more representative comparison. A novel approach involves using sterile forceps enclosed in a sheet with a plug at the tip to sample the mucosa-associated bacteria as previously described by Shanahan et al. (2016). This approach could then allow to reach the sampling site without contamination from the entry channel and possibly limit contaminations with colon bacteria.

9 SUSTAINABILITY PARAGRAPH

As established during this thesis, the small intestinal gut microbiome is involved in several diseases, including small intestinal bacterial overgrowth and inflammatory bowel disease. Research aimed at defining a "healthy" small intestinal microbiome, as well as identifying disease-associated microbiomes, can aid in treating conditions like those aforementioned. By developing and validating an *in vitro* model that simulates the small intestinal bacteria in both health and disease, this thesis contributes to good health and well-being of individuals, which is one of the 17 sustainable development goals.

The developed *in vitro* model offers a sustainable alternative to *in vivo* sampling and animal models for research purposes. *In vivo* sampling is invasive, costly, and time-consuming. While the SI M-SHIME model is also costly and time-consuming, it avoids the invasiveness associated with the *in vivo* sampling. Additionally, animal models are expensive, animal-unfriendly, and not fully representative of the human gut microbiome. In this way, the SI M-SHIME contributes to the 3R principle: Reduce, Replace, and Refine. Therefore, it fits within the Belgium RE-Place project, which aims to identify and collect all the New Approach Methodologies (RE-Place) in a database, aiding the avoidance of animals.

Beyond this, implementing more sustainable lab practices is also crucial. For instance, the UV light in the laminar flow could be programmed to turn off automatically to prevent it from being left on unintentionally. Additionally, computers that are not in use for extended periods could be switched off to save energy. In the lab, aluminum foil is frequently used. Often, this foil is discarded after use, but if there is no risk of biological/chemical contamination, it could be reused to reduce waste. Additionally, instead of autoclaving scissors and tweezers completely enfolded in aluminum foil, reusable aluminum containers/glass bowls could be implemented.

10 APPENDIX

10.1 Material and methods

Table S 1: Pancreatic juice and bile acid medium composition.

Sterile SI pancreatic juice & bile acid	**g L^{-1}**	**Supplier**
$NaHCO_3$	12.5	Carl Roth, Karlsruhe, Germany
Bile salts	16.75 (~6mM)	Difco, Bierbeek, Belgium
Pancreatin	0.9	Sigma Aldrich, Hoeilaart, Belgium

Table S 2: Agar-mucin composition.

Agar-mucin	**.100mL^{-1}**	**Supplier**
Mucin type III (for ileum and proximal small intestine) OR type II (for colon)	5 g	Sigma Aldrich, Hoeilaart, Belgium
Agar	1 g	Carl Roth, Karlsruhe, Germany
10 M NaOH	350 µL	Chem-Lab NV, Zedelgem, Belgium
Distillated H_2O	100 mL	

Table S 3: Nutritional saliva medium.

Nutritional saliva medium	**Mixed (g L^{-1})**	**Supplier**
Urea solution	**10 mL**	
Urea	0,06	Oxoid, Merelbeke, Belgium
Nutritional solution	**1000 mL**	
Yeast extract	1	Carl Roth, Karlsruhe, Belgium
Bacteriological peptone	2	Oxoid, Merelbeke, Belgium
Tryptone (= Trypticase peptone)	1	Carl Roth, Karlsruhe, Germany
Mucin	1,5	Sigma Aldrich, Hoeilaart, Belgium
Sucrose	1	Merck Millipore, Darmstadt, Germany
Cysteine HCl	0.1	Calbiochem, Darmstadt, Germany
K2HPO4		Carl Roth, Karlsruhe, Germany
KH2PO4		Carl Roth, Karlsruhe, Germany
Hemin stock	**1 mL**	
Hemin	0,001	Sigma Aldrich, Hoeilaart, Belgium
1M NaOH		Chem-Lab NV, Zedelgem, Belgium
Distilled autoclaved water		
Menadione stock	**200 µL**	
Menadione	0,0002	Sigma Aldrich, Hoeilaart, Belgium
EtOH (96%, pure EtOH)		

Table S 4: Overview of the amount of feed added to a certain compartment per cyclus, with three cycli per day.

Addition	Amount (mL/cyclus)	Compartment
Nutritional saliva	100	mouth
SI-M-SHIME feed	130	Stomach
PJ/BA SI SHIME	60	Proximal small intestine
Dialysis buffer	360	Dialysis membrane
Fiber solution	16.67	Ileum

Table S 5: Pump settings first SI-M-SHIME run with PSI = Proximal small intestine, PC = proximal colon, and distal colon = distal colon, BA = bile acids, PJ = pancreatic juice.

Compartment	Volume (mL) Speed (mL/min)	Time	Cycle 1	Cycle 2	Cycle 3
Nutritional saliva -> Mouth	99 mL 3.3 mL/min	30 min	5:35 –6:05	13:35 –14:05	21:35 –22: 05
Mouth -> Waste (Excess volume)	79 mL 3.3 mL/min	24 min 19+5min	5:40 – 5:57	13:40 – 13:57	21:40 – 21:57
Mouth -> Stomach	20 mL 3.3 mL/min	6 min	5:57 – 6:00	13:57 – 14:00	21:57 – 22:00
Feed -> Stomach	130 mL 4.33 mL/min	30 min	5:30 – 6:00 5:30 – 8:30	13:30 – 14:00 13:30 – 16:30	21:30 – 22:00 21:30 – 00:30
pH regulation Stomach			6:00 – 6:30 - 07:38 – 08:25 – 08:58	14:00 – 14:30 - 15:38 – 16:25 – 16:58	22:00 – 22:30 - 23:38 – 00:25 – 00:58
Stomach -> PSI	65.8 mL 1.4 mL/min	47 min	Gradual 3.25 – 2.0 07:38 – 08:25	Gradual 3.25 – 2.0 15:38 – 16:25	Gradual 3.25 – 2.0 23:38 – 00:25
	75.8 mL + 8 mL 2.5 mL/min	33,5 min	Rest 2.0 08:25– 08:58:30	Rest 2.0 16:25–16:58:30	Rest 2.0 00:25–00:58:30
BA/PJ -> PSI	60 mL 1.4 mL/min (start with 1:1 ratio for Feed:Bile and then slowly decrease bile to 7:3)	43 min	07:38 – 08:21	15:38 – 16:21	23:38 – 00:21
pH regulation PSI			08:13 – 10:09 1h56	16:13 – 18:09	00:13 – 02:09
PSI -> Dialysis	200mL 20mL/min	11 min	10:09 – 10:20	18:09 – 18:20	02:09 – 02:20
Dialysis -> Ileum (Extern)	200mL (+extra volume) 20mL/min	11 min	10:09 – 10:20	18:09 – 18:20	02:09 – 02:20
Serosal fluid IN/OUT (Extern)	3 00mL 30 mL/min	11 min	10:09 – 10:20	18:09 – 18:20	02:09 – 02:20
Ileum -> PC	200 mL 4 mL/min	50 min	11:19 – 12:09	19:19 – 20:09	03:19 – 04:09

pH regulation Ileum			10:20 – 11:44	18:20 – 19:44	02:20 – 03:44
PC -> distal colon (Extern)	200 mL 1.67 mL/min	120 min	11:50 – 13:50	19:50 – 21:50	03:50 – 05:50
pH reg. PC			Continuous	Continuous	Continuous
distal colon -> Waste	200 mL 1.67 mL/min	120 min	12:50 – 14:50	20:50 – 22:50	04:50 – 06:50
pH reg. distal colon			Continuous	Continuous	Continuous

Table S 6: Pump setting second and third SI-M-SHIME run with PSI = Proximal small intestine, PC = proximal colon, and distal colon = distal colon, BA = bile acids, PJ = pancreatic juice.

Compartment	**Volume (mL)** **Speed (mL/min)**	**Time**	**Cycle 1**	**Cycle 2**	**Cycle 3**
pH Mouth	-		Continuous	Continuous	Continuous
Nutritional saliva -> Mouth	99 mL 3.3 mL/min	30 min	6:05 – 6:35	14:05 – 14:35	22:05 – 22:35
Mouth -> Waste (Excess volume)	79 mL 3.3 mL/min	24 min 19+5min	6:10 – 6:25 6:20 – 6:39	14:10 – 14:25 14:20 – 14:39	22:10 – 22:25 22:20 – 22:39
Mouth -> Stomach	20 mL 3.3 mL/min	6 min	6:16 – 6:22	14:16 – 14:22	22:16 – 22:22
Feed -> Stomach	130 mL 4.33 mL/min	30 min	6:00 – 6:30 6:00 – 8:00	14:00 – 14:30 14:00 – 16:30	22:00 – 22:30 *22:00 – 00:30*
Flush stomach	After entering Prior removal	2 min	06:30 – 06:32 07:40 – 07:42	14:30 – 14:32 15:40 – 15:42	22:30 – 22:32
pH regulation Stomach			6:30 – 07:00 - 07:44 – 08:27 – 09:07	14:30 – 15:00 - 15:44 – 16:27 – 17:07	22:00 – 22:30 - 23:38 –00:00 - 00:25 – 00:58
Stomach -> PSI	60.2 mL 1.4 mL/min Rest volume 2.5 mL/min	43 min 40 min	Gradual 3.0 – 2.0 07:44 – 08:27 Rest 2.0 08:27 – 09:07	Gradual 3.0 – 2.0 15:44 – 16:27 Rest 2.0 16:27 – 17:07	Gradual 3.0 – 2.0 23:44 – 23:59 00:00 - 00:27 Rest 2.0 00:27 – 01:07
BA/PJ -> PSI	60 mL 1.4 mL/min	43 min	07:44 – 08:27	15:44 – 16:27	23:44 – 23:59 00:00 - 00:27
Flush PSI	Before entering After removal	2 min 2 min	07:40 – 07:42 10:25 – 10:27	15:40 – 15:42 18:25 – 18:27	23:40 – 23:42 02:25 – 02:27
pH regulation PSI	(after 35 min)		08:13 – 10:09 1h56	16:13 – 18:09	00:13 – 02:09
Prox. SI -> Dialysis	200mL 20mL/min	11 min	10:09 – 10:20	18:09 – 18:20	02:09 – 02:20
Dialysis -> Ileum (Extern)	200mL (+extra volume)	11 min	10:09 – 10:20	18:09 – 18:20	02:09 – 02:20

	20mL/min				
Serosal fluid IN/OUT (Extern)	3 00mL 30 mL/min	11 min	10:09 – 10:20	18:09 – 18:20	02:09 – 02:20
Fiber mix -> Ileum	50 mL 4 mL/min	12.5 min	10:20 – 10:32:30	18:20 – 18:32:30	02:10 – 02:22:30
Flush ileum	After entering During removal/ After removal	2 min 2 min	10:34 – 10:36 12:11 – 12:13	18:34 – 18:36 20:11 – 20:13	02:34 – 02:36 04:11 – 04:13
Ileum -> Proximal colon	200 mL 4 mL/min	50 min	11:19 – 12:09	19:19 – 20:09	03:19 – 04:09
Ileum -> waste	50 mL 4 mL/min	12.5 min	12:10 – 12:22:30	20:10 – 20:22:30	04:10 – 04:22:30
pH regulation Ileum			10:20 – 11:30	18:20 – 19:44	02:20 – 03:30
PC -> distal colon (Extern)	200 mL 1.67 mL/min	120 min	11:50 – 13:50	19:50 – 21:50	03:50 – 05:50
pH reg. PC			Continuous	Continuous	Continuous
distal colon -> Waste	200 mL 1.67 mL/min	120 min	12:50 – 14:50	20:50 – 22:50	04:50 – 06:50
pH reg. distal colon			Continuous	Continuous	Continuous

Table S 7: Composition of modified Mineral Wolin's solution.

Compound	**Concentration (g L^{-1})**
Nitrilotriacetic acid	1.5
$MgSO_4$ x 7 H_2O	3
$MnSO_4$ x H_2O	0.5
NaCl	1
$FeSO_4$ x 7 H_2O	0.1
$CoSO_4$ x 7 H_2O	0.18
$CaCl_2$ x 2 H_2O	0.1
$ZnSO_4$ x 7 H_2O	0.18
$CuSO_4$ x 5 H_2O	0.01
$AlK(SO_4)_2$ x 12 H_2O	0.02
H_3BO_3	0.01
Na_2MoO_4 x 2 H_2O	0.01
$NiCl_2$ x 6 H_2O	0.03
Na_2SeO_3 x 5 H_2O	0.0003
Na_2WO_4 x 2 H_2O	0.0004

10.2 Results

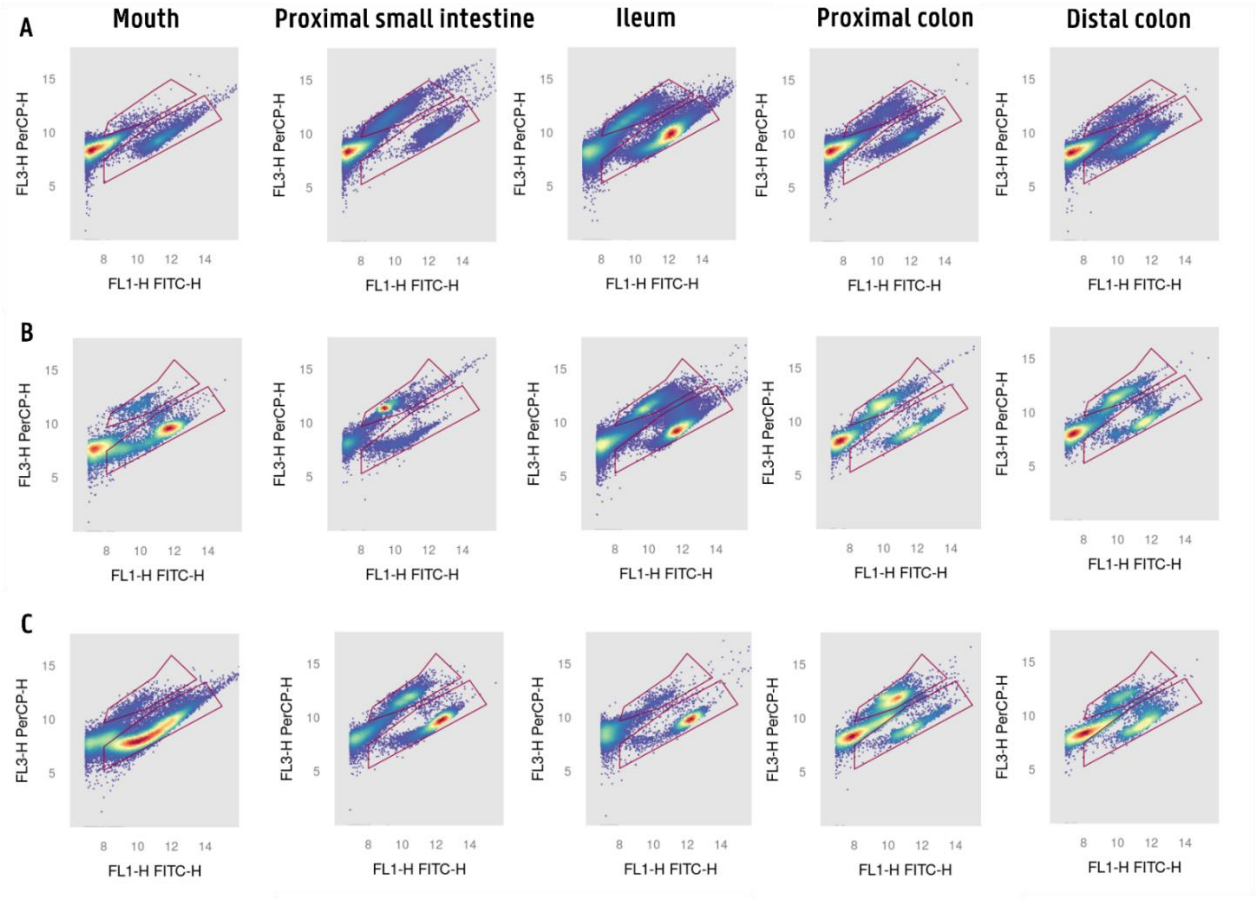

*Figure S 1: Flowcytometry cell counts based on SGPI staining in the different compartments of the SHIME of **A** of the first donor on day 13, **B** the second donor on day 12, and **C** the third donor on day 12.*

Table S 8: Mean total and intact bacterial cells/mL measured during the SHIME runs of the three donors. The mean is taken of the stable SHIME days for the first and third donor (n = 10), while for the second donor all days are taken into account (days 5 to 19) (n = 12 for the proximal small intestine and ileum, and 14 for mouth, proximal colon and distal colon). Total bacterial cell count was measured by flowcytometry using SG for the first and third donor, and SGPI for the second donor, while the intact bacterial cell counts are obtained using SGPI.

		Donor 1		Donor 2		Donor 3	
Counts type	**SHIME Compartment**	**Average (cells/mL)**	**Standard deviation**	**Average (cells/mL)**	**Standard deviation**	**Average (cells/mL)**	**Standard deviation**
Total bacterial cell count	**Mouth**	9.43E+08	2.34E+08	7.33E+08	1.67E+08	1.58E+09	4.1E+08
	Proximal small intestine	2.28E+08	1.53E+08	9.99E+08	3.68E+08	5.11E+08	1.59E+08
	Ileum	6.66E+08	2.11E+08	1.81E+09	7.34E+08	1.37E+09	2.31E+08
	Proximal colon	1.11E+09	5.23E+08	1.66E+09	64528112	2.2E+09	4.77E+08
	Distal colon	1.56E+09	8.82E+08	1.62E+09	1.61E+08	2.19E+09	5.6E+08
Intact bacterial cell count	**Mouth**	9.06E+08	2.24E+08	6.82E+08	1.66E+08	1.74E+09	4.94E+08
	Proximal small intestine	1.16E+08	1.37E+08	4.66E+08	6.35E+07	2.10E+08	7.42E+07
	Ileum	5.57E+08	1.98E+08	1.22E+09	6.39E+08	1.17E+09	2.32E+08
	Proximal colon	6.46E+08	3.2E+08	7.18E+08	3.61E+07	8.31E+08	3.17E+08
	Distal colon	1.18E+09	7.73E+08	8.03E+08	7.26E+07	1.18E+09	2.79E+08

Table S 9: Mean concentration (mM) and standard deviation of the organic acid found in the different compartments during the stable days of the first donor and 3 (n = 4) and during all days for the second donor (n = 3 for the mouth, proximal small intestine, ileum, and n = 4 for proximal colon and distal colon) with SD: standard deviation and n.d.: no data.

		Donor 1		Donor 2		Donor 3	
Compartment	**Variables**	**Mean (mM)**	**SD**	**Mean (mM)**	**SD**	**Mean (mM)**	**SD**
Mouth	Formate	0.01	0.03	0.32	0.04	0.36	0.13
	Acetate	24.14	0.64	2.91	0.45	5.98	0.49
	Lactate	0.003	0.002	0.33	0.20	0.11	0.10
	Propionate	6.54	0.17	2.31	0.54	5.29	0.18
	Isobutyrate	1.03	0.05	0	0	0.84	0.03
	Butyrate	1.51	0.30	0	0	3.55	0.22
	Isovalerate	0.85	0.04	0.09	0.15	1.48	0.06
	Valerate	0.21	0.01	0	0	0	0
	Isocaproate	1.17	0.03	0	0	0	0
	Caproate	0	0	0	0	0	0
	Heptanoate	0	0	0	0	0	0
	Octanoate	0	0	n.d.	n.d.	0	0
Proximal small intestine	Formate	0.94	0.67	2.27	0.24	1.07	0.33
	Acetate	4.41	0.46	2.57	0.18	2.81	0.20
	Lactate	2.03	0.12	1.14	0.09	3.74	2.33
	Propionate	0.58	0.07	0.19	0.02	0.26	0.03
	Isobutyrate	0.15	0.01	0	0	0.04	0.003
	Butyrate	0.13	0.03	0	0	0.22	0.01
	Isovalerate	0.12	0.002	0	0	0.08	0.01

	Valerate	0	0	0	0	0	0
	Isocaproate	0.11	0.01	0	0	0	0
	Caproate	0.03	0.04	0.14	0.003	0	0
	Heptanoate	0	0	0	0	0	0
	Octanoate	0	0	n.d.	n.d.	0	0
Ileum	Formate	7.51	1.33	5.98	1.08	6.63	0.43
	Acetate	11.01	2.14	5.73	0.78	7.93	1.47
	Lactate	3.41	1.35	2.06	0.06	3.78	3.48
	Propionate	1.21	0.25	0.31	0.08	1.35	0.29
	Isobutyrate	0.06	0.07	0	0	0.01	0.01
	Butyrate	0.13	0.03	0.04	0.07	0.09	0.05
	Isovalerate	0.07	0.05	0.08	0.07	0.02	0.01
	Valerate	0	0	0	0	0	0
	Isocaproate	0.05	0.04	0	0	0	0
	Caproate	0	0	0.04	0.08	0	0
	Heptanoate	0	0	0	0	0	0
	Octanoate	0	0	n.d.	n.d.	0	0
Proximal colon	Formate	3.71	1.06	5.92	0.67	0.58	0.71
	Acetate	38.50	1.46	23.34	4.51	25.35	0.59
	Lactate	0.19	0.19	3.22	0.29	0.14	0.24
	Propionate	15.40	0.36	20.94	4.48	21.41	0.84
	Isobutyrate	0.66	0.10	0	0	0.63	0.02
	Butyrate	12.07	0.94	0.41	0.44	11.12	1.37
	Isovalerate	0.98	0.15	0.30	0.20	1.14	0.01
	Valerate	0.15	0.001	0	0	0.0003	0.0006
	Isocaproate	0.03	0.03	0	0	0	0
	Caproate	0	0	0	0	0	0
	Heptanoate	0	0	0	0	0	0
	Octanoate	0	0	n.d.	n.d.	0	0
Distal colon	Formate	0	0	3.88	0.09	0	0
	Acetate	44.19	0.88	38.92	4.13	33.83	2.72
	Lactate	0	0	1.18	0.55	0.00	0.00
	Propionate	14.76	0.51	28.74	4.58	23.14	2.03
	Isobutyrate	1.03	0.01	0.37	0.05	0.85	0.06
	Butyrate	11.33	1.16	7.94	4.94	14.14	1.13
	Isovalerate	1.36	0.01	0.63	0.04	1.46	0.09
	Valerate	2.70	0.31	0.07	0.14	0.05	0.01
	Isocaproate	0.03	0.03	0	0	0	0
	Caproate	4.20	1.07	0	0	0	0
	Heptanoate	1.94	0.61	0	0	0	0
	Octanoate	0.17	0.07	n.d.	n.d.	0	0

Table S 10: The mean net daily production (mM) in the proximal colon and distal colon over the stable days for the first donor and 3, and over days 5, 9, and 12 for the second donor, with n.d. = no data.

		Donor 1	Donor 2	Donor 3
Compartment	Organic acid	Mean (mM)	Mean (mM)	Mean (mM)
Proximal colon	Formate	-5.69	-0.09	-9.09
	Acetate	41.23	26.40	26.13
	Lactate	-4.83	1.74	-5.47
	Propionate	21.28	30.95	30.08
	Isobutyrate	0.91	0	0.93
	Butyrate	17.49	0.55	16.55
	Isovalerate	1.36	0.33	1.67
	Valerate	0.22	0	0
	Isocaproate	-0.03	0	0
	Caproate	0	-0.07	0
	Heptanoate	0	0	0
	Octanoate	0	n.d.	0
Distal colon	Formate	-3.45	-1.88	-0.53
	Acetate	6.17	14.39	7.83
	Lactate	-0.21	-1.88	-0.13
	Propionate	-0.69	7.21	1.60
	Isobutyrate	0.40	0.34	0.20
	Butyrate	-0.81	6.95	2.78
	Isovalerate	0.41	0.31	0.30
	Valerate	2.77	0.07	0.04
	Isocaproate	-0.0004	0	0
	Caproate	4.55	0	0
	Heptanoate	2.10	0	0
	Octanoate	0.19	n.d.	0

Table S 11: Absolute abundances of the genera present in the saliva and feces of the first donor.

Compartment	Genus	Mean
Saliva	*Actinomyces*	1.06E+08
	Alloprevotella	2.29E+06
	Atopobium	6.86E+06
	Butyrivibrio	1.37E+06
	Capnocytophaga	9.15E+05
	Catonella	1.37E+06
	Cutibacterium	4.58E+05
	Dialister	4.58E+05
	Fusobacterium	3.20E+06
	Gemella	1.37E+06
	Granulicatella	9.15E+05
	Haemophilus	2.75E+06
	Johnsonella	4.58E+05
	Lachnoanaerobaculum	1.37E+06
	Lautropia	4.58E+05
	Leptotrichia	2.10E+07
	Megasphaera	1.19E+07
	Neisseria	1.83E+06

	Oribacterium	2.75E+06
	Prevotella	2.29E+06
	Prevotella_7	2.20E+07
	Rothia	3.57E+07
	Selenomonas	5.49E+06
	Solobacterium	1.37E+06
	Stomatobaculum	2.75E+06
	Streptococcus	1.66E+08
	TM7x	2.29E+06
	Treponema	4.58E+05
	Unknown	4.58E+06
	Veillonella	4.58E+07
	[Eubacterium] nodatum group	9.15E+05
Feces	*Adlercreutzia*	4.66E+07
	Agathobacter	7.82E+07
	Akkermansia	1.43E+09
	Alistipes	1.72E+08
	Anaerostipes	3.79E+08
	Bacteroides	4.29E+08
	Barnesiella	1.60E+07
	Bifidobacterium	8.01E+08
	Bilophila	2.74E+06
	Blautia	2.03E+09
	Butyricicoccus	1.70E+08
	Butyrivibrio	3.20E+06
	CAG-352	9.98E+08
	CAG-56	1.14E+08
	Catenisphaera	1.37E+07
	Christensenellaceae R-7 group	1.12E+09
	Clostridium sensu stricto 1	1.17E+09
	Colidextribacter	7.18E+07
	Collinsella	4.44E+09
	Coprococcus	1.30E+09
	Coriobacteriaceae UCG-002	2.29E+06
	DNF00809	4.12E+06
	Defluviitaleaceae UCG-011	1.83E+06
	Desulfovibrio	9.60E+06
	Dorea	6.33E+08
	Enterorhabdus	9.65E+07
	Erysipelotrichaceae UCG-003	8.64E+07
	Escherichia-Shigella	2.74E+06
	Faecalibacterium	1.05E+09
	Family XIII AD3011 group	2.57E+08
	Family XIII UCG-001	1.92E+07
	Flavonifractor	2.29E+06
	Fournierella	8.69E+06
	Fusicatenibacter	2.92E+08
	Fusobacterium	5.49E+06
	Holdemania	2.29E+06
	Incertae Sedis	6.31E+07
	Intestinibacter	1.92E+07

	Intestinimonas	6.40E+06
	Lachnoclostridium	3.06E+07
	Lachnospiraceae AC2044 group	1.19E+07
	Lachnospiraceae FCS020 group	1.49E+08
	Lachnospiraceae ND3007 group	1.01E+07
	Lachnospiraceae NK4A136 group	6.26E+07
	Lachnospiraceae UCG-001	2.01E+07
	Marvinbryantia	2.06E+08
	Methanobrevibacter	2.52E+09
	Monoglobus	6.63E+07
	NK4A214 group	5.56E+08
	Negativibacillus	5.94E+06
	Odoribacter	3.20E+06
	Oscillibacter	1.19E+07
	Oscillospira	8.69E+06
	Paludicola	1.01E+07
	Parabacteroides	4.39E+08
	Parvimonas	1.83E+06
	Phascolarctobacterium	2.48E+08
	Prevotella_7	1.05E+08
	Prevotella_9	1.79E+09
	Prevotellaceae UCG-001	9.79E+07
	Rikenellaceae RC9 gut group	4.94E+07
	Romboutsia	2.21E+09
	Roseburia	3.22E+08
	Ruminococcus	3.02E+07
	S5-A14a	1.37E+06
	Shuttleworthia	6.40E+06
	Slackia	6.86E+06
	Streptococcus	1.37E+06
	Subdoligranulum	3.40E+09
	Terrisporobacter	5.72E+07
	Turicibacter	2.38E+07
	UBA1819	3.34E+07
	UCG-002	6.16E+08
	UCG-003	4.21E+07
	UCG-005	2.39E+08
	UCG-009	1.23E+07
	Unknown	5.17E+09
	[Eubacterium] eligens group	3.20E+06
	[Eubacterium] fissicatena group	1.05E+07
	[Eubacterium] hallii group	4.88E+08
	[Eubacterium] ruminantium group	5.85E+07
	[Eubacterium] siraeum group	3.70E+07
	[Eubacterium] ventriosum group	2.02E+08
	[Eubacterium] xylanophilum group	3.20E+07
	[Ruminococcus] gauvreauii group	2.38E+08
	[Ruminococcus] torques group	7.17E+08

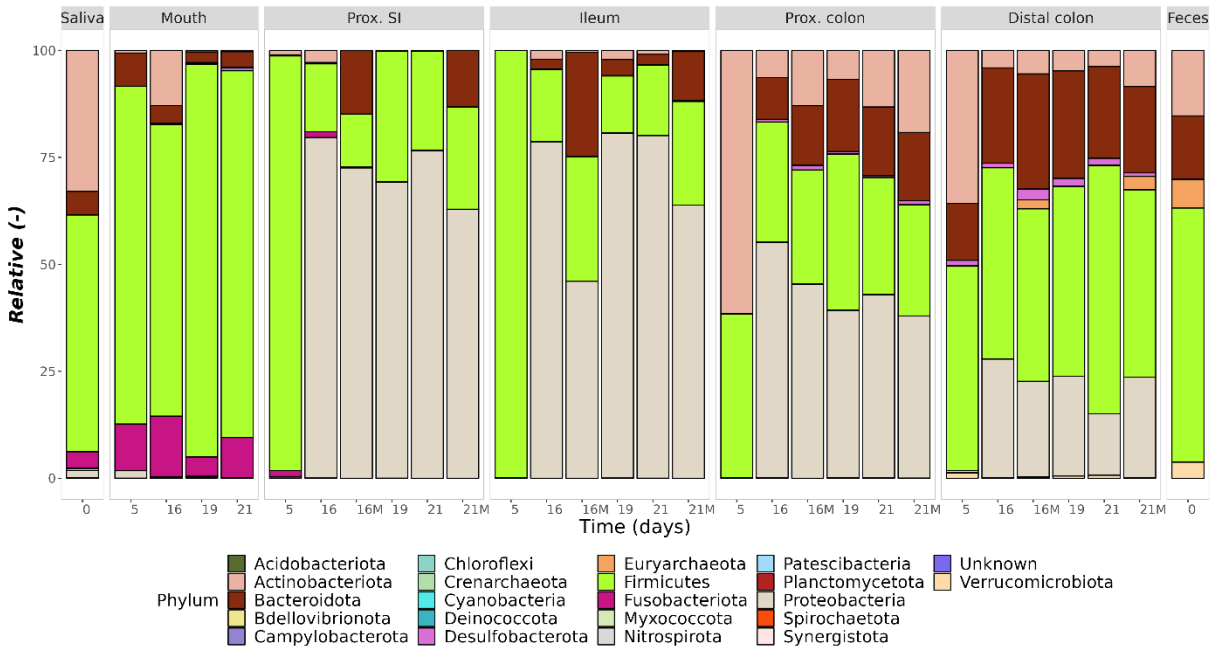

Figure S 2: Relative abundance of the phyla present in the different compartments of the SHIME, saliva and feces. Prox. small intestine indicates the proximal small intestine and prox. colon for the proximal colon.

11 REFERENCES

Aas, J. A., Paster, B. J., Stokes, L. N., Olsen, I., & Dewhirst, F. E. (2005). Defining the normal bacterial flora of the oral cavity. *Journal of clinical microbiology*, *43*(11), 5721-5732. https://doi.org/10.1128/jcm.43.11.5721-5732.2005

Aburub, A., Fischer, M., Camilleri, M., Semler, J., & Fadda, H. (2018). Comparison of pH and motility of the small intestine of healthy subjects and patients with symptomatic constipation using the wireless motility capsule. *International Journal of Pharmaceutics*, *544*(1), 158-164. https://doi.org/10.1016/j.ijpharm.2018.04.031

Ahluwalia, B., Magnusson, M. K., & Öhman, L. (2017). Mucosal immune system of the gastrointestinal tract: maintaining balance between the good and the bad. *Scandinavian journal of gastroenterology*, *52*(11), 1185-1193. https://doi.org/10.1080/00365521.2017.1349173

Ahn, J., Yang, L., Paster, B. J., Ganly, I., Morris, L., Pei, Z., & Hayes, R. B. (2011). Oral microbiome profiles: 16S rRNA pyrosequencing and microarray assay comparison. *PloS one*, *6*(7), e22788. https://doi.org/10.1371/journal.pone.0022788

Albenberg, L., Esipova, T. V., Judge, C. P., Bittinger, K., Chen, J., Laughlin, A., Grunberg, S., Baldassano, R. N., Lewis, J. D., & Li, H. (2014). Correlation between intraluminal oxygen gradient and radial partitioning of intestinal microbiota. *Gastroenterology*, *147*(5), 1055-1063. e1058. https://doi.org/10.1053/j.gastro.2014.07.020

Ali, S. M. F., & Tanwir, F. (2012). Oral microbial habitat a dynamic entity. *Journal of oral biology and craniofacial research*, *2*(3), 181-187. https://doi.org/10.1016/j.jobcr.2012.07.001

Allen, A., Flemstrom, G., Garner, A., & Kivilaakso, E. (1993). Gastroduodenal mucosal protection. *Physiological reviews*, *73*(4), 823-857.

Appert, O., Garcia, A. R., Frei, R., Roduit, C., Constancias, F., Neuzil-Bunesova, V., Ferstl, R., Zhang, J., Akdis, C., & Lauener, R. (2020). Initial butyrate producers during infant gut microbiota development are endospore formers. *Environmental microbiology*, *22*(9), 3909-3921. https://doi.org/10.1111/1462-2920.15167

Atuma, C., Strugala, V., Allen, A., & Holm, L. (2001). The adherent gastrointestinal mucus gel layer: thickness and physical state in vivo. *American Journal of Physiology-Gastrointestinal and Liver Physiology*, *280*(5), G922-G929.

Baltazar-Díaz, T. A., González-Hernández, L. A., Aldana-Ledesma, J. M., Peña-Rodríguez, M., Vega-Magaña, A. N., Zepeda-Morales, A. S. M., López-Roa, R. I., del Toro-Arreola, S., Martínez-López, E., & Salazar-Montes, A. M. (2022). Escherichia/Shigella, SCFAs, and Metabolic Pathways—The Triad That Orchestrates Intestinal Dysbiosis in Patients with Decompensated Alcoholic Cirrhosis from Western Mexico. *Microorganisms*, *10*(6), 1231. https://doi.org/10.3390/microorganisms10061231

Barbosa, F., Irino, K., Carbonell, G., & Mayer, M. P. A. (2006). Characterization of Serratia marcescens isolates from subgingival biofilm, extraoral infections and environment by prodigiosin production, serotyping, and genotyping. *Oral microbiology and immunology*, *21*(1), 53-60. https://doi.org/10.1111/j.1399-302X.2005.00254.x

Barlow, J. T., Leite, G., Romano, A. E., Sedighi, R., Chang, C., Celly, S., Rezaie, A., Mathur, R., Pimentel, M., & Ismagilov, R. F. (2021). Quantitative sequencing clarifies the role of disruptor taxa, oral microbiota, and strict anaerobes in the human small-intestine microbiome. *Microbiome*, *9*, 1-17. https://doi.org/10.1186/s40168-021-01162-2

Barret, K. E., Barman, S. M., Boitano, S., & Brooks, H. L. (2018). Overview of Gastrointestinal Function & Regulation. In *Ganong's Review of Medical Physiology*.

Begley, M., Gahan, C. G., & Hill, C. (2005). The interaction between bacteria and bile. *FEMS microbiology reviews*, *29*(4), 625-651. https://doi.org/10.1016/j.femsre.2004.09.003

Benn, A., Heng, N., Broadbent, J., & Thomson, W. (2018). Studying the human oral microbiome: challenges and the evolution of solutions. *Australian dental journal*, *63*(1), 14-24. https://doi.org/10.1111/adj.12565

Benson, A. K., Kelly, S. A., Legge, R., Ma, F., Low, S. J., Kim, J., Zhang, M., Oh, P. L., Nehrenberg, D., & Hua, K. (2010). Individuality in gut microbiota composition is a complex polygenic trait shaped by multiple environmental and host genetic factors. *Proceedings of the National Academy of Sciences*, *107*(44), 18933-18938. https://doi.org/10.1073/pnas.1007028107

Berg, R. D. (1996). The indigenous gastrointestinal microflora. *Trends in microbiology*, *4*(11), 430-435. https://doi.org/10.1016/0966-842X(96)10057-3

Bergman, E. (1990). Energy contributions of volatile fatty acids from the gastrointestinal tract in various species. *Physiological reviews*, *70*(2), 567-590. https://doi.org/10.1152/physrev.1990.70.2.567

Biagini, F., Daddi, C., Calvigioni, M., De Maria, C., Zhang, Y. S., Ghelardi, E., & Vozzi, G. (2023). Designs and methodologies to recreate in vitro human gut microbiota models. *Bio-Design and Manufacturing*, *6*(3), 298-318. https://doi.org/10.1007/s42242-022-00210-6

Bik, E. M., Eckburg, P. B., Gill, S. R., Nelson, K. E., Purdom, E. A., Francois, F., Perez-Perez, G., Blaser, M. J., & Relman, D. A. (2006). Molecular analysis of the bacterial microbiota in the human stomach. *Proceedings of the National Academy of Sciences*, *103*(3), 732-737. https://doi.org/10.1073/pnas.0506655103

Bik, E. M., Long, C. D., Armitage, G. C., Loomer, P., Emerson, J., Mongodin, E. F., Nelson, K. E., Gill, S. R., Fraser-Liggett, C. M., & Relman, D. A. (2010). Bacterial diversity in the oral cavity of 10 healthy individuals. *The ISME journal*, *4*(8), 962-974. https://doi.org/10.1038/ismej.2010.30

Blachier, F., Mariotti, F., Huneau, J.-F., & Tomé, D. (2007). Effects of amino acid-derived luminal metabolites on the colonic epithelium and physiopathological consequences. *Amino acids*, *33*, 547-562. https://doi.org/10.1007/s00726-006-0477-9

Booijink, C. C., El-Aidy, S., Rajilić-Stojanović, M., Heilig, H. G., Troost, F. J., Smidt, H., Kleerebezem, M., De Vos, W. M., & Zoetendal, E. G. (2010). High temporal and inter-individual variation detected in the human ileal microbiota. *Environmental microbiology*, *12*(12), 3213-3227. https://doi.org/10.1111/j.1462-2920.2010.02294.x

Bresalier, R. S., & Chapkin, R. S. (2020). Human microbiome in health and disease: the good, the bad, and the bugly. In (Vol. 65, pp. 671-673): Springer.

Burisch, J., Jess, T., Martinato, M., Lakatos, P. L., & ECCO-EpiCom. (2013). The burden of inflammatory bowel disease in Europe. *Journal of Crohn's and Colitis*, *7*(4), 322-337. https://doi.org/10.1016/j.crohns.2013.01.010

Bushyhead, D., & Quigley, E. M. (2022). Small intestinal bacterial overgrowth—pathophysiology and its implications for definition and management. *Gastroenterology*, *163*(3), 593-607. https://doi.org/10.1053/j.gastro.2022.04.002

Callahan, B. J., Sankaran, K., Fukuyama, J. A., McMurdie, P. J., & Holmes, S. P. (2016). Bioconductor workflow for microbiome data analysis: from raw reads to community analyses. *F1000Research*, *5*. https://doi.org/10.12688/f1000research.8986.2

Calvigioni, M., Panattoni, A., Biagini, F., Donati, L., Mazzantini, D., Massimino, M., Daddi, C., Celandroni, F., Vozzi, G., & Ghelardi, E. (2023). Development of an in vitro model of the gut microbiota enriched in mucus-adhering bacteria. *Microbiology Spectrum*, *11*(4), e00336-00323. https://doi.org/10.1128/spectrum.00336-23

Campbell, I. (2015). The mouth, stomach and intestines. *Anaesthesia & Intensive Care Medicine*, *16*(1), 37-39.

Campbell, J., Berry, J., & Liang, Y. (2019). Anatomy and physiology of the small intestine. In *Shackelford's Surgery of the Alimentary Tract, 2 Volume Set* (pp. 817-841). Elsevier. https://doi.org/10.1016/B978-0-323-40232-3.00071-6

Cavender-Bares, J., Kozak, K. H., Fine, P. V., & Kembel, S. W. (2009). The merging of community ecology and phylogenetic biology. *Ecology letters*, *12*(7), 693-715. https://doi.org/10.1111/j.1461-0248.2009.01314.x

Chen, H., & Jiang, W. (2014). Application of high-throughput sequencing in understanding human oral microbiome related with health and disease. *Frontiers in microbiology*, *5*, 508. https://doi.org/10.3389/fmicb.2014.00508

Chen, P.-S., & Li, C.-S. (2005). Real-time quantitative PCR with gene probe, fluorochrome and flow cytometry for microorganism analysis. *Journal of environmental monitoring*, *7*(3), 257-262. https://doi.org/10.1039/B415250F

Chiang, J. Y., & Ferrell, J. M. (2018). Bile acid metabolism in liver pathobiology. *Gene expression*, *18*(2), 71. https://doi.org/10.3727/105221618X15156018385515

Chung, C.-S., Chang, P.-F., Liao, C.-H., Lee, T.-H., Chen, Y., Lee, Y.-C., Wu, M.-S., Wang, H.-P., & Ni, Y.-H. (2016). Differences of microbiota in small bowel and faeces between irritable bowel syndrome patients and healthy subjects. *Scandinavian journal of gastroenterology*, *51*(4), 410-419. https://doi.org/10.3109/00365521.2015.1116107

Cieplak, T., Wiese, M., Nielsen, S., Van de Wiele, T., van den Berg, F., & Nielsen, D. S. (2018). The smallest intestine (TSI)—a low volume in vitro model of the small intestine with increased throughput. *FEMS microbiology letters*, *365*(21), fny231. https://doi.org/10.1093/femsle/fny231

Claudel, T., Staels, B., & Kuipers, F. (2005). The Farnesoid X receptor: a molecular link between bile acid and lipid and glucose metabolism. *Arteriosclerosis, thrombosis, and vascular biology*, *25*(10), 2020-2030. https://doi.org/10.1161/01.ATV.0000178994.21828.a7

Clausen, M. R., & Mortensen, P. B. (1997). Lactulose, disaccharides and colonic flora: clinical consequences. *Drugs*, *53*, 930-942. https://doi.org/10.2165/00003495-199753060-00003

Collins, J. T., Nguyen, A., & Badireddy, M. (2017). Anatomy, abdomen and pelvis, small intestine.

Cragg, R., Phillips, S., Piper, J., Varma, J., Campbell, F., Mathers, J., & Ford, D. (2005). Homeostatic regulation of zinc transporters in the human small intestine by dietary zinc supplementation. *Gut*, *54*(4), 469-478. https://doi.org/10.1136/gut.2004.041962

Cummings, J., & Macfarlane, G. (1992). The control and consequences of bacterial fermentation in the human colon.

Cummings, J. H., Pomare, E., Branch, W., Naylor, C., & MacFarlane, G. (1987). Short chain fatty acids in human large intestine, portal, hepatic and venous blood. *Gut*, *28*(10), 1221-1227. https://doi.org/10.1136/gut.28.10.1221

Davami, F., Eghbalpour, F., Nematollahi, L., Barkhordari, F., & Mahboudi, F. (2015). Effects of peptone supplementation in different culture media on growth, metabolic pathway and productivity of CHO DG44 cells; a new insight into amino acid profiles. *Iranian biomedical journal*, *19*(4), 194. https://doi.org/10.7508/ibj.2015.04.002

Davidson, J., Linforth, R., & Taylor, A. (1998). In-mouth measurement of pH and conductivity during eating. *Journal of agricultural and food chemistry*, *46*(12), 5210-5214. https://doi.org/10.1021/jf9806558

Davis, S., Hardy, J., & Fara, J. (1986). Transit of pharmaceutical dosage forms through the small intestine. *Gut*, *27*(8), 886-892. https://doi.org/10.1136/gut.27.8.886

Day, R. M. (2019). Chapter 64 - Alimentary Tract, . *Principles of Regenerative Medicine (Third Edition)*,, 1131-1148. https://doi.org/10.1016/B978-0-12-809880-6.00064-3.

De Paepe, K., Kerckhof, F. M., Verspreet, J., Courtin, C. M., & Van de Wiele, T. (2017). Inter-individual differences determine the outcome of wheat bran colonization by the human gut microbiome. *Environmental microbiology*, *19*(8), 3251-3267. https://doi.org/10.1111/1462-2920.13819

De Paepe, K., Verspreet, J., Verbeke, K., Raes, J., Courtin, C. M., & Van de Wiele, T. (2018). Introducing insoluble wheat bran as a gut microbiota niche in an in vitro dynamic gut model stimulates propionate and butyrate production and induces colon region specific shifts in the luminal and mucosal microbial community. *Environmental microbiology*, *20*(9), 3406-3426. https://doi.org/10.1111/1462-2920.14381

Delaroque, C., Wu, G. D., Compher, C., Ni, J., Albenberg, L., Liu, Q., Tian, Y., Patterson, A. D., Lewis, J. D., & Gewirtz, A. T. (2022). Diet standardization reduces intra-individual microbiome variation. *Gut microbes*, *14*(1), 2149047. https://doi.org/10.1080/19490976.2022.2149047

Dewhirst, F. E., Chen, T., Izard, J., Paster, B. J., Tanner, A. C., Yu, W.-H., Lakshmanan, A., & Wade, W. G. (2010). The human oral microbiome. *Journal of bacteriology*, *192*(19), 5002-5017. https://doi.org/10.1128/jb.00542-10

Deyaert, S., Moens, F., Pirovano, W., van den Bogert, B., Klaassens, E. S., Marzorati, M., Van de Wiele, T., Kleerebezem, M., & Van den Abbeele, P. (2023). Development of a reproducible small intestinal microbiota model and its integration into the SHIME®-system, a dynamic in vitro gut model. *Frontiers in microbiology*, *13*, 1054061. https://doi.org/10.3389/fmicb.2022.1054061

Di Ciaula, A., Garruti, G., Baccetto, R. L., Molina-Molina, E., Bonfrate, L., Portincasa, P., & Wang, D. Q. (2018). Bile acid physiology. *Annals of hepatology*, *16*(1), 4-14. https://doi.org/10.5604/01.3001.0010.5493

Dixit, Y., Kanojiya, K., Bhingardeve, N., Ahire, J. J., & Saroj, D. (2023). In Vitro Human Gastrointestinal Tract Simulation Systems: A Panoramic Review. *Probiotics and Antimicrobial Proteins*, 1-18. https://doi.org/10.1007/s12602-023-10052-y

Dlugosz, A., Winckler, B., Lundin, E., Zakikhany, K., Sandström, G., Ye, W., Engstrand, L., & Lindberg, G. (2015). No difference in small bowel microbiota between patients with irritable bowel syndrome and healthy controls. *Scientific reports*, *5*(1), 8508. https://doi.org/10.1038/srep08508

Donaldson, G. P., Lee, S. M., & Mazmanian, S. K. (2016). Gut biogeography of the bacterial microbiota. *Nature Reviews Microbiology*, *14*(1), 20-32. https://doi.org/10.1038/nrmicro3552

Durruty, J., Mattsson, T., & Theliander, H. (2017). Local filtration properties of Kraft lignin: The influence of residual xylan. *Separation and Purification Technology*, *179*, 455-466. https://doi.org/10.1016/j.seppur.2017.01.068

El Aidy, S., Van Den Bogert, B., & Kleerebezem, M. (2015). The small intestine microbiota, nutritional modulation and relevance for health. *Current opinion in biotechnology*, *32*, 14-20. https://doi.org/10.1016/j.copbio.2014.09.005

Engstrand, L., & Lindberg, M. (2013). Helicobacter pylori and the gastric microbiota. *Best practice & research Clinical gastroenterology*, *27*(1), 39-45. https://doi.org/10.1016/j.bpg.2013.03.016

Falony, G., Joossens, M., Vieira-Silva, S., Wang, J., Darzi, Y., Faust, K., Kurilshikov, A., Bonder, M. J., Valles-Colomer, M., & Vandeputte, D. (2016). Population-level analysis of gut microbiome variation. *science*, *352*(6285), 560-564. https://doi.org/10.1126/science.aad3503

Fan, P., Liu, P., Song, P., Chen, X., & Ma, X. (2017). Moderate dietary protein restriction alters the composition of gut microbiota and improves ileal barrier function in adult pig model. *Scientific Reports*, *7*(1), 43412. https://doi.org/10.1038/srep43412

Fatahi-Bafghi, M. (2021). Characterization of the Rothia spp. and their role in human clinical infections. *Infection, Genetics and Evolution*, *93*, 104877. https://doi.org/10.1016/j.meegid.2021.104877

Federle, M. P., Poullos, P. D., & Sinha, S. R. (2019). *Imaging in Gastroenterology E-Book: Imaging in Gastroenterology E-Book*. Elsevier Health Sciences.

Fehlbaum, S., Chassard, C., Haug, M. C., Fourmestraux, C., Derrien, M., & Lacroix, C. (2015). Design and investigation of PolyFermS in vitro continuous fermentation models inoculated with immobilized fecal microbiota mimicking the elderly colon. *PloS one*, *10*(11), e0142793. https://doi.org/10.1371/journal.pone.0142793

Fish, E. M., & Burns, B. (2022). Physiology, small bowel. In *StatPearls [Internet]*. StatPearls Publishing.

Flemström, G., & Kivilaakso, E. (1983). Demonstration of a pH gradient at the luminal surface of rat duodenum in vivo and its dependence on mucosal alkaline secretion. *Gastroenterology*, *84*(4), 787-794. https://doi.org/10.1016/0016-5085(83)90147-6

Flint, H. J., Duncan, S. H., Scott, K. P., & Louis, P. (2015). Links between diet, gut microbiota composition and gut metabolism. *Proceedings of the Nutrition Society*, *74*(1), 13-22. https://doi.org/10.1017/S0029665114001463

Flint, H. J., Scott, K. P., Louis, P., & Duncan, S. H. (2012). The role of the gut microbiota in nutrition and health. *Nature reviews Gastroenterology & hepatology*, *9*(10), 577-589. https://doi.org/10.1038/nrgastro.2012.156

Gacesa, R., Kurilshikov, A., Vich Vila, A., Sinha, T., Klaassen, M. A., Bolte, L. A., Andreu-Sánchez, S., Chen, L., Collij, V., & Hu, S. (2022). Environmental factors shaping the gut microbiome in a Dutch population. *Nature*, *604*(7907), 732-739. https://doi.org/10.1038/s41586-022-04567-7

Garabedian, E. M., Roberts, L. J., McNevin, M. S., & Gordon, J. I. (1997). Examining the role of Paneth cells in the small intestine by lineage ablation in transgenic mice. *Journal of Biological Chemistry*, *272*(38), 23729-23740. https://doi.org/10.1074/jbc.272.38.23729

Germerodt, S., Bohl, K., Lück, A., Pande, S., Schröter, A., Kaleta, C., Schuster, S., & Kost, C. (2016). Pervasive selection for cooperative cross-feeding in bacterial communities. *PLoS computational biology*, *12*(6), e1004986. https://doi.org/10.1371/journal.pcbi.1004986

Glover, J. S., Ticer, T., & Engevik, M. (2022). Identifying Mucus-Degrading Microbes Within the Human Gut Microbiota. *The FASEB Journal*, *36*. https://doi.org/10.1096/fasebj.2022.36.S1.R5626

Grabitske, H. A., & Slavin, J. L. (2008). Low-digestible carbohydrates in practice. *Journal of the American Dietetic Association*, *108*(10), 1677-1681. https://doi.org/10.1016/j.jada.2008.07.010

Guerra, A., Etienne-Mesmin, L., Livrelli, V., Denis, S., Blanquet-Diot, S., & Alric, M. (2012). Relevance and challenges in modeling human gastric and small intestinal digestion. *Trends in biotechnology*, *30*(11), 591-600. https://doi.org/10.1016/j.tibtech.2012.08.001

Guzman-Rodriguez, M., McDonald, J. A., Hyde, R., Allen-Vercoe, E., Claud, E. C., Sheth, P. M., & Petrof, E. O. (2018). Using bioreactors to study the effects of drugs on the human microbiota. *Methods*, *149*, 31-41. https://doi.org/10.1016/j.ymeth.2018.08.003

Haddy, R. I., Mann, B. L., Nadkarni, D. D., Cruz, R. F., Elshoff, D. J., Buendia, F. C., Domers, T. A., & Oberheu, A. M. (1996). Nosocomial infection in the community hospital: severe infection due to Serratia species. *Journal of Family Practice*, *42*(3), 273-277.

Haschek, W. M., Rousseaux, C. G., & Wallig, M. A. (2010). Gastrointestinal tract. *Fundamentals of toxicologic pathology*, 163-196. https://doi.org/10.1016/b978-0-12-370469-6.00008-8

Hayase, E., Hayase, T., Jamal, M. A., Miyama, T., Chang, C.-C., Ortega, M. R., Ahmed, S. S., Karmouch, J. L., Sanchez, C. A., & Brown, A. N. (2022). Mucus-degrading Bacteroides link carbapenems to aggravated graft-versus-host disease. *Cell*, *185*(20), 3705-3719. e3714. https://doi.org/10.1111/j.1399-302X.2005.00254.x

Hayashi, H., Takahashi, R., Nishi, T., Sakamoto, M., & Benno, Y. (2005). Molecular analysis of jejunal, ileal, caecal and recto-sigmoidal human colonic microbiota using 16S rRNA gene libraries and terminal restriction fragment length polymorphism. *Journal of medical microbiology*, *54*(11), 1093-1101. https://doi.org/10.1099/jmm.0.45935-0

He, G., Shankar, R. A., Chzhan, M., Samouilov, A., Kuppusamy, P., & Zweier, J. L. (1999). Noninvasive measurement of anatomic structure and intraluminal oxygenation in the gastrointestinal tract of living mice with spatial and spectral EPR imaging. *Proceedings of the National Academy of Sciences*, *96*(8), 4586-4591. https://doi.org/10.1073/pnas.96.8.4586

Helander, H. F., & Fändriks, L. (2014). Surface area of the digestive tract–revisited. *Scandinavian journal of gastroenterology*, *49*(6), 681-689. https://doi.org/10.3109/00365521.2014.898326

Hillman, E. T., Lu, H., Yao, T., & Nakatsu, C. H. (2017). Microbial ecology along the gastrointestinal tract. *Microbes and environments*, *32*(4), 300-313. https://doi.org/10.1264/jsme2.ME17017

Hofmann, A. F., & Eckmann, L. (2006). How bile acids confer gut mucosal protection against bacteria. *Proceedings of the National Academy of Sciences*, *103*(12), 4333-4334. https://doi.org/10.1073/pnas.0600780103

Höllwarth, M. E. (1999). Short bowel syndrome: pathophysiological and clinical aspects. *Pathophysiology*, *6*(1), 1-19. https://doi.org/10.1016/S0928-4680(98)00035-2

Holmes, R., & Lobley, R. (1989). Intestinal brush border revisited. *Gut*, *30*(12), 1667. https://doi.org/10.1136/gut.30.12.1667

Hooper, L. V., Littman, D. R., & Macpherson, A. J. (2012). Interactions between the microbiota and the immune system. *science*, *336*(6086), 1268-1273. https://doi.org/10.1126/science.1223490

Hooton, D., Lentle, R., Monro, J., Wickham, M., & Simpson, R. (2015). The secretion and action of brush border enzymes in the mammalian small intestine. *Reviews of physiology, biochemistry and pharmacology*, 59-118. https://doi.org/10.1007/112_2015_24

Hugenholtz, P. (2002). Exploring prokaryotic diversity in the genomic era. *Genome biology*, *3*, 1-8. https://doi.org/10.1186/gb-2002-3-2-reviews0003

Huus, K. E., Petersen, C., & Finlay, B. B. (2021). Diversity and dynamism of IgA–microbiota interactions. *Nature Reviews Immunology*, *21*(8), 514-525. https://doi.org/10.1038/s41577-021-00506-1

Hylemon, P. B., Zhou, H., Pandak, W. M., Ren, S., Gil, G., & Dent, P. (2009). Bile acids as regulatory molecules. *Journal of lipid research*, *50*(8), 1509-1520. https://doi.org/10.1194/jlr.R900007-JLR200

Johansson, M. E., Ambort, D., Pelaseyed, T., Schütte, A., Gustafsson, J. K., Ermund, A., Subramani, D. B., Holmén-Larsson, J. M., Thomsson, K. A., & Bergström, J. H. (2011). Composition and functional role of the mucus layers in the intestine. *Cellular and molecular life sciences*, *68*, 3635-3641. https://doi.org/10.1007/s00018-011-0822-3

Johansson, M. E., Sjövall, H., & Hansson, G. C. (2013). The gastrointestinal mucus system in health and disease. *Nature reviews Gastroenterology & hepatology*, *10*(6), 352-361. https://doi.org/10.1038/nrgastro.2013.35

Kageyama, A., & Benno, Y. (2015). Solobacterium. *Bergey's Manual of Systematics of Archaea and Bacteria*, 1-4. https://doi.org/10.1002/9781118960608.gbm00765

Kalantzi, L., Goumas, K., Kalioras, V., Abrahamsson, B., Dressman, J. B., & Reppas, C. (2006). Characterization of the human upper gastrointestinal contents under conditions simulating bioavailability/bioequivalence studies. *Pharmaceutical research*, *23*, 165-176. https://doi.org/10.1007/s11095-005-8476-1

Kaoutari, A. E., Armougom, F., Gordon, J. I., Raoult, D., & Henrissat, B. (2013). The abundance and variety of carbohydrate-active enzymes in the human gut microbiota. *Nature Reviews Microbiology*, *11*(7), 497-504. https://doi.org/10.1038/nrmicro3050

Kastl Jr, A. J., Terry, N. A., Wu, G. D., & Albenberg, L. G. (2020). The structure and function of the human small intestinal microbiota: current understanding and future directions. *Cellular and molecular gastroenterology and hepatology*, *9*(1), 33-45. https://doi.org/10.1016/j.jcmgh.2019.07.006

Kazor, C., Mitchell, P., Lee, A., Stokes, L., Loesche, W., Dewhirst, F., & Paster, B. (2003). Diversity of bacterial populations on the tongue dorsa of patients with halitosis and healthy patients. *Journal of clinical microbiology*, *41*(2), 558-563. https://doi.org/10.1128/jcm.41.2.558-563.2003

Kern, L., Abdeen, S. K., Kolodziejczyk, A. A., & Elinav, E. (2021). Commensal inter-bacterial interactions shaping the microbiota. *Current opinion in microbiology*, *63*, 158-171. https://doi.org/10.1016/j.mib.2021.07.011

Klappenbach, J. A., Dunbar, J. M., & Schmidt, T. M. (2000). rRNA operon copy number reflects ecological strategies of bacteria. *Applied and environmental microbiology*, *66*(4), 1328-1333. https://doi.org/10.1128/AEM.66.4.1328-1333.2000

König, H., & Fröhlich, J. (2017). Lactic acid bacteria. *Biology of Microorganisms on Grapes, in Must and in Wine*, 3-41. https://doi.org/10.1007/978-3-319-60021-5_1

Korpela, K. (2018). Diet, microbiota, and metabolic health: trade-off between saccharolytic and proteolytic fermentation. *Annual review of food science and technology*, *9*, 65-84. https://doi.org/10.1146/annurev-food-030117-012830

Kotarski, S. F., & Salyers, A. A. (1981). Effect of long generation times on growth of Bacteroides thetaiotaomicron in carbohydrate-limited continuous culture. *Journal of bacteriology*, *146*(3), 853-860. https://doi.org/10.1128/jb.146.3.853-860.1981

Kwon, Y.-J., Kwak, H. J., Lee, H. K., Lim, H. C., & Jung, D.-H. (2021). Comparison of bacterial community profiles from large intestine specimens, rectal swabs, and stool samples. *Applied Microbiology and Biotechnology*, *105*, 9273-9284. https://doi.org/10.1007/s00253-021-11650-y

Lane, D. (1991). 16S/23S rRNA sequencing. *Nucleic acid techniques in bacterial systematics*.

Lee, S. M., Donaldson, G. P., Mikulski, Z., Boyajian, S., Ley, K., & Mazmanian, S. K. (2013). Bacterial colonization factors control specificity and stability of the gut microbiota. *Nature*, *501*(7467), 426-429. https://doi.org/10.1038/nature12447

Leite, G., Morales, W., Weitsman, S., Celly, S., Parodi, G., Mathur, R., Barlow, G. M., Sedighi, R., Millan, M. J. V., & Rezaie, A. (2020). The duodenal microbiome is altered in small intestinal bacterial overgrowth. *PloS one*, *15*(7), e0234906. https://doi.org/10.1371/journal.pone.0234906

Leonidou, N., Ostyn, L., Coenye, T., Crabbé, A., & Dräger, A. (2024). Genome-scale model of Rothia mucilaginosa predicts gene essentialities and reveals metabolic capabilities. *Microbiology Spectrum*, e04006-04023. https://doi.org/10.1128/spectrum.04006-23

Li, G., Yang, M., Zhou, K., Zhang, L., Tian, L., Lv, S., Jin, Y., Qian, W., Xiong, H., & Lin, R. (2015). Diversity of duodenal and rectal microbiota in biopsy tissues and luminal contents in healthy volunteers. *Journal of microbiology and biotechnology*, *25*(7), 1136-1145. https://doi.org/10.4014/jmb.1412.12047

Li, X.-X., Wong, G. L.-H., To, K.-F., Wong, V. W.-S., Lai, L. H., Chow, D. K.-L., Lau, J. Y.-W., Sung, J. J.-Y., & Ding, C. (2009). Bacterial microbiota profiling in gastritis without Helicobacter pylori infection or non-steroidal anti-inflammatory drug use. *PloS one*, *4*(11), e7985. https://doi.org/10.1371/journal.pone.0007985

Li, Y., & Kong, F. (2022). Simulating human gastrointestinal motility in dynamic in vitro models. *Comprehensive Reviews in Food Science and Food Safety*, *21*(5), 3804-3833. https://doi.org/10.1111/1541-4337.13007

Lim, C. C., Ferguson, L. R., & Tannock, G. W. (2005). Dietary fibres as "prebiotics": implications for colorectal cancer. *Molecular nutrition & food research*, *49*(6), 609-619.

Liu, B., Faller, L. L., Klitgord, N., Mazumdar, V., Ghodsi, M., Sommer, D. D., Gibbons, T. R., Treangen, T. J., Chang, Y.-C., & Li, S. (2012). Deep sequencing of the oral microbiome reveals signatures of periodontal disease. *PloS one*, *7*(6), e37919. https://doi.org/10.1371/journal.pone.0037919

Liu, S., Wang, Y., Zhao, L., Sun, X., & Feng, Q. (2020). Microbiome succession with increasing age in three oral sites. *Aging (albany NY)*, *12*(9), 7874. https://doi.org/10.18632/aging.103108

Louca, S., Doebeli, M., & Parfrey, L. W. (2018). Correcting for 16S rRNA gene copy numbers in microbiome surveys remains an unsolved problem. *Microbiome*, *6*, 1-12. https://doi.org/10.1186/s40168-018-0420-9

Lowry, O. H., Rosebrough, N. J., Farr, A. L., & Randall, R. J. (1951). Protein measurement with the Folin phenol reagent. *J biol Chem*, *193*(1), 265-275.

Lu, R., Meng, H., Gao, X., Xu, L., & Feng, X. (2014). Effect of non-surgical periodontal treatment on short chain fatty acid levels in gingival crevicular fluid of patients with generalized aggressive periodontitis. *Journal of periodontal research*, *49*(5), 574-583. https://doi.org/10.1111/jre.12137

Lundberg, J. O., & Govoni, M. (2004). Inorganic nitrate is a possible source for systemic generation of nitric oxide. *Free Radical Biology and Medicine*, *37*(3), 395-400. https://doi.org/10.1016/j.freeradbiomed.2004.04.027

Macfarlane, G., Gibson, G., Beatty, E., & Cummings, J. (1992). Estimation of short-chain fatty acid production from protein by human intestinal bacteria based on branched-chain fatty acid measurements. *FEMS microbiology ecology*, *10*(2), 81-88. https://doi.org/10.1111/j.1574-6941.1992.tb00002.x

Macfarlane, G., Gibson, G., & Cummings, J. (1992). Comparison of fermentation reactions in different regions of the human colon. *Journal of Applied Bacteriology*, *72*(1), 57-64. https://doi.org/10.1111/j.1365-2672.1992.tb04882.x

Macfarlane, G. T., & Macfarlane, S. (2012). Bacteria, colonic fermentation, and gastrointestinal health. *Journal of AOAC International*, *95*(1), 50-60. https://doi.org/10.5740/jaoacint.SGE_Macfarlane

Machen, T. E., & Paradiso, A. M. (1987). Regulation of intracellular pH in the stomach. *Annual review of physiology*, *49*(1), 19-33. https://doi.org/10.1146/annurev.ph.49.030187.000315

Mafra, D., Barros, A. F., & Fouque, D. (2013). Dietary protein metabolism by gut microbiota and its consequences for chronic kidney disease patients. *Future microbiology*, *8*(10), 1317-1323. https://doi.org/10.2217/fmb.13.103

Mager, D. L., Ximenez-Fyvie, L. A., Haffajee, A. D., & Socransky, S. S. (2003). Distribution of selected bacterial species on intraoral surfaces. *Journal of clinical periodontology*, *30*(7), 644-654. https://doi.org/10.1034/j.1600-051X.2003.00376.x

Mahlen, S. D. (2011). Serratia infections: from military experiments to current practice. *Clinical microbiology reviews*, *24*(4), 755-791. https://doi.org/10.1128/cmr.00017-11

Malagelada, J.-R., Longstreth, G., Summerskill, W., & Go, V. (1976). Measurement of gastric functions during digestion of ordinary solid meals in man. *Gastroenterology*, *70*(2), 203-210. https://doi.org/10.1016/S0016-5085(76)80010-8

Martinez-Medina, M., Aldeguer, X., Gonzalez-Huix, F., Acero, D., & Garcia-Gil, J. L. (2006). Abnormal microbiota composition in the ileocolonic mucosa of Crohn's disease patients as revealed by polymerase chain reaction-denaturing gradient gel electrophoresis. *Inflammatory bowel diseases*, *12*(12), 1136-1145. https://doi.org/10.1097/01.mib.0000235828.09305.0c

Maurer, A. H., & Krevsky, B. (1995). Whole-gut transit scintigraphy in the evaluation of small-bowel and colon transit disorders. Seminars in nuclear medicine,

McLaren, M. R., & Callahan, B. J. (2021). Silva 138.1 prokaryotic SSU taxonomic training data formatted for DADA2. *Zenodo*.

Minekus, M., Marteau, P., Havenaar, R., & Veld, J. H. H. i. t. (1995). A multicompartmental dynamic computer-controlled model simulating the stomach and small intestine. *Alternatives to laboratory animals*, *23*(2), 197-209. https://doi.org/10.1177/026119299502300205

Minnebo, Y., De Paepe, K., Raes, J., & Van de Wiele, T. (2023). Eating patterns contribute to shaping the gut microbiota in the mucosal simulator of the human intestinal microbial ecosystem. *FEMS microbiology ecology*, fiad149. https://doi.org/10.1093/femsec/fiad149

Minnebo, Y., Delbaere, K., Goethals, V., Raes, J., Van de Wiele, T., & De Paepe, K. (2023). Gut microbiota response to in vitro transit time variation is mediated by microbial growth rates, nutrient use efficiency and adaptation to in vivo transit time. *Microbiome*, *11*(1), 240. https://doi.org/10.1186/s40168-023-01691-y

Molly, K., Vande Woestyne, M., & Verstraete, W. (1993). Development of a 5-step multi-chamber reactor as a simulation of the human intestinal microbial ecosystem. *Applied microbiology and biotechnology*, *39*, 254-258. https://doi.org/10.1007/BF00228615

Molly, K., Woestyne, M. V., Smet, I. D., & Verstraete, W. (1994). Validation of the simulator of the human intestinal microbial ecosystem (SHIME) reactor using microorganism-associated activities. *Microbial ecology in health and disease*, *7*(4), 191-200. https://doi.org/10.3109/08910609409141354

Nagasue, T., Hirano, A., Torisu, T., Umeno, J., Shibata, H., Moriyama, T., Kawasaki, K., Fujioka, S., Fuyuno, Y., & Matsuno, Y. (2022). The compositional structure of the small intestinal microbial community via balloon-assisted enteroscopy. *Digestion*, *103*(4), 308-318. https://doi.org/10.1159/000524023

Nagata, N., Tohya, M., Fukuda, S., Suda, W., Nishijima, S., Takeuchi, F., Ohsugi, M., Tsujimoto, T., Nakamura, T., & Shimomura, A. (2019). Effects of bowel preparation on the human gut microbiome and metabolome. *Scientific Reports*, *9*(1), 4042. https://doi.org/10.1038/s41598-019-40182-9

Nava, G. M., & Stappenbeck, T. S. (2011). Diversity of the autochthonous colonic microbiota. *Gut microbes*, *2*(2), 99-104. https://doi.org/10.4161/gmic.2.2.15416

Neis, E. P., Dejong, C. H., & Rensen, S. S. (2015). The role of microbial amino acid metabolism in host metabolism. *Nutrients*, *7*(4), 2930-2946. https://doi.org/10.3390/nu7042930

Neyraud, E., Cabaret, S., Brignot, H., Chabanet, C., Labouré, H., Guichard, E., & Berdeaux, O. (2017). The basal free fatty acid concentration in human saliva is related to salivary lipolytic activity. *Scientific Reports*, *7*(1), 5969. https://doi.org/10.1038/s41598-017-06418-2

Nightingale, J. M., & Spiller, R. (2023). Normal intestinal anatomy and physiology. In *Intestinal Failure* (pp. 13-33). Springer. https://doi.org/10.1007/978-3-031-22265-8_2

Nobel, Y. R., Snider, E. J., Compres, G., Freedberg, D. E., Khiabanian, H., Lightdale, C. J., Toussaint, N. C., & Abrams, J. A. (2018). Increasing dietary fiber intake is associated with a distinct esophageal microbiome. *Clinical and translational gastroenterology*, *9*(10). https://doi.org/10.1038/s41424-018-0067-7

O'Toole, P. W., & Jeffery, I. B. (2018). Microbiome–health interactions in older people. *Cellular and molecular life sciences*, *75*, 119-128. https://doi.org/10.1007/s00018-017-2673-z

Olajide, A. M., & LaPointe, G. (2022). *Encyclopedia of Dairy Sciences (Third edition)*. https://doi.org/10.1016/B978-0-12-818766-1.00023-4

Pabst, O. (2012). New concepts in the generation and functions of IgA. *Nature Reviews Immunology*, *12*(12), 821-832. https://doi.org/10.1038/nri3322

Patrascu, O., Béguet-Crespel, F., Marinelli, L., Le Chatelier, E., Abraham, A.-L., Leclerc, M., Klopp, C., Terrapon, N., Henrissat, B., & Blottière, H. M. (2017). A fibrolytic potential in the human ileum mucosal microbiota revealed by functional metagenomic. *Scientific Reports*, *7*(1), 40248. https://doi.org/10.1038/srep40248

Payling, L., Fraser, K., Loveday, S., Sims, I., Roy, N., & McNabb, W. (2020). The effects of carbohydrate structure on the composition and functionality of the human gut microbiota. *Trends in Food Science & Technology*, *97*, 233-248. https://doi.org/10.1016/j.tifs.2020.01.009

Pei, Z., Bini, E. J., Yang, L., Zhou, M., Francois, F., & Blaser, M. J. (2004). Bacterial biota in the human distal esophagus. *Proceedings of the National Academy of Sciences*, *101*(12), 4250-4255. https://doi.org/10.1073/pnas.030639810

Penna, T. C. V., Mazzola, P. G., & Silva Martins, A. M. (2001). The efficacy of chemical agents in cleaning and disinfection programs. *BMC Infectious Diseases*, *1*, 1-8. https://doi.org/10.1186/1471-2334-1-16

Pepino, M. Y., Love-Gregory, L., Klein, S., & Abumrad, N. A. (2012). The fatty acid translocase gene CD36 and lingual lipase influence oral sensitivity to fat in obese subjects. *Journal of lipid research*, *53*(3), 561-566. https://doi.org/10.1194/jlr.M021873

Petras, R. E., & Frankel, W. L. (2009). Large intestine (colon). *Modern Surgical Pathology*, 755. https://doi.org/10.1016/B978-1-4160-3966-2.00023-0

Profet, M. (1991). The function of allergy: immunological defense against toxins. *The Quarterly review of biology*, *66*(1), 23-62.

Props, R., Monsieurs, P., Mysara, M., Clement, L., & Boon, N. (2016). Measuring the biodiversity of microbial communities by flow cytometry. *Methods in Ecology and Evolution*, *7*(11), 1376-1385. https://doi.org/10.1111/2041-210X.12607

Pullan, R., Thomas, G., Rhodes, M., Newcombe, R., Williams, G., Allen, A., & Rhodes, J. (1994). Thickness of adherent mucus gel on colonic mucosa in humans and its relevance to colitis. *Gut*, *35*(3), 353. https://doi.org/10.1136/gut.35.3.353

Qin, J., Li, R., Raes, J., Arumugam, M., Burgdorf, K. S., Manichanh, C., Nielsen, T., Pons, N., Levenez, F., & Yamada, T. (2010). A human gut microbial gene catalogue established by metagenomic sequencing. *Nature*, *464*(7285), 59-65. https://doi.org/10.1038/nature08821

Raimondi, S., Musmeci, E., Candeliere, F., Amaretti, A., & Rossi, M. (2021). Identification of mucin degraders of the human gut microbiota. *Scientific Reports*, *11*(1), 11094. https://doi.org/10.1038/s41598-021-90553-4

Rajilic-Stojanovic, M., Maathuis, A., Heilig, H. G., Venema, K., de Vos, W. M., & Smidt, H. (2010). Evaluating the microbial diversity of an in vitro model of the human large intestine by phylogenetic microarray analysis. *Microbiology*, *156*(11), 3270-3281. https://doi.org/10.1099/mic.0.042044-0

Ramsay, P. T., & Carr, A. (2011). Gastric acid and digestive physiology. *Surgical Clinics*, *91*(5), 977-982. https://doi.org/10.1016/j.suc.2011.06.010

Ramsey, M., Hartke, A., & Huycke, M. (2014). The physiology and metabolism of enterococci. *Enterococci: From Commensals to Leading Causes of Drug Resistant Infection [Internet]*.

RE-Place. (n.d.). *RE-Place project* https://www.re-place.be/

Rehan, M., Al-Bahadly, I., Thomas, D. G., Young, W., Cheng, L. K., & Avci, E. (2024). Smart capsules for sensing and sampling the gut: status, challenges and prospects. *Gut*, *73*(1), 186-202. https://doi.org/10.1136/gutjnl-2023-329614

Richardson, M. (2006). Gastrointestinal tract. Part 4: the small intestine. *Nursing times*, *102*(9), 24-25.

Rios-Covian, D., Arboleya, S., Hernandez-Barranco, A. M., Alvarez-Buylla, J. R., Ruas-Madiedo, P., Gueimonde, M., & de los Reyes-Gavilan, C. G. (2013). Interactions between Bifidobacterium and Bacteroides species in cofermentations are affected by carbon sources, including exopolysaccharides produced by bifidobacteria. *Applied and environmental microbiology*, *79*(23), 7518-7524. https://doi.org/10.1128/AEM.02545-13

Rios-Covian, D., Cuesta, I., Alvarez-Buylla, J. R., Ruas-Madiedo, P., Gueimonde, M., & de Los Reyes-Gavilán, C. G. (2016). Bacteroides fragilis metabolises exopolysaccharides produced by bifidobacteria. *BMC microbiology*, *16*, 1-8. https://doi.org/10.1186/s12866-016-0773-9

Rios-Covian, D., Sánchez, B., Salazar, N., Martınez, N., Redruello, B., & Gueimonde, M. (2015). Different metabolic features of Bacteroides fragilis growing in the presence of glucose and exopolysaccharides of bifidobacteria. Front Microbiol. 2015; 6: 825. In.

Rivière, A., Selak, M., Lantin, D., Leroy, F., & De Vuyst, L. (2016). Bifidobacteria and butyrate-producing colon bacteria: importance and strategies for their stimulation in the human gut. *Frontiers in microbiology*, *7*, 979. https://doi.org/10.3389/fmicb.2016.00979

Rogowski, A., Briggs, J. A., Mortimer, J. C., Tryfona, T., Terrapon, N., Lowe, E. C., Baslé, A., Morland, C., Day, A. M., & Zheng, H. (2015). Glycan complexity dictates microbial resource allocation in the large intestine. *Nature communications*, *6*(1), 7481. https://doi.org/10.1038/ncomms8481

Rosier, B., Buetas, E., Moya-Gonzalvez, E., Artacho, A., & Mira, A. (2020). Nitrate as a potential prebiotic for the oral microbiome. *Scientific Reports*, *10*(1), 12895. https://doi.org/10.1038/s41598-020-69931-x

Rosier, B. T., Moya-Gonzalvez, E. M., Corell-Escuin, P., & Mira, A. (2020). Isolation and characterization of nitrate-reducing bacteria as potential probiotics for oral and systemic health. *Frontiers in microbiology*, *11*, 555465. https://doi.org/10.3389/fmicb.2020.555465

Roussel, C., De Paepe, K., Galia, W., De Bodt, J., Chalancon, S., Leriche, F., Ballet, N., Denis, S., Alric, M., & Van de Wiele, T. (2020). Spatial and temporal modulation of enterotoxigenic E. coli H10407 pathogenesis and interplay with microbiota in human gut models. *BMC biology*, *18*(1), 1-21. https://doi.org/10.1186/s12915-020-00860-x

Rumney, C. J., & Rowland, I. R. (1992). In vivo and in vitro models of the human colonic flora. *Critical Reviews in Food Science & Nutrition*, *31*(4), 299-331. https://doi.org/10.1080/10408399209527575

Rumsey, D. (2005). SMALL INTESTINE | Structure and Function. In *Encyclopedia of Human Nutrition* (second ed., pp. 126-133). https://doi.org/https://doi.org/10.1016/B0-12-226694-3/02255-9

Sagar, N. M., Cree, I. A., Covington, J. A., & Arasaradnam, R. P. (2015). The interplay of the gut microbiome, bile acids, and volatile organic compounds. *Gastroenterology research and practice*, *2015*. https://doi.org/10.1155/2015/398585

Salter, S. J., Cox, M. J., Turek, E. M., Calus, S. T., Cookson, W. O., Moffatt, M. F., Turner, P., Parkhill, J., Loman, N. J., & Walker, A. W. (2014). Reagent and laboratory contamination can critically impact sequence-based microbiome analyses. *BMC biology*, *12*, 1-12. https://doi.org/10.1186/s12915-014-0087-z

Savage, D. C. (1978). Factors involved in colonization of the gut epithelial surface. *The American journal of clinical nutrition*, *31*(10), S131-S135. https://doi.org/10.1093/ajcn/31.10.S131

Schmidt, T. S., Hayward, M. R., Coelho, L. P., Li, S. S., Costea, P. I., Voigt, A. Y., Wirbel, J., Maistrenko, O. M., Alves, R. J., & Bergsten, E. (2019). Extensive transmission of microbes along the gastrointestinal tract. *Elife*, *8*, e42693. https://doi.org/10.7554/eLife.42693

Schneeman, B. O. (1987). Dietary fiber and gastrointestinal function.

Scholtens, S., Smidt, N., Swertz, M. A., Bakker, S. J., Dotinga, A., Vonk, J. M., Van Dijk, F., van Zon, S. K., Wijmenga, C., & Wolffenbuttel, B. H. (2015). Cohort Profile: LifeLines, a three-generation cohort study and biobank. *International journal of epidemiology*, *44*(4), 1172-1180. https://doi.org/10.1093/ije/dyu229

Schömig, V. J., Käsdorf, B. T., Scholz, C., Bidmon, K., Lieleg, O., & Berensmeier, S. (2016). An optimized purification process for porcine gastric mucin with preservation of its native functional properties. *RSC advances*, *6*(50), 44932-44943.

Schroeder, B. O., Birchenough, G. M., Ståhlman, M., Arike, L., Johansson, M. E., Hansson, G. C., & Bäckhed, F. (2018). Bifidobacteria or fiber protects against diet-induced microbiota-mediated colonic mucus deterioration. *Cell Host & Microbe*, *23*(1), 27-40. e27. https://doi.org/10.1016/j.chom.2017.11.004

Seekatz, A. M., Schnizlein, M. K., Koenigsknecht, M. J., Baker, J. R., Hasler, W. L., Bleske, B. E., Young, V. B., & Sun, D. (2019). Spatial and temporal analysis of the stomach and small-intestinal microbiota in fasted healthy humans. *MSphere*, *4*(2), 10.1128/msphere. 00126-00119. https://doi.org/10.1128/msphere.00126-19

Segata, N., Haake, S. K., Mannon, P., Lemon, K. P., Waldron, L., Gevers, D., Huttenhower, C., & Izard, J. (2012). Composition of the adult digestive tract bacterial microbiome based on seven mouth surfaces, tonsils, throat and stool samples. *Genome Biology*, *13*(6), Article R42. https://doi.org/10.1186/gb-2012-13-6-r42

Sender, R., Fuchs, S., & Milo, R. (2016). Revised estimates for the number of human and bacteria cells in the body. *PLoS biology*, *14*(8), e1002533. https://doi.org/10.1371/journal.pbio.1002533

Shah, H. N., Olsen, I., Bernard, K., Finegold, S. M., Gharbia, S., & Gupta, R. S. (2009). Approaches to the study of the systematics of anaerobic, gram-negative, non-sporeforming rods: current status and perspectives. *Anaerobe*, *15*(5), 179-194. https://doi.org/10.1016/j.anaerobe.2009.08.003

Shalon, D., Culver, R. N., Grembi, J. A., Folz, J., Treit, P. V., Shi, H., Rosenberger, F. A., Dethlefsen, L., Meng, X., & Yaffe, E. (2023). Profiling the human intestinal environment under physiological conditions. *Nature*, *617*(7961), 581-591. https://doi.org/10.1038/s41586-023-05989-7

Shanahan, E., Zhong, L., Talley, N., Morrison, M., & Holtmann, G. (2016). Characterisation of the gastrointestinal mucosa-associated microbiota: a novel technique to prevent cross-contamination during endoscopic procedures. *Alimentary pharmacology & therapeutics*, *43*(11), 1186-1196. https://doi.org/10.1111/apt.13622

Sharma, S., Hashmi, M. F., & Valentino III, D. J. (2018). Actinomycosis.

Sheridan, W. G., Lowndes, R. H., & Young, H. L. (1990). Intraoperative tissue oximetry in the human gastrointestinal tract. *The American Journal of Surgery*, *159*(3), 314-319. https://doi.org/10.1016/S0002-9610(05)81226-7

Shim, J. E., Lee, T., & Lee, I. (2017). From sequencing data to gene functions: co-functional network approaches. *Animal cells and systems*, *21*(2), 77-83. https://doi.org/10.1080/19768354.2017.1284156

Singhal, R., & Shah, Y. M. (2020). Oxygen battle in the gut: Hypoxia and hypoxia-inducible factors in metabolic and inflammatory responses in the intestine. *Journal of Biological Chemistry*, *295*(30), 10493-10505. https://doi.org/10.1074/jbc.REV120.011188

Solé, M., Rius, N., & Lorén, J. G. (2000). Rapid extracellular acidification induced by glucose metabolism in non-proliferating cells of Serratia marcescens. *International Microbiology*, *3*(1), 39-43.

Sommer, F., & Bäckhed, F. (2016). Know your neighbor: Microbiota and host epithelial cells interact locally to control intestinal function and physiology. *BioEssays*, *38*(5), 455-464. https://doi.org/10.1002/bies.201500151

Song, Y., & Finegold, S. M. (2011). Peptostreptococcus, finegoldia, anaerococcus, peptoniphilus, veillonella, and other anaerobic cocci. *Manual of clinical microbiology*, 803-816. https://doi.org/10.1128/9781555816728.ch48

Souto, R., Silva-Boghossian, C. M., & Colombo, A. P. V. (2014). Prevalence of Pseudomonas aeruginosa and Acinetobacter spp. in subgingival biofilm and saliva of subjects with chronic periodontal infection. *Brazilian Journal of Microbiology*, *45*, 495-501. https://doi.org/10.1590/S1517-83822014000200017

Soybel, D. I. (2005). Anatomy and physiology of the stomach. *Surgical Clinics*, *85*(5), 875-894. https://doi.org/10.1016/j.suc.2005.05.009

Staley, J. T., & Konopka, A. (1985). Measurement of in situ activities of nonphotosynthetic microorganisms in aquatic and terrestrial habitats. *Annual review of microbiology*, *39*(1), 321-346. https://doi.org/10.1146/annurev.mi.39.100185.001541

Stearns, J. C., Lynch, M. D., Senadheera, D. B., Tenenbaum, H. C., Goldberg, M. B., Cvitkovitch, D. G., Croitoru, K., Moreno-Hagelsieb, G., & Neufeld, J. D. (2011). Bacterial biogeography of the human digestive tract. *Scientific Reports*, *1*(1), 170. https://doi.org/10.1038/srep00170

Stephen, A., Haddad, A., & Phillips, S. (1983). Passage of carbohydrate into the colon: direct measurements in humans. *Gastroenterology*, *85*(3), 589-595. https://doi.org/10.1016/0016-5085(83)90012-4

Stolaki, M., Minekus, M., Venema, K., Lahti, L., Smid, E. J., Kleerebezem, M., & Zoetendal, E. G. (2019). Microbial communities in a dynamic in vitro model for the human ileum resemble the human ileal microbiota. *FEMS microbiology ecology*, *95*(8), fiz096. https://doi.org/10.1093/femsec/fiz096

Strockbine, N. A., & Maurelli, A. T. (2015). Shigella. *Bergey's Manual of Systematics of Archaea and Bacteria*, 1-26. https://doi.org/10.1002/9781118960608.gbm01168

Sundin, O. H., Mendoza-Ladd, A., Zeng, M., Diaz-Arévalo, D., Morales, E., Fagan, B. M., Ordoñez, J., Velez, P., Antony, N., & McCallum, R. W. (2017). The human jejunum has an endogenous microbiota that differs from those in the oral cavity and colon. *BMC microbiology*, *17*(1), 1-17. https://doi.org/10.1186/s12866-017-1059-6

Suzuki, H., & Sugiyama, Y. (2000). Role of metabolic enzymes and efflux transporters in the absorption of drugs from the small intestine. *European journal of pharmaceutical sciences*, *12*(1), 3-12. https://doi.org/10.1016/S0928-0987(00)00178-0

Takahashi, N. (2015). Oral microbiome metabolism: from "who are they?" to "what are they doing?". *Journal of dental research*, *94*(12), 1628-1637. https://doi.org/10.1177/0022034515606045

Tap, J., Mondot, S., Levenez, F., Pelletier, E., Caron, C., Furet, J. P., Ugarte, E., Muñoz-Tamayo, R., Paslier, D. L., & Nalin, R. (2009). Towards the human intestinal microbiota phylogenetic core. *Environmental microbiology*, *11*(10), 2574-2584. https://doi.org/10.1111/j.1462-2920.2009.01982.x

Thuenemann, E. C. (2015). Dynamic Digestion Models: General Introduction. In K. Verhoeckx, P. Cotter, I. López-Expósito, C. Kleiveland, T. Lea, A. Mackie, T. Requena, D. Swiatecka, & H. Wichers (Eds.), *The Impact of Food Bioactives on Health: in vitro and ex vivo models* (pp. 33-36). Springer International Publishing. https://doi.org/10.1007/978-3-319-16104-4_4

Thuenemann, E. C., Mandalari, G., Rich, G. T., & Faulks, R. M. (2015). Dynamic gastric model (DGM). *The Impact of Food Bioactives on Health: in vitro and ex vivo models*, 47-59.

Tian, Y., Gui, W., Koo, I., Smith, P. B., Allman, E. L., Nichols, R. G., Rimal, B., Cai, J., Liu, Q., & Patterson, A. D. (2020). The microbiome modulating activity of bile acids. *Gut microbes*, *11*(4), 979-996. https://doi.org/10.1080/19490976.2020.1732268

Tomb, J.-F., White, O., Kerlavage, A. R., Clayton, R. A., Sutton, G. G., Fleischmann, R. D., Ketchum, K. A., Klenk, H. P., Gill, S., & Dougherty, B. A. (1997). The complete genome sequence of the gastric pathogen Helicobacter pylori. *Nature*, *388*(6642), 539-547. https://doi.org/10.1038/41483

Topping, D. L., & Clifton, P. M. (2001). Short-chain fatty acids and human colonic function: roles of resistant starch and nonstarch polysaccharides. *Physiological reviews*, *81*(3), 1031-1064. https://doi.org/10.1152/physrev.2001.81.3.1031

Towner, K. J. (1992). The genus acinetobacter. In *The Prokaryotes: A Handbook on the Biology of Bacteria: Ecophysiology, Isolation, Identification, Applications* (pp. 3137-3143). Springer. https://doi.org/10.1007/978-1-4757-2191-1_2

Treuting, P. M., Arends, M. J., & Dintzis, S. M. (2018a). Lower gastrointestinal tract. In *Comparative anatomy and histology* (pp. 213-228). Elsevier. https://doi.org/10.1016/B978-0-12-802900-8.00012-9

Treuting, P. M., Arends, M. J., & Dintzis, S. M. (2018b). Upper gastrointestinal tract. In *Comparative anatomy and histology* (pp. 191-211). Elsevier. https://doi.org/https://doi.org/10.1016/B978-0-12-802900-8.00011-7

Turnbaugh, P. J., Ley, R. E., Hamady, M., Fraser-Liggett, C. M., Knight, R., & Gordon, J. I. (2007). The human microbiome project. *Nature*, *449*(7164), 804-810. https://doi.org/10.1038/nature06244

Uchibori, S., Tsuzukibashi, O., Kobayashi, T., & Aida, M. (2013). Localization of the genus Rothia in the oral cavity. *International Journal of Oral-Medical Sciences*, *11*(3), 207-210. https://doi.org/10.5466/ijoms.11.207

Uranga, C. C., Arroyo Jr, P., Duggan, B. M., Gerwick, W. H., & Edlund, A. (2020). Commensal oral Rothia mucilaginosa produces enterobactin, a metal-chelating siderophore. *Msystems*, *5*(2), 10.1128/msystems. 00161-00120. https://doi.org/10.1128/msystems.00161-20

Van de Graaff, K. M. (1986). Anatomy and physiology of the gastrointestinal tract. *The Pediatric Infectious Disease Journal*, *5*(1), 11-16. https://journals.lww.com/pidj/fulltext/1986/01001/anatomy_and_physiology_of_the_gastrointestinal.5.aspx

Van de Wiele, T., Van den Abbeele, P., Ossieur, W., Possemiers, S., & Marzorati, M. (2015). The simulator of the human intestinal microbial ecosystem (SHIME®). *The Impact of Food Bioactives on Health: in vitro and ex vivo models*, 305-317. https://doi.org/10.1007/978-3-319-16104-4_27

Van den Abbeele, P., Belzer, C., Goossens, M., Kleerebezem, M., De Vos, W. M., Thas, O., De Weirdt, R., Kerckhof, F.-M., & Van de Wiele, T. (2013). Butyrate-producing Clostridium cluster XIVa species specifically colonize mucins in an in vitro gut model. *The ISME journal*, *7*(5), 949-961. https://doi.org/10.1038/ismej.2012.158

Van den Abbeele, P., Grootaert, C., Marzorati, M., Possemiers, S., Verstraete, W., Gérard, P., Rabot, S., Bruneau, A., El Aidy, S., & Derrien, M. (2010). Microbial community development in a dynamic gut model is reproducible, colon region specific, and selective for Bacteroidetes and Clostridium cluster IX. *Applied and environmental microbiology*, *76*(15), 5237-5246. https://doi.org/10.1128/AEM.00759-10

Van den Abbeele, P., Roos, S., Eeckhaut, V., MacKenzie, D. A., Derde, M., Verstraete, W., Marzorati, M., Possemiers, S., Vanhoecke, B., & Van Immerseel, F. (2012). Incorporating a mucosal environment in a dynamic gut model results in a more representative colonization by lactobacilli. *Microbial biotechnology*, *5*(1), 106-115. https://doi.org/10.1111/j.1751-7915.2011.00308.x

van den Bogert, B. (2013). *Community and genomic analysis of the human small intestine microbiota*. Wageningen University and Research.

Van den Bogert, B., Erkus, O., Boekhorst, J., Goffau, M. d., Smid, E. J., Zoetendal, E. G., & Kleerebezem, M. (2013). Diversity of human small intestinal Streptococcus and Veillonella populations. *FEMS microbiology ecology*, *85*(2), 376-388. https://doi.org/10.1111/1574-6941.12127

Vandeputte, D., Kathagen, G., D'hoe, K., Vieira-Silva, S., Valles-Colomer, M., Sabino, J., Wang, J., Tito, R. Y., De Commer, L., & Darzi, Y. (2017). Quantitative microbiome profiling links gut community variation to microbial load. *Nature*, *551*(7681), 507-511. https://doi.org/10.1038/nature24460

Vasapolli, R., Schütte, K., Schulz, C., Vital, M., Schomburg, D., Pieper, D. H., Vilchez-Vargas, R., & Malfertheiner, P. (2019). Analysis of transcriptionally active bacteria throughout the gastrointestinal tract of healthy individuals. *Gastroenterology*, *157*(4), 1081-1092. e1083. https://doi.org/10.1053/j.gastro.2019.05.068

Venema, K., & Van den Abbeele, P. (2013). Experimental models of the gut microbiome. *Best practice & research Clinical gastroenterology*, *27*(1), 115-126. https://doi.org/10.1016/j.bpg.2013.03.002

Verma, D., Garg, P. K., & Dubey, A. K. (2018). Insights into the human oral microbiome. *Archives of microbiology*, *200*, 525-540. https://doi.org/10.1007/s00203-018-1505-3

Vila, T., Rizk, A. M., Sultan, A. S., & Jabra-Rizk, M. A. (2019). The power of saliva: Antimicrobial and beyond. *PLoS pathogens*, *15*(11), e1008058. https://doi.org/10.1371/journal.ppat.1008058

Villmones, H. C. (2022). Investigating the human small intestinal microbiota: Microbiological characterization of jejunal and ileal samples collected during surgery. https://doi.org/10.1038/s41598-018-23198-5

Villmones, H. C., Halland, A., Stenstad, T., Ulvestad, E., Weedon-Fekjær, H., & Kommedal, Ø. (2021). The cultivable microbiota of the human distal ileum. *Clinical Microbiology and Infection*, *27*(6), 912. e917-912. e913. https://doi.org/10.1016/j.cmi.2020.08.021

Villmones, H. C., Haug, E. S., Ulvestad, E., Grude, N., Stenstad, T., Halland, A., & Kommedal, Ø. (2018). Species level description of the human ileal bacterial microbiota. *Scientific Reports*, *8*(1), 4736. https://doi.org/10.1038/s41598-018-23198-5

Voigt, N., Stein, J., Galindo, M. M., Dunkel, A., Raguse, J.-D., Meyerhof, W., Hofmann, T., & Behrens, M. (2014). The role of lipolysis in human orosensory fat perception. *Journal of lipid research*, *55*(5), 870-882. https://doi.org/10.1194/jlr.M046029

von Martels, J. Z., Sadabad, M. S., Bourgonje, A. R., Blokzijl, T., Dijkstra, G., Faber, K. N., & Harmsen, H. J. (2017). The role of gut microbiota in health and disease: In vitro modeling of host-microbe interactions at the aerobe-anaerobe interphase of the human gut. *Anaerobe*, *44*, 3-12. https://doi.org/10.1016/j.anaerobe.2017.01.001

Vuik, F., Dicksved, J., Lam, S. Y., Fuhler, G., van der Laan, L., van de Winkel, A., Konstantinov, S., Spaander, M., Peppelenbosch, M., & Engstrand, L. (2019). Composition of the mucosa-associated microbiota along the entire gastrointestinal tract of human individuals. *United European gastroenterology journal*, *7*(7), 897-907. https://doi.org/10.1177/2050640619852225

Wächtershäuser, A., & Stein, J. (2000). Rationale for the luminal provision of butyrate in intestinal diseases. *European journal of nutrition*, *39*, 164-171. https://doi.org/10.1007/s003940070020

Walter, J., & Ley, R. (2011). The human gut microbiome: ecology and recent evolutionary changes. *Annual review of microbiology*, *65*, 411-429. https://doi.org/10.1146/annurev-micro-090110-102830

Wan, J., Zhang, Y., He, W., Tian, Z., Lin, J., Liu, Z., Li, Y., Chen, M., Han, S., & Liang, J. (2022). Gut microbiota and metabolite changes in patients with ulcerative colitis and Clostridioides difficile infection. *Frontiers in microbiology*, *13*, 802823. https://doi.org/10.3389/fmicb.2022.802823

Wang, M., Ahrné, S., Jeppsson, B., & Molin, G. (2005). Comparison of bacterial diversity along the human intestinal tract by direct cloning and sequencing of 16S rRNA genes. *FEMS microbiology ecology*, *54*(2), 219-231. https://doi.org/10.1016/j.femsec.2005.03.012

Wang, M., Wichienchot, S., He, X., Fu, X., Huang, Q., & Zhang, B. (2019). In vitro colonic fermentation of dietary fibers: Fermentation rate, short-chain fatty acid production and changes in microbiota. *Trends in Food Science & Technology*, *88*, 1-9. https://doi.org/10.1016/j.tifs.2019.03.005

Wang, Q., Garrity, G. M., Tiedje, J. M., & Cole, J. R. (2007). Naive Bayesian classifier for rapid assignment of rRNA sequences into the new bacterial taxonomy. *Applied and environmental microbiology*, *73*(16), 5261-5267. https://doi.org/10.1128/AEM.00062-07

Williams, C., Walton, G., Jiang, L., Plummer, S., Garaiova, I., & Gibson, G. R. (2015). Comparative analysis of intestinal tract models. *Annual review of food science and technology*, *6*, 329-350. https://doi.org/10.1146/annurev-food-022814-015429

Wilson, M. M. (2004). The gastrointestinal tract and its indigenous microbiota. In *Microbial inhabitants of humans : their ecology and role in health and disease*. https://doi.org/10.1017/cbo9780511735080.008

Wright, E. M., Sala-Rabanal, M., Ghezzi, C., & Loo, D. D. (2018). Sugar absorption. In *Physiology of the gastrointestinal tract* (pp. 1051-1062). Elsevier. https://doi.org/10.1016/B978-0-12-809954-4.00046-3

Wu, G. (1998). Intestinal mucosal amino acid catabolism. *The Journal of nutrition*, *128*(8), 1249-1252.

Zoetendal, E. G., Raes, J., Van Den Bogert, B., Arumugam, M., Booijink, C. C., Troost, F. J., Bork, P., Wels, M., De Vos, W. M., & Kleerebezem, M. (2012). The human small intestinal microbiota is driven by rapid uptake and conversion of simple carbohydrates. *The ISME journal*, *6*(7), 1415-1426. https://doi.org/10.1038/ismej.2011.212

ZR, V. (1990). 13. Physiology and pathophysiology of enterohepatic circulation of bile acids. *Hepatology: a textbook of liver desease*.